

**Human Interleukin-4 binding protein epitope involved in high-affinity
binding of Interleukin-4: Molecular analysis and characterisation**

Dissertation zur Erlangung des
naturwissenschaftlichen Doktorgrades
der Bayerischen Julius-Maximilians-Universität Würzburg

vorgelegt von

Irina Wietek

aus
Sofia, Bulgarien

Würzburg, Juli 2001

Eingereicht am: 23. Juli 2001

Mitglieder der Promotionskommission:

Vorsitzender:

Gutachter: Prof. Dr. Walter Sebald

Gutachter: Prof. Dr. Erich Buchner

Tag des Promotionskolloquiums:

Doktorurkunde ausgehändigt am:

Contents

1 INTRODUCTION.....	4
2. MATERIALS AND METHODS.....	22
2.1 Abbreviations.....	22
2.2 Chemicals and Enzymes	25
2.3 Bacterial Strains.....	25
2.4 Cell Lines.....	25
2.5 Antibodies	26
2.6 Vectors and Oligonucleotides.....	26
2.6.1 Expression Vector for E.coli	26
2.6.2 Baculovirus Transfer Vector pAcGP67-B	26
2.6.3 Oligonucleotides	26
2.7 Microbiological Methods	28
2.7.1 Sterilization	28
2.7.2 Culture Media.....	29
2.7.3 Culturing of Bacteria.....	29
2.7.4 Electrocompetent E.coli	30
2.7.4.1 Preparation of electrocompetent bacterial cells.....	30
2.7.4.2 Electrotransformation of competent E.coli.....	30
2.7.5 Storage of Bacterial Cultures	30
2.8 Molecular Biological Methods	31
2.8.1 Determination of the Concentration of Nucleic Acids.....	31
2.8.2 Phenol Extraction of DNA	31
2.8.3 Ethanol Precipitation of DNA.....	31
2.8.4 DNA Molecular Standards.....	32
2.8.5 DNA Agarose Gel Electrophoresis	32
2.8.6 Purification of DNA by Agarose Gel Electrophoresis.....	33
2.8.7 Site-directed Mutagenesis by PCR.....	33
2.8.8 Site-directed Mutagenesis Using DNA Cassettes	35
2.8.9 Digestion of DNA	35
2.8.10 Ligation of DNA	36
2.8.11 Preparation of Plasmid DNA	36
2.8.11.1 Lysozyme-alkaline-lysis procedure.....	36
2.8.11.2 PEG precipitation procedure.....	37
2.8.11.3 Preparation of plasmid DNA with LiCl.....	38
2.8.12 DNA Sequencing	39
2.9 Protein Chemical Methods	39
2.9.1 Determination of the Protein Concentration	39
2.9.2 Lyophilization of Proteins.....	40
2.9.3 Molecular Weight Standard for Protein Samples.....	40

2.9.4 SDS - Polyacrylamide Gel Electrophoresis	40
2.9.5 Concentration of Protein Samples by TCA.....	41
2.9.6 Biotinylation of Proteins	42
2.10 Immunological methods - Western Blot.....	42
2.10.1 Transfer of Proteins to a Nitrocellulose Membrane.....	42
2.10.2 Detection of Western Blots by a Peroxidase Coupled Antibody	43
2.11 Expression of Recombinant Proteins in E.coli	44
2.11.1 Temperature Induced Protein Expression	44
2.11.2 Preparation of Inclusion Bodies	45
2.11.3 Denaturation and Renaturation of Proteins	45
2.12 Expression of Recombinant Proteins in Sf9 cells	46
2.12.1 General Handling Techniques.....	46
2.12.1.1 Insect cell culture media	46
2.12.1.2 Cultivation of Sf9 cells	46
2.12.1.3 Staining and counting of Sf9 cells.....	47
2.12.1.4 Long-term cell storage.....	47
2.12.1.5 Monolayer culture.....	48
2.12.1.6 Suspension culture	48
2.12.2 Generation of Recombinant Baculoviruses.....	49
2.12.2.1 The Baculovirus expression system.....	49
2.12.2.2 Co-transfection of BaculoGold DNA and a transfer vector into insect cells	49
2.12.2.3 Generating pure virus stocks by plaque purification	51
2.12.3 Amplification of Virus Stocks	52
2.12.3.1 Virus amplification from a single virus plaque	52
2.12.3.2 Virus amplification in a small volume scale.....	53
2.12.3.3 Virus amplification in a large volume scale	53
2.12.3.4 Determination of virus titer by plaque assay	53
2.12.3.5 Virus storage.....	54
2.12.4 Protein Expression	54
2.13 Purification of Recombinant Proteins.....	55
2.13.1 Purification of Proteins Expressed in E.coli	55
2.13.1.1 Protein purification by ion exchange chromatography.....	55
2.13.1.2 Protein purification by RP-HPLC.....	55
2.13.2 Purification of Proteins Expressed in Sf9 Cells	57
2.13.2.1 Affinity chromatography using IL-4 as a ligand	57
2.13.2.2 Affinity chromatography using X14/38 as a ligand	57
2.13.2.3 Dialysis	58
2.13.2.4 Concentration of proteins by ultrafiltration	58
2.14 Analysis of Protein-Protein Interactions by BIAcore Technology	59
2.14.1 Immobilization of Proteins by Streptavidin-Biotin Coupling.....	60
2.14.2 Measuring and Evaluation of Protein-Protein Interactions.....	60
2.14.3 Assessment of the Energetic Effects of Introduced Mutations	61
3. RESULTS	62
3.1 Preparation of Recombinant IL-4BP and Its Variants	62
3.1.1 Cloning of IL-4BP and Its Variants in the Baculovirus Transfer Vector pAcGP67B	64

3.1.2 Co-transfection into SF9 Insect Cells and Amplification of the Recombinant Virus.....	68
3.1.3 Expression and Purification of Recombinant IL-4BP and Its Variants	69
3.1.3.1 Purification of IL-4BP and its variants by IL-4 affinity column	69
3.1.3.2 Purification of IL-4BP variants through Antibody column	74
3.1.4 Biotinylation of IL-4BP Recombinant Variants	77
3.2 Preparation of Recombinant IL-4 Variants	78
3.2.1 Cloning of IL-4 Mutant Variants	78
3.2.2 Expression and Purification of IL-4 Variants	81
3.3 Kinetic Analysis of the Interaction of IL-4 with the IL-4BP Variants Using BIAcore Technology.....	84
3.3.1 Immobilization of the Biotinylated IL-4BP and its Variants on the Sensor Chips.....	84
3.3.2 Kinetics of the Interaction of IL-4 and IL-4BP.....	87
3.3.3 Effects of Site-Specific Perturbations in IL-4BP on the Interaction with IL-4.....	89
3.3.3.1 Kinetics of the binding of IL-4 to the alanine variants of IL-4BP.....	89
3.3.3.2 Thermodynamic aspects of the interaction between IL-4 and the IL-4BP variants included in the alanine scanning mutagenesis.....	99
3.3.3.3 Analysis of the binding of IL-4 to the IL-4BP tyrosine variants.....	103
3.3.4 Analysis of IL-4BP Double Mutants.....	105
3.4 Biosensor Analysis of the Kinetics of Binding of IL-4 Variants to the IL-4BP	110
4. DISCUSSION	112
4.1 Structural Features and Binding Site of Human IL-4BP.....	112
4.2 Defining Functional Important Residues from The Interface of Human IL-4BP for the Interaction with IL-4	116
4.3 Additivity and Cooperativity in the Functional Epitope of IL-4BP	124
4.4 Comparison of the Structural and the Functional IL-4BP Epitopes	126
4.5 Complementarity between the Functional Epitopes of Human IL-4 and IL-4BP	129
4.6 Comparison of the IL-4BP Functional Epitope to Other Cytokine Receptors	131
5. SUMMARY.....	135
6. LITERATURE.....	137
7. APPENDICES	146
ACKNOWLEDGEMENTS	155
LEBENS LAUF	156
ERKLÄRUNG	157

1 Introduction

The immune system is a remarkably adaptive defense system that has evolved in vertebrates to protect them from invading pathogens and cancer. It is able to generate an enormous variety of cells and molecules capable of specifically recognizing and eliminating an apparently limitless variety of foreign invaders. These cells and molecules act together in an exquisitely adaptable, dynamic and complex network.

Immunity has both non-specific and specific components, which work in a synchronized manner that provides an effective biological defense. Innate, or non-specific immunity refers to the basic resistance to disease that comprises four types of defensive barriers: anatomic, physiologic, endocytic and phagocytic, and inflammatory. Acquired, or specific, immunity reflects the presence of a functional immune system that is capable of specific and selective immune responses: humoral and cell-mediated. Generation of an effective humoral immune response requires cell interactions between macrophages, T_H cells and B cells leading to the production of large numbers of antibody molecules specific for a foreign pathogen. The cell-mediated immunity is characterized by the generation of various effector immune cells: $CD4^+$ and $CD8^+$ T lymphocytes (antigen-specific), macrophages, neutrophils, eosinophils and natural killer cells (antigen-non-specific). Unlike the humoral branch of the immune system, which serves mainly to eliminate extracellular bacteria and their products, the cell-mediated immunity is responsible for the clearance of intracellular pathogens, virus-infected cells, tumor cells and foreign grafts (Kuby, 1994).

The large number of distinct cell types which are involved in the immune responses and their functions must be coordinated to insure a response that is appropriate in quality and in magnitude to the eliciting antigenic stimulus. A central role in this regulation and co-ordination of functions has the action of T lymphocytes, whose receptors are specific for peptides derived from the eliciting antigen, bound to a groove in a class I or a class II MHC molecules. Much of their function is mediated by a set of small proteins whose expression, secretion, or both is induced as a result of antigen-stimulated cellular activation. These proteins, designated cytokines, act by binding to high-affinity receptors expressed on target cells and by inducing biochemical signals within those cells that profoundly affect their behavior.

Cytokines are a diverse group of proteins, which can be subdivided into several families, including the haematopoietins, the interferons, tumor necrosis factor (TNF)-related molecules, immunoglobulin super-family members, and the chemokines (Paul & Seder, 1994). Among these molecules substantial overlap in functions is observed. These pleiotropic mediators act synergistically or antagonistically to orchestrate the behavior, proliferation and death of cells, acting directly or by regulating the expression of other cytokines. A paradigm of cytokine biology arises from the regulation of the differentiation of naive T cells. Among cloned lines of $CD4^+$ T cells, two major subsets (T_{H1} and T_{H2}) have been identified, which have shown a great degree of polarization in their cytokine-producing phenotype (Romagnani, 1991). T_{H1} clones tend to produce IL-2, $IFN\gamma$ and $TNF\beta$ as their unique products, while T_{H2} clones express IL-4, IL-5, IL-6, IL-10 and IL-13. T_{H1} and T_{H2} cells develop from precursors of T helper cells (pT_H), which are bi-potent and their differentiation is determined by the present cytokines (Figure 1.1). IL-4 appears to be essential for priming the differentiation of pT_H cells into T_{H2} cells, while $IFN\gamma$ inhibits it (Seder et al., 1992). The differentiation into T_{H1} cells is enhanced by IL-12 and diminished by IL-4 (Hsieh et al., 1993; Seder et al., 1993).

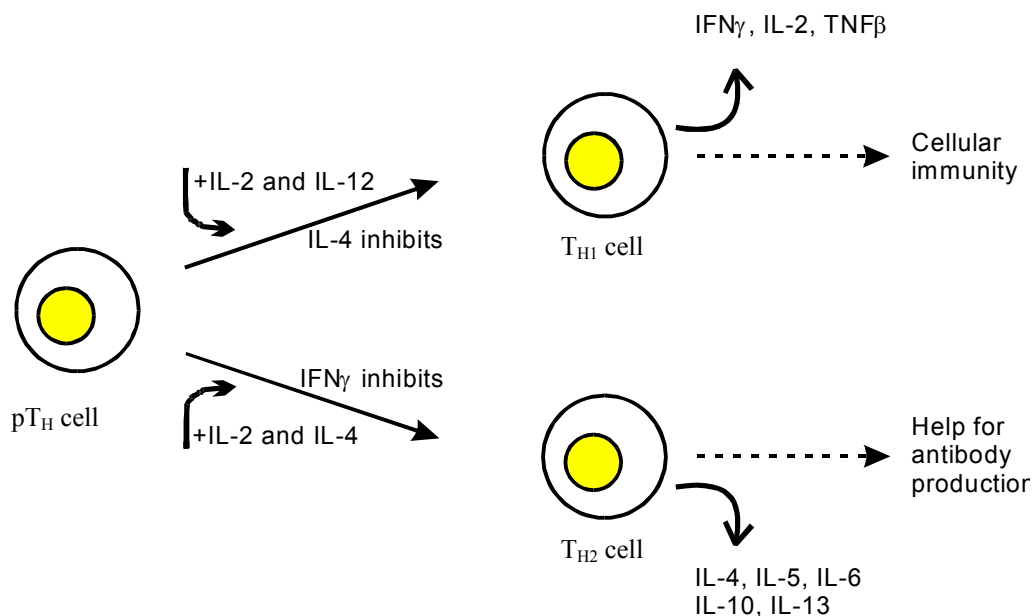


Figure 1.1: Differentiation of pT_H cells into T_{H1} and T_{H2} subtypes is determined by cytokines. A system through which the polarization of $CD4^+$ T cell response toward the production of $IFN\gamma$ and the expression of cellular immunity or toward the production of IL-4 and expression of help for antibody production is mediated (Paul & Seder, 1994).

Interleukin-4 (IL-4) belongs to the haematopoietin family of cytokines. It was initially described in 1982 and first designated B-cell growth factor (Howard et al., 1982). IL-4 is produced by T_{H2} cells (Figure 1.1), basophils and mast cells in response to receptor-mediated activation events (Seder & Paul, 1994). A specialized subset of T cells, some of which express NK1.1 and appear to be specific for CD-1 (NK T cells), has been also shown to produce IL-4 (Yoshimoto & Paul, 1994; Chen & Paul, 1997). Eosinophils have also been reported to be capable of producing IL-4 (Dubucquoi et al., 1994).

Among the cytokine family, IL-4 is one that displays a wide range of biological effects on numerous cell types. These effects are either direct or indirect through the modulation of secretion of other cytokines. As mentioned above, IL-4 plays a central role in regulating the differentiation of antigen stimulated naive T cells into T_{H1} or T_{H2} subtypes and determines the kind of the following immune response (McKenzie, 2000).

A second function of major physiologic importance is IL-4's control of specificity of immunoglobulin class switching. IL-4 determines that human B cells switch to the expression of IgE and IgG4 and mouse B cells to IgE and IgG1 (Gascan et al., 1991; Coffman et al., 1986). This switching function is antagonized by IFN γ . Similarly, IL-4 inhibits the production of IgG2a in B cells treated with IFN γ (Pene et al, 1988). Thus, the control of production of these two cytokines is a key element in the qualitative nature of immune responses. Indeed, in IL-4 and IL-4 receptor α (IL-4R α) deficient mice the serum levels of IgE and IgG1 are strongly reduced (Kopf et al., 1993; Kuehn et al., 1991; Noben-Trauth et al., 1997). Taken together, these facts have established an important role of IL-4 in Ig isotype selection *in vitro* and *in vivo*.

IL-4 has a variety of other effects in cells of the immune system. It is involved in activation and proliferation of T and B cells (Nicola, 1994; Rebollo et al, 1996; Friedrich & Wietek, 2001). In resting B cells IL-4 increases the expression of class II MHC molecules (Noelle et al., 1984), enhances expression of CD23 (Defrance et al., 1987), up-regulates the expression of the IL-4 receptor (Ohara & Paul, 1988), and in association with lipopolysaccharide allows B cells to express Thy1 (Snapper et al., 1988). It also acts as a co-mitogen for B cell growth (Howard et al., 1982). Although not a growth factor by itself for resting lymphocytes, it can substantially prolong the lives of T and B lymphocytes in culture (Hu-Li et al., 1987). IL-4 also has activity as a stimulant of IL-3-mediated mast cell growth. IL-4 acts on macrophages to inhibit the release of proinflammatory molecules such as TNF, IL-1, IL-8 and other cytokines (Nicola & Hilton, 1999). IL-4 also has an important role in tissue adhesion and inflammation. It acts with TNF to induce expression of vascular cell adhesion molecule-1 on vascular endothelial cells (Thornhill et al., 1991) and it down-regulates the expression of E-selectin (Bennett et al., 1997). This shift in

balance of expression of adhesion molecules by IL-4 is thought to favor the recruitment of T cells and eosinophils, rather than granulocytes, to the side of inflammation.

Many cell types respond to IL-4, including some without apparent connection to haematopoiesis or to the immune system, e.g. osteoblasts, keratinocytes, or fibroblasts (Duschl & Sebald, 1996). IL-4 acts as a chemotactic factor for fibroblasts and induces dermal fibroblasts to secrete extracellular matrix proteins, such as type I and type III colagens and fibronectin (Chomarat & Banchereau, 1997). Although the mechanism remains unclear, IL-4 has been observed to enhance the killing of tumor cells *in vivo* (Tepper & Mule, 1994).

Studies with transgenic mice have revealed that over-expression of IL-4 results not only in high serum IgE levels, but also in inflammatory lesions, which severity and frequency directly correlates with the level of transgenically expressed IL-4. These lesions histologically resemble those seen in human allergic disorders suggesting the importance of IL-4 in the pathogenesis of allergic diseases (Tepper et al., 1990). The pathophysiological features of allergic asthma are thought to result of aberrant expression of T_{H2} cells producing IL-4, IL-5 and IL-13. Such conclusion is supported by the fact that T_{H2} cells are necessary for induction of allergic asthma in murine models (Gavett et al., 1994). The type 2 cytokines undergo expansion in these models as well as in patients with allergic asthma (Walker et al., 1992). High amounts of these cytokines have been detected especially in the airway tissue of asthmatics and animal models (Gavett et al., 1995; Tsicopoulos et al., 2000). Experiments using IL-4 deficient mice have shown significantly attenuated asthma phenotype after repeated allergen exposure, in contrast to wild-type control animals, where all asthmatic symptoms have developed (Brusselle et al., 1994; Brusselle et al., 1995; Hamelmann et al., 1999).

Recent studies have demonstrated the contribution of another type 2 cytokine, IL-13 for inducing allergic asthma in a IL-4-independent manner (Wills-Karp et al., 1998; Gruenig et al., 1998; Cohn et al., 1999, Izuhara et al., 2000). IL-13 is a cytokine closely related to IL-4 and both bind to IL-4R α . Linkage analysis has mapped susceptibility to allergic asthma to a region on human chromosome 5q25-33, which includes the genes for both IL-4 and IL-13 (Marsh et al., 1996, Lonjou et al., 2000). A number of additional regions in the genome have been linked to asthma in human studies, suggesting a complex multifactorial phenotype (Nanavaty et al., 2001). However, diverse forms of asthma, implicating IL-4 and IL-13 might follow a final common effector pathway mediated through signals transduced by IL-4R α .

Allergy comprises a group of syndromes that includes asthma, atopic dermatitis and hay fever. These diseases have classically been described as caused by an allergic response characterized by immediate (type 1) hypersensitivity reactions, increased serum IgE, and increased bronchial reactivity to specific or non-specific inhaled allergens. Allergic asthma is a complex disorder

characterized by local and systemic allergic inflammation and reversible airway obstruction (Anderson & Morrison, 1998). Asthma develops because of both a genetic predisposition and the exposure to environmental factors, such as allergens, respiratory tract infections and atmospheric pollutants (Manian, 1997). Most major allergens are extremely well characterized. They are usually soluble proteins with dimensions that allow penetration into the airways of the nose or lung. Allergen sources include house dust mites, domestic and farm animals, and grass or tree pollen.

Recent decades have brought dramatic increases in the prevalence and severity of allergic asthma. It is especially an important problem in developed societies, where 10% of the children are affected (Cookson & Moffatt, 1998).

Although some details of the asthmatic pathogenesis remain unclear, the main mechanism and the role of IL-4 are well established (Figure 1.2). Processing of the allergen by antigen-presenting cells (APC) leads to the formation of an allergen peptide that is presented to the T-cell receptors (TCR) of CD4⁺ T cells in association with MHC class II molecules. IL-4 released by eosinophils, basophils and mast cells facilitates the differentiation of pT_H cells into T_{H2} cells which secrete IL-4, IL-5, IL-6, IL-10 and IL-13. Activated T_{H2} cells interact through the TCR with the peptide-MHC complex on B cells. Adhesive interaction between T_{H2} and B cells are also mediated by the surface expression of CD40 ligand on T_{H2} cells and CD40 on B cells. IL-4 and IL-13, secreted to a varied extent by T_{H2} cells, basophils, mast cells and eosinophils, induce immunoglobulin class switching to IgE in B cells. Allergic disease is initiated when allergen comes into contact with IgE bound to the high affinity IgE receptor (FcεRI) on mast cells and basophils. Receptor cross-linking releases a mixture of inflammatory mediators (histamine, peptide leukotrienes and platelet-activating factor) that are responsible for the symptoms of allergic asthma. Immediate inflammation and associated symptoms resolve and are followed by a second phase, which typically peaks 6 to 20 hours after antigen exposure (Marone, 1998).

The conventional therapy of patients with allergic asthma includes symptomatic treatment with inhaled corticosteroids. The long term of steroid therapy has shown different side effects such as osteoporosis, skin thinning and hypertension. New, alternative strategies specifically target the T_{H1}/T_{H2} balance of the immune response. Potent candidates for development of anti-allergic drugs are IL-4, IL-5 and IL-13. Possible therapies include the use of inhibitory antibodies, soluble cytokine receptors or antagonistic cytokine variants (Prasad et al., 2000; Ramshaw et al., 2001). An antibody-mediated blockade of IL-4 in a murine model has ablated the development

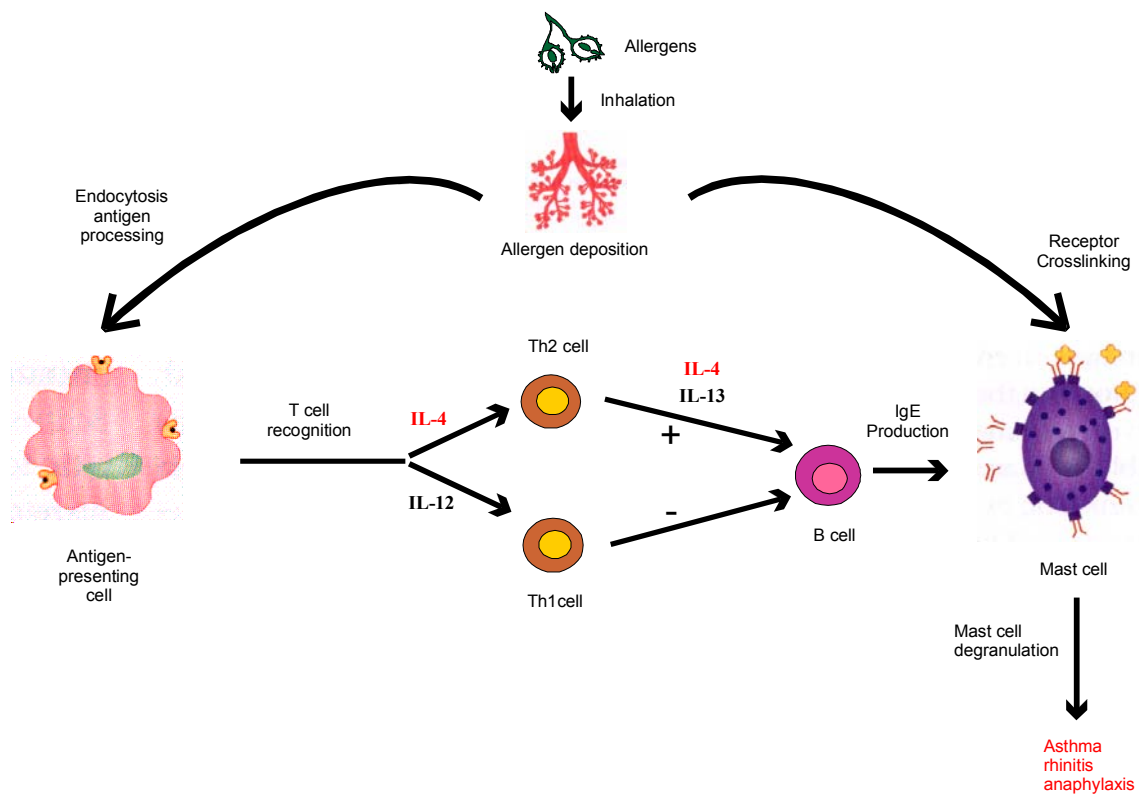


Figure 1.2: Mechanism of immediate (type I) hypersensitivity reactions. Allergens induce disease in sensitized individuals by the crosslinking of IgE bound to high-affinity receptors on mast cells. Mast cell degranulation initiates an inflammatory cascade and allergic symptoms. Th2 cells up-regulate IgE production, whereas Th1 cells down-regulate it (Cookson & Moffatt, 1998).

of allergic asthma only when the monoclonal antibody has been administered during the period of systemic immunization. No effect has been observed when anti-IL-4 has been administered during the period of allergen challenge (Corry et al., 1996; Tanaka et al., 1998). Treatment of sensitized mice with soluble IL-4 receptor (sIL-4R) has demonstrated partial success, since the late phase pulmonary inflammation has been blocked to some degree (Henderson et al, 2000). Antagonistic IL-4 variants have been first described for human IL-4 (Kruse et al., 1992; Kruse et al., 1993). The most efficient human antagonist described so far is [R121D, Y124D]-IL-4 (Tony et al., 1994). A murine antagonistic variant, [Q116D, Y119D]-mIL-4, has shown inhibition of mIL-4 and has prevented completely the development of an allergy phenotype in treated animals (Grunewald et al., 1998). Another mutant variant of murine IL-4 (C118 deletion) was recently reported to prevent the development of allergic airway eosinophilia and airway hyperresponsiveness in mice (Tomkison et al, 2001). These examples demonstrated the

therapeutic potential of IL-4 mutant proteins as receptor antagonists that are able to inhibit both IL-4 and IL-13 in treatment of allergic asthma.

Murine IL-4 is a glycoprotein with an approximate molecular weight of 19 kDa when purified from T-cell source (Ohara et al., 1985; Grabstein et al., 1986). Recombinant IL-4 produced in baculovirus expression system has an approximate molecular weight of 14 to 15 kDa, whereas recombinant IL-4 produced in yeast is quite heterogeneous in molecular weight with some forms having size of ~50 kDa. These differences represent variable glycosylation. IL-4 that has been deglycosylated has full biologic activity (Le et al., 1988), as does recombinant IL-4 produced in E.coli. Human IL-4 has very similar characteristics (Table 1.1). It exists in molecular weight forms between 15 and 19 kDa.

Table 1.1: Characteristics of murine and human IL-4 (Beckmann, 1992)

Characteristic	Murine IL-4	Human IL-4
Amino acids		
Precursor	140	153
Mature	120	129
Molecular weight, kDa		
Predicted	14	14
Expressed	15-19	15-19
N-linked glycosylation sites	3	2
Disulphide bonds	Yes (6 Cys)	Yes (6 Cys)
Gene size, Kbp	~ 6	~ 10
Number of exons	4	4
Chromosomal location	11	5q23.3-31.2

cDNA for both mouse and human IL-4 have been cloned (Lee et al., 1986; Yokota et al., 1986), and the proteins encoded by the murine and human cDNAs contain 140 and 153 amino acids, respectively. Both murine and human IL-4 contain putative signal sequences at their N-termini which following cleavage, result in mature proteins of 120 and 129 amino acids, respectively. There is approximately 50% overall identity between human and murine IL-4.

The gene for human IL-4 has been mapped to the long arm of chromosome 5 at 5q23-31 (Le Beau et al., 1988). The IL-4 gene is linked to the genes of a few other cytokines: IL-13, IL-5, granulocyte/macrophage colony-stimulating factor (GM-CSF) and IL-3. Due to their close localization, the similar exon structure of the genes and their primary sequence homology, this cytokines have been termed the IL-4 family (Paul & Seder, 1994). A homologous region has been found at mouse chromosome 11 (D'Eustachio et al, 1988).

The secondary structure of IL-4 has been described in crystals and in solution (Powers et al., 1992; Smith et al., 1992; Walter et al., 1992; Wlodawer et al., 1992). IL-4 displays the four α -

helix bundle structure, which is a characteristic of the ligands from class 1 of the cytokine superfamily. The four-helix bundles of haematopoietic ligands have an “up-up-down-down” orientation in which the first two helices are parallel to each other and anti-parallel to the last two. This is achieved by cross-over connections linking helix A to B and helix C to D. Based on the overall length of the polypeptide chain, the length of the main helices, and the inter-helix angles, class 1 of cytokine superfamily is further classified into two groups: a “long chain” and a “short chain” group (Sprang & Bazan, 1993). As seen from the structures of GH, G-CSF, LIF, EPO, IL-6, and leptin, members of the long-chain group have about 160 to 200 amino acids, long helices (about 25 residues), and an angle between the AD and BC helix pairs of about 160°. Based on sequence comparisons, it is expected that PRL, ONC, CNTR, IL-11, and IL-12 belong to this group as well. In contrast, the ligands of the short-chain group are 105 to 145 amino acids long, have shorter helices (about 15 residues), and a large AD/BC packing angle (about 35°), as seen from the structure of GM- and M-CSF, IL-2, IL-4, and IL-5. Also IL-3, IL-7, IL-9, IL-13, and CSF are expected to show similar structural topology. Most of the ligands are monomeric, with the exceptions of the disulfide-linked dimers of M-CSF and IL-5 (for a review see Kossiskoff & de Vos, 1998; Nicola & Hilton, 1998).

The overall structure of IL-4 is highly compact and globular with a predominantly hydrophobic core. The helices range in length from 14 to 25 residues. They are connected by one short and two long segments to form a left handed bundle topology (Figure 1.3). These connecting segments include residues 19-40 (loop AB), 59-69 (loop BC), and 95-108 (loop CD). Residues 27-31 and 105-108 within the two long connections form a two-stranded anti-parallel β -sheet (Walter, et al., 1992).

Human recombinant IL-4 contains three disulfide bonds and no free cysteine residues. Cys³ and Cys¹²⁷ form a disulfide bond that links the N- and C-termini of the molecule. Cys²⁴ is located at the C terminal end of helix A and forms a disulfide bond with Cys⁶⁵, which is in the BC loop. Cys⁴⁶ is in the middle of helix B and forms a disulfide bond with Cys⁹⁹ located in the CD loop. The three disulfide bonds link the polypeptide chain at the three most spatially parts of the molecule (Walter et al., 1992). Exchange of the cysteine residues in human IL-4 with threonine residues has revealed that the disulfide bridge formed by Cys⁴⁶–Cys⁹⁹ is structural and functional essential, whereas the other two disulfide bridges (Cys³–Cys¹²⁷ and Cys²⁴–Cys⁶⁵) are less important (Kruse et al., 1991). Human IL-4 contains two potential sites for N-linked glycosylation at positions 38-40 and 105-107.

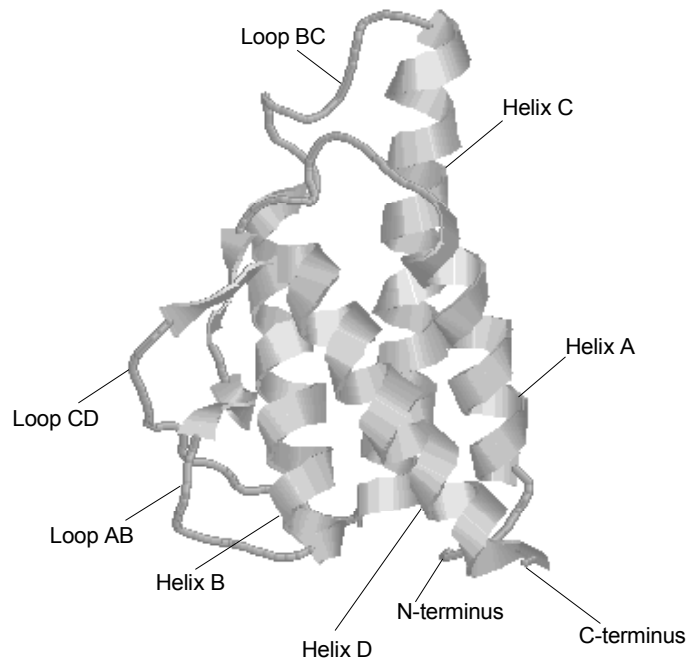


Figure 1.3: Ribbon model of the IL-4 molecule.

The ability of cytokines to influence the course of cell growth and differentiation uniquely depends on their recognition and binding by specific receptors. These are cell surface molecules that transduce the binding of messenger cytokines into cytoplasmic signals and trigger developmental processes within the cell (Nicola & Hilton, 1998).

IL-4 receptors (IL-4R) are present in haematopoietic, endothelial, epithelial, muscle, fibroblast, hepatocyte and brain tissues. Two types of IL-4R have been established, so far (Table 1.2). The type I IL-4R is constituted by the association of a high-affinity ($K_d \sim 100$ pM) IL-4R α -chain, (IL-4R α) and the IL-2R γ -chain, known as IL-2R γ or γ_c (Russell et al., 1993). This kind of receptor is especially found on T and B lymphocytes, and monocytes. The type II IL-4R, which is expressed on non-haematopoietic cells, is composed of the IL-4R α and the low-affinity binding chain for IL-13 termed IL-13R α 1 (Obiri et al., 1995). The type II receptor is used by both IL-4 and IL-13, whereas the type I is used only by IL-4 (Murata et al., 1998; Jensen, 2000).

Table 1.2: Comparison of IL-4R type I and II. Data from Jensen, 2000 is used.

	Chain composition	Type of cells	Binding to IL-4	Binding to IL-13
IL-4R type I	IL-4R α , γ_c	T and B lymphocytes, monocytes	high affinity	no binding
IL-4R type II	IL-4R α , IL-13R α 1	Cos-7, A431, Colo201 cells	competition with IL-13	high affinity; competition with IL-4

Cytokine receptors are type I membrane proteins, where extracellular and intracellular domains may operate rather independent from each other. Transmembrane signaling is achieved by dimerization or oligomerization of receptor subunits. For IL-4, binding is a strictly sequential process (Figure 1.4). The ligand is first bound with high affinity by the ectodomain of IL-4R α , and then this 1:1 complex can associate the γ_c creating in this way an active dimer. A cellular signal is generated because the joined intracellular domains can recruit signaling molecules from the cytoplasm (Duschl & Sebald, 1996).

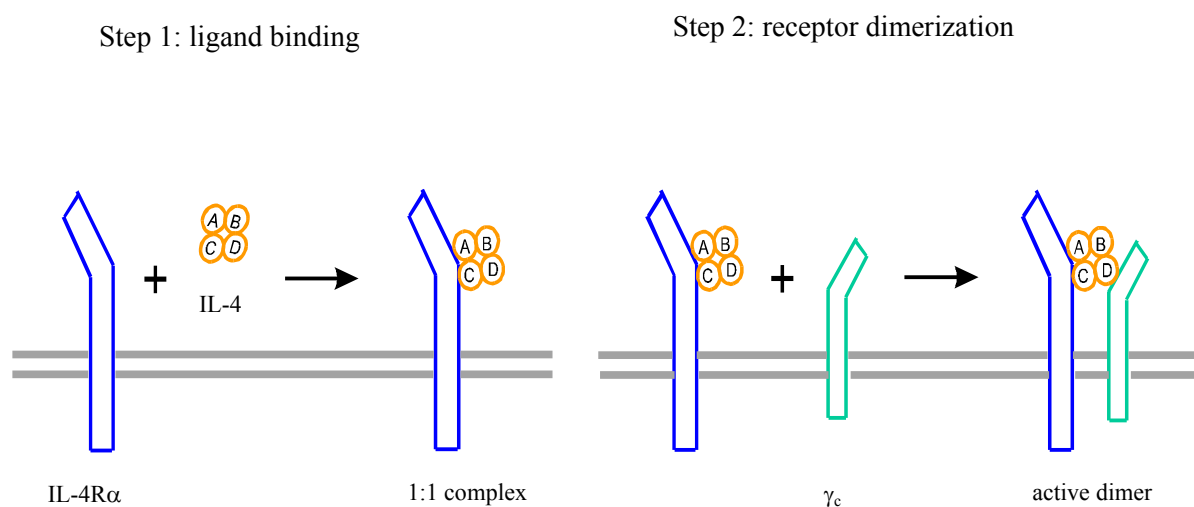


Figure 1.4: A two step mechanism of receptor activation by IL-4 (Duschl & Sebald, 1996).

Based on *in vitro* and *in vivo* binding studies, two binding sites have been described in the IL-4 molecule. Site 1 binds to IL-4R α and is marked by Glu9 in helix A and Arg88 in helix C. Site 2, which is important for the IL-4-dependent association between IL-4R α and γ_c , is located at the end of helix D, including particularly Arg121, Tyr124, and Ser125. (Kruse et al., 1993). The

mechanism of sequential receptor dimerization and the established two binding sites have been exploited for design of antagonistic variants of IL-4. Such mutants cannot recruit the γ_c into the receptor complex, since the site 2 has been destroyed, but they bind to IL-4R α with high affinity and in this way block the signaling pathways (Kruse et al., 1992).

Ligand induced dimerization of cytokine receptors results in the activation of tyrosine kinases that phosphorylate cellular substrates and initiate signaling cascades (Miyajima et al., 1992). Neither the IL-4R α nor the γ_c has endogenous kinase activity and therefore the IL-4R requires receptor-associated kinases for the initiation of signal transduction. The Janus-family (Jak) tyrosine kinases are critical in the initiation of signaling through the IL-4R system. Jak1 has been proposed to associate with IL-4R α , while Jak3 associates with γ_c (Miyazaki et al., 1994). IL-4 stimulation results in tyrosine phosphorylation of Jak1 and Jak3 (Figure 1.5). Activation of IL-4R-associated kinases leads to tyrosine phosphorylation of the IL-4R α chain itself, a process that occurs rapidly after IL-4R engagement (Smerz-Bertling & Duschl, 1995). The cytoplasmic domain of human IL-4R α contains six conserved tyrosine residues, which are potential sites of phosphorylation and subsequent interaction with downstream signaling proteins through Src-homology 2 (SH2) or phosphotyrosine-binding (PTB) domains within these molecules. The cytoplasmic region of IL-4R α chain appears to have three functionally distinct domains, one that acts as an interaction site for Jaks, one required for activation of proliferative pathways (containing Tyr497), and a third involved in the activation of pathways leading to induction of gene expression (Tyr575, Tyr603, Tyr631).

Analysis of IL-4R α deletion mutants have indicated that the region between residues 557 and 657 of the human IL-4R α is critical for the induction of signaling pathways leading to expression of IL-4-responsive genes (Wang et al., 1996). The three conserved tyrosine residues within this region (Tyr575, Tyr603, Tyr631) are potential sites of phosphorylation and subsequent association of SH2-containing proteins. As a direct connection between the cytokine receptor and the transcription apparatus act molecules termed signal transducers and activators of transcription, or STATs. Experimentally it has been shown that Jak activation is required for STAT activation (Velazquez et al., 1992). Thus, the STAT activation pathway is often referred to as the Jak-STAT pathway. STAT6 is the primary STAT activated in response to IL-4 stimulation. IL-4 engagement results in the activation of Jak1 and Jak3, and phosphorylation of specific tyrosine residues in the receptor cytoplasmic region. STAT6 then binds to the phosphorylated receptor through a highly conserved SH2 domain, enabling the activated kinases to phosphorylate STAT6 at a C-terminal tyrosine residue. The conserved Tyr575, Tyr603, Tyr631 have been proposed to be docking sites for the SH2 domains of STAT6 (Figure 1.5).

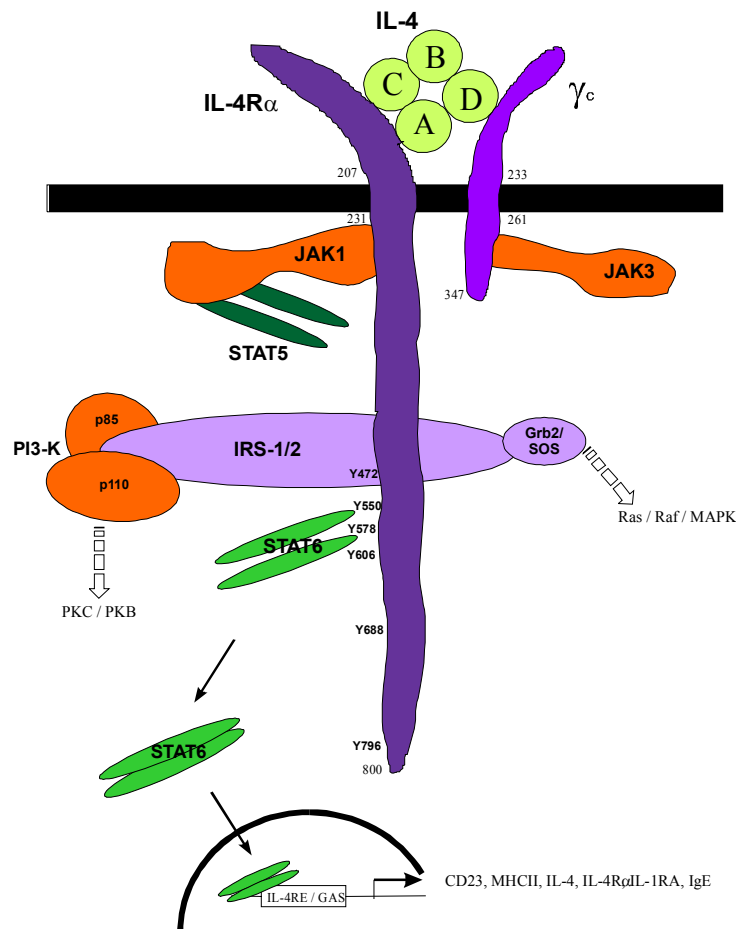


Figure 1.5: Signal transduction through the IL-4R complex. A, B, C, and D, IL-4 helices; IL-4RE, IL-4 responsive element; IL-1RA, IL-1R antagonist; GAS, IFN γ activated sequence.

Once phosphorylated, the STAT6 molecule disengages from the receptor and forms homodimers through interaction of its SH2 domain with the C-terminal phosphotyrosine residue of a second STAT6 molecule. The dimerized STAT6 complexes translocate to the nucleus where they bind to specific DNA motifs in the promoter of responsive genes. The DNA motifs bound by different STATs bear remarkable similarity to each other and reflect a dyad symmetry. STAT6 appears to bind in particular to the sequence TTC-N₄-GAA (Leonard & O'Shea, 1998). The exact mechanism by which STATs activate transcription is still being determined. Activation of gene transcription by STAT6 may require co-operative interaction with additional transcription factors (Schaefer et al., 1995; Look et al., 1995), or phosphorylation by kinases activated in the Ras/MAP kinase cascade (David et al., 1995). Alternatively spliced forms of STAT6 have

deletions in the N-terminal (STAT6b) or SH2 (STAT6c) regions (Patel et al., 1998) and may play a role in STAT6 regulation.

Stimulation with IL-4 or IL-13 induces tyrosine phosphorylation of a 170 kDa protein designated insulin receptor substrate-2 (IRS-2), due to its high similarity to IRS-1 (Turner et al., 1991; Miossec, 1993). The IRS-1/2 molecules link IL-4R to signaling pathways involved in cellular proliferation (Sun et al., 1995). It has been shown that IRS-2 becomes phosphorylated as a result of interaction with a phosphorylated motif of the IL-4R α including Tyr497, presumably through the action of receptor-associated kinases (Wang et al., 1996). Among the molecules that interact with the phosphorylated IRS-1/2 are the regulatory subunit of phosphoinositide-3-kinase (PI-3-K) and the adapter molecule, Grb-2 (Figure 1.5). These interactions lead to the activation of the PI-3-K and Ras/MAPK signaling pathways, respectively. The interaction between the regulatory subunit of PI-3-K and IRS-1/2 is followed by activation of the catalytic subunit of PI-3-K. Once activated, the catalytic subunit is capable of phosphorylating membrane lipids as well as Ser/Thr residues of proteins (Dh et al., 1994). The lipid kinase activity mediates phosphorylation of inositol in the cellular membrane (Toker et al., 1997). Since phosphoinositides have been implicated in the activation of a number of downstream kinases that play a key role in cell survival (Franke et al., 1997), it is hypothesized that activation of the PI-3-K pathway by IL-4 may prevent apoptosis in haematopoietic cells. Although the importance of the Ser/Thr kinase activity has not yet been fully defined, it has been suggested that this pathway may result in a negative feedback loop, which contributes to the regulation of the IRS-1/2 signaling pathway. IL-4 activation of Ras/MAPK is not consistently observed. In particular, this activation critically depends on cell type and more specifically on the variety of signaling molecules expressed in these cells. (Welham et al., 1995; Zamorano et al., 1998)

The signaling pathways that are activated by IL-4R engagement, such as the Jak-STAT and IRS1/2 pathways, mirror those activated by a number of other cytokines. Nevertheless, the activation of these pathways results in a unique pattern of cellular responses to IL-4. In the case of IL-4, specificity is in part achieved through the activation of STAT6, an event that, among class I cytokine receptors, has been demonstrated to occur only through engagement of IL-4R α . Specific cellular responses to IL-4 may also result from the unique character of the IL-4R (for a review, see Nelms et al., 1999).

cDNA encoding the human high-affinity IL-4R α have been obtained (Idzerda et al., 1990). The full-length cDNA contains an open reading frame encoding a 825 amino acids protein, which includes a signal sequence of 25 amino acids. The mature receptor chain is a glycoprotein with molecular weight of 140 kDa, which displays a 207-amino-acid extracellular domain, a transmembrane domain of 24 amino acids, and a 569-amino-acid cytoplasmic domain. It contains

six potential N-glycosylation sites. Furthermore, an alternatively spliced form of IL-4R α has been identified in mouse serum. It encodes a soluble product (sIL-4R) which binds IL-4 with an affinity comparable with that determined for the cell surface receptor chain (Fernandez-Botran & Vitetta, 1990). A role of a transport protein that prevents enzymatic degradation of IL-4, has been suggested for sIL-4R (Fernandez-Botran & Vitetta, 1991).

The γ_c , first identified as a component of IL-2R, has been found to be shared as a common subunit among receptors for IL-2, IL-4, IL-7, IL-9 and IL-15. Therefore, it is now called the common γ_c . Neither IL-4 nor any other cytokine up to now could be demonstrated to bind directly to a solitary γ_c in whole cells (Sugamura et al., 1995). Molecular binding studies have indicated that the γ_c recognizes a complex of IL-4 and IL-4R α and binds to it exhibiting a high dissociation constant $K_d = 3 \mu\text{M}$ (Letzelter et al., 1998). Although γ_c does not contribute to the affinity of the IL-4R complex for IL-4, it is essential for formation of the functional IL-4R and activation of signaling pathways by IL-4 (Russel et al., 1993). Human cDNA clones encoding the 64 kDa-protein of the common γ_c have been isolated (Takeshita et al., 1992). The mature form of γ_c consists of 347 amino acids, including an extracellular domain of 232 amino acids, a transmembrane domain of 29 amino acids, and an 86-amino-acid cytoplasmic domain that contains two SH2 regions. The human γ_c gene has been mapped on the same chromosomal locus (Xq13) as the putative gene responsible for the human X-linked severe combined immunodeficiency (XSCID) characterized by a complete or profound T cell defect. XSCID is now understood to be caused by mutations of γ_c (Sugamura et al., 1996).

The human IL-13R α 1 cDNA encodes for an open reading frame of 427 amino acids. The signal sequence is represented by 20 amino acids and the mature receptor chain is constituted by an extracellular domain of 322 amino acids, a transmembrane domain of 24 amino acids, and a 60-amino acid cytoplasmic domain. The IL-13R α 1 binds IL-13 with a weak affinity ($K_d = 2\text{-}10 \text{ nM}$), but its co-expression with the IL-4R α markedly increases the affinity of the interaction ($K_d = 400 \text{ pM}$) (Aman et al., 1996). However, in the interaction between IL-13 and IL-4R type II, IL-13R α 1 is the specificity chain and such an interaction occurs only when this chain is present. Thus, IL-4R α has a high-affinity epitope for IL-4 and a low-affinity epitope for IL-13. The epitopes for the two ligands overlap, since both IL-4- and IL-13-dependent responses can be inhibited by antagonistic IL-4 variants blocking the IL-4R α chain (Tony et al., 1994; Tomkinson et al., 2001). All three chains, which are components of the IL-4R/IL-13R system, belong to the class 1 of the cytokine receptor superfamily. The structural basis for the classification of the cytokine receptors in one superfamily is a conserved cytokine receptor homology (CRH) region within their extracellular portion. This CRH contains the ligand-binding determinants of the receptor. As first

proposed by Bazan (1990), the 200 to 250-amino acids long CRH region consists of two domains connected by a short linker. Both domains can be classified as fibronectin type III (FNIII) modules based on their overall fold and topology. Each domain consists of a β sandwich containing seven β strands, sequentially labeled A, B, C, C', E, F and G following the accepted FNIII convention (Leahy et al., 1992). The CHR regions of receptors of class 1 of the superfamily have four strictly conserved cysteine residues in their N-terminal domain and a strongly conserved Trp-Ser-X-Trp-Ser sequence, the so-called "WSXWS motif", near the C-terminus of the second domain (X being any residue).

The crystal structure of the 1:1 complex between human IL-4 and IL-4BP revealed that IL-4BP exhibits all features characterizing the class I of the cytokine receptor superfamily (Hage et al., 1999). It has an overall L shape (Figure 1.6) and is organized in two covalently linked domains, D1 (residues 1-91) and D2 (residues 97-197). The antiparallel β sheets are arranged in three-strand (A, B, E) and four-strand (G, F, C, C') β -pleated sheets that are twisted against each other by $\sim 40^\circ$. Domain D1 belongs to the h-type topological subclass of the immunoglobulin fold where strand C' interacts first with strand C, and then its direct continuation (designated D) switches to interact with strand E. It contains an additional single helical turn in BC loop and six cysteine residues that are engaged in three disulfide bridges as follows: Cys⁹-Cys¹⁹, Cys⁴⁹-Cys⁶¹, and Cys²⁹-Cys⁵⁹. The first two are conserved among class I CHR's (Bazan, 1990), while the third is unique to IL-4BP. D2 domain also shows FN III topology with two additional short helices and no disulfide bridges.

The quaternary structure of the complex is assembled by IL-4BP binding to the helix AC face of IL-4 and is characterized by an almost perpendicular orientation of the L-shaped IL-4BP to the helical axes of αC and αA of IL-4 (Figure 1.7). Loops of IL-4BP that interact with IL-4 are almost co-linear with the axes of the IL-4 helices and are oriented in a stack-like fashion. They comprise four different levels, namely loop L2 from IL-4BP interacting with helix B of IL-4, loops L3 and L1 interacting with αC , and loops L5 and L6 interacting with αA . Loop L4 connects domains D1 and D2 and has no interaction with IL-4.

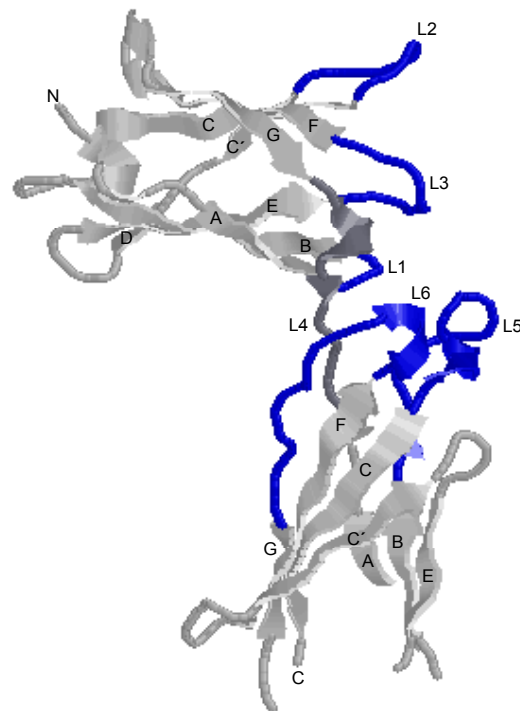


Figure 1.6: A ribbon model of IL-4BP. Loops which make contacts to IL-4 are showed in blue. In the dark gray is loop L2 connecting D1 and D2.

An important feature revealed by the complex is the polar character of the interacting epitopes, which are highly discontinuous and comprise multiple sequence segments. Contact residues on IL-4 are distributed over three helices and comprise mainly polar and charged residues. The complementary receptor epitope is assembled from residues of five loops and has a midline of hydrophobic side chains. The binding epitope reveals a mosaic-like assembly consisting of three discrete clusters of *trans*-interacting residues. Two of them exhibit conspicuous amphipathic structure with an outer mantle of hydrophobic side chain moieties and an inner core of polar groups. The third cluster has a completely different design and is dominated by electrostatic interactions.

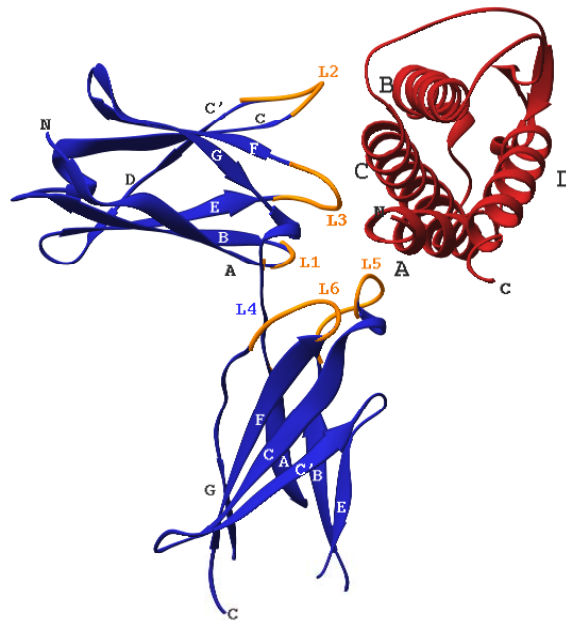


Figure 1.7: A ribbon view of the structure of the IL-4/IL-4BP complex (IL-4BP, blue/yellow; IL-4, red). The five IL-4BP loops that interact with IL-4 are highlighted in yellow. The loop depicted in blue connects D1-D2 and has no interactions with IL-4 (Hage et al., 1999).

A mosaic-binding pattern has been independently confirmed by a systematic mutational and kinetic analysis of IL-4 contacting residues (Wang et al., 1997). This study has shown that charged and polar determinants located on helices A and C predominate in the high-affinity binding epitope of human IL-4. The binding epitope has been established as a set of side chains determining the dissociation rate constant (k_{off}) and a partially overlapping set determining the association rate constant (k_{on}) of IL-4/IL-4BP complex. Based on these results, the k_{off} epitope is represented by two juxtaposed main determinants (Glu9 and Arg88) surrounded by a few side chains of lower importance (Ile5, Thr13, Arg53, Asn89, and Trp91). The k_{on} epitope has been postulated as formed by five positively charged residues on helix C (Lys77, Arg81, Lys84, Arg85, and Arg88) and two neighboring residues on helix A (Glu9 and Thr13). Thus, both the data from the crystal structure and from the mutation analysis have revealed novel features, which are different from these known for the hGH, and are unique for the IL-4 functional epitope. The formation of complexes between proteins and the specific interactions between a ligand and its receptor in particular, are critical events in many biological processes. Structural analysis can

reveal the interactions that contribute to protein-protein recognition in atomic details (Jones & Thornton, 1996). However, it alone cannot show how these interactions contribute to the overall affinity and specificity. Ideally, the high-resolution structure of a complex would be used to guide a comprehensive functional survey of residues presented at the interface using site-directed mutagenesis, to allow their individual contribution to be assessed. Since the effects of alanine and glutamine substitution in IL-4 variants have been examined (Wang et al., 1997), the present study concentrates on functional mapping of IL-4BP binding surface. To analyze the contribution of individual side chains to overall binding energy in the interaction between IL-4 and IL-4BP, residues of the receptor interface implicated in ligand binding were subjected to systematic alanine substitution (alanine scanning). The IL-4BP variants were expressed in a eukaryotic expression system that allowed their glycosylation. The binding kinetics was measured by the means of the BIAcore technology. For this, the IL-4BP variants were immobilized at the biosensor matrix. Variants, which demonstrated large changes of the kinetic constants comparing to the wild-type interaction, were additionally mutated to a more conservative residue. That gave the possibility to assess whether the loss of binding affinity was due to gross conformational changes caused during the alanine substitution. In addition, energetic coupling between two residues was analyzed using variants in which two different mutations were introduced simultaneously. The effects on binding that was produced by the double mutants were compared to those observed when the corresponding residues were mutated singly.

The nature of the interactions between cytokines and their receptors is of fundamental importance for detailed understanding of the immune response. While these receptors are clearly specific to their ligands, some of them share receptor functions between more than one different ligand. Understanding of the similarities and differences between these related proteins, and the molecular mechanisms involved in their binding, will provide insights into more general protein-protein interactions. Moreover, knowledge about the structural and functional binding epitope of both IL-4 and IL-4BP, provides the basis for developing molecules with antagonistic properties to IL-4 and design of highly effective anti-allergic drugs.

2. Materials and Methods

2.1 Abbreviations

γ_c	“common γ chain”
Ab	antibody
AcNPV	<i>Autographa californica</i> nuclear polyhedrosis virus
Amp	ampicillin
APC	antigen presenting cell
APS	ammonium persulfate
BEVS	Baculovirus expression vector system
bp	base pair
BPB	bromphenol blue
BSA	bovine serum albumin
CD	cluster of differentiation
cDNA	complementary deoxyribonucleic acid
CNTF	ciliary neurotrophic factor
CRH	cytokine receptor homology
Da	Dalton
$\Delta\Delta G$	change of binding free energy
$\Delta\Delta G_{\text{add}}$	the $\Delta\Delta G$ value for a double mutant predicted by adding the $\Delta\Delta G$ values for the corresponding individual mutants
ddNTPs	2',3'-dideoxyribonucleoside triphosphates
DMSO	dimethylsulfoxide
DNA	deoxyribonucleic acid
dNTPs	deoxyribonucleoside triphosphates
dsDNA	double-stranded deoxyribonucleic acid
DTT	dithiothreitol
<i>E.coli</i>	<i>Escherichia coli</i>
EBP	erythropoietin binding protein
EDTA	ethylenediaminetetraacetic acid
EPO/EPOR	erythropoietin/ erythropoietin receptor
eq., equilib.	equilibrium
EtBr	ethidium bromide
EtOH	ethanol

FCS	fetal calf serum
FNIII	fibronectin type III
GCSF	granulocyte colony-stimulating factor
GCSF-R	granulocyte colony-stimulating factor receptor
GH	growth hormone
GM-CSF	granulocyte-macrophage colony-stimulating factor
GuHCl	guanidine hydrochloride
hGH	human growth hormone
hGHbp	human growth hormone-binding protein
HMS	high molecular standard
HPLC	high pressure liquid chromatography
Ig	immunoglobulin
IL-13R α 1	interleukin-13 receptor α 1
IL-4R α	interleukin-4 receptor α chain
IL-x	interleukin-x
IL-xBP	interleukin-x binding protein
IL-xR	interleukin-x receptor
INF	interferon
IRS-1/2	insulin receptor substrate-1/2
Jak	Janus kinase
kbp	kilo base pair
K _d	dissociation equilibrium constant
kin.	kinetic data
k _{off}	dissociation rate constant
k _{on}	association rate constant
LB	Luria Broth
LIF	leukaemia inhibitory factor
LMS	low molecular standard
ln	logarithm to the basis of “e”
m	mouse
max.	maximal
MCS	multiple cloning site
M-CSF	macrophage colony-stimulating factor
MHC	major histocompatibility complex
min	minute(s)

MOI	multiplicity of infection (plaque-forming units/cell number)
mRNA	messenger ribonucleic acid
MS	molecular standard
n	number of measurements
NK	natural killer (cell)
NMR	nuclear magnetic resonance
ORF	Open Reading Frame
PAGE	polyacrylamide gel electrophoresis
PBS	phosphate buffered saline
PCR	polymerase chain reaction
PEG	polyethylene glycol
pfu	plaque forming unit(s) = virus
pg130	glycoprotein 130 (kDa)
PI-3-K	phosphoinositide-3-kinase
PTB	phosphotyrosine-binding
rel.	relative value
RNA	ribonucleic acid
RP-HPLC	reverse phase high pressure liquid chromatography
RT	room temperature
RU	resonance units
s	soluble
SDS	sodium dodecyl sulfate
SDS-PAGE	sodium dodecyl sulfate polyacrylamide gel electrophoresis
SE	standard error
sec	second(s)
<i>Sf</i>	<i>Spodoptera frugiperda</i>
SH	src homology (domain)
SPR	surface plasmon resonance
ssDNA	single-stranded deoxyribonucleic acid
STAT	signal transducer and activator of transcription
TB	Terrific Broth
TCA	trichloroacetic acid
TCR	T cell receptor
TEMED	N,N,N',N'-tetramethylethylenediamine
TGR	transforming growth factor

T _H	T helper (cell)
TNF	tumor necrosis factor
TRIS	tris(-hydroxymethyl)-aminomethane
U	unit
UV	ultraviolet
v/v	volume: volume ratio
Vol	volume
wt	wildtype
XSCID	x-linked severe combined immunodeficiency

2.2 Chemicals and Enzymes

All chemicals and enzymes were purchased from the following companies: Amersham, Biorad, Boehringer Mannheim, Fermentas, Fluka, Gibco-BRL, Merck, Pharmacia, Roth, Serva, Sigma. All solutions used in the experiments were made with deionized water (Millipore-Q-System).

2.3 Bacterial Strains

The following genotypes *E. coli* were used:

E. coli JM103 *recA*⁻ (McCarthy et al., 1985)
Genotype: *endA*, *D* (*lac-pro*), *thi-1*, *strA*, *sbcB15*, *hsdR4*, *supE*, *F'**traD36*, *proAB*⁺, *lacI*^q, *zDM15*, *lambda*⁻/*F*⁻

E. coli JM109 (Yanisch-Perron et al., 1985)
Genotype: *recA1*, *endA1*, *thi*, *gyrA96*, *hsdR17*, *supE44*, *relA1*, *D* (*lac-proAB*), *F'**traD36*, *proAB*⁺, *lacI*^q

2.4 Cell Lines

Sf9 cell line - a cell line, which was originally established from ovarian tissues of *Spodoptera frugiperda* larvae (Vaughn et al., 1977). Sf9 cells may be grown in a monolayer or in a suspension.

2.5 Antibodies

For detection of Western Blot the following antibodies were used:

X14/38: mAb from mouse against the extracellular domain of IL-4R α (Reusch et al., 1994)
anti-mouse IgG-POD: pAb from goat, POD-coupled (Sigma)

2.6 Vectors and Oligonucleotides

2.6.1 Expression Vector for E.coli

(McCarthy et al., 1985)

The bacterial vector R^{TS}pRC109 (3988 bp) was used for expression of recombinant protein under the control of the right λ -phage promoter. It contains the CI857 repressor gene coding temperature-induced protein translation.

2.6.2 Baculovirus Transfer Vector pAcGP67-B

(Baixeras, E. et al., 1990)

The Baculovirus transfer vector pAcGP67-B (Pharming) contains gp67 signal sequence upstream of a multiple cloning site. After co-transfection with Baculovirus DNA into Sf9 cells, the cloned gene is expressed as a gp67 signal peptide fusion protein under the control of the strong Baculovirus polyhedrin promoter.

2.6.3 Oligonucleotides

The oligonucleotides, which were used for cloning and sequencing in the work presented here, are presented in Table 2.1.

Table 2.1: Sequence and function of the used oligonucleotides. The mutated codons are underlined.

Name	Sequence	Function
5'Y13A	5'CGTCTCCGAC <u>GCC</u> ATGAGCATC 3'	PCR induced mutagenesis/ IL-4R α in AA at position 13
3'Y13A	5'GATGCTCAT <u>GGC</u> GTCGGAGACG 3'	PCR induced mutagenesis/ IL-4R α in AA at position 13
5'Y13F	5'CGTCTCCGACT <u>T</u> CATGAGCATC 3'	PCR induced mutagenesis/ IL-4R α in AA at position 13
3'Y13F	5'GATGCTCAT <u>GAA</u> GTCGGAGACG 3'	PCR induced mutagenesis/ IL-4R α in AA at position 13
5'L39A	5'CCTGTTGTACCAG <u>GCG</u> GTTTTTCTGC 3'	PCR induced mutagenesis/ IL-4R α in AA at position 39
3'L39A	5'GCAGAAAAAC <u>CGC</u> CTGGTACAACAGG 3'	PCR induced mutagenesis/ IL-4R α in AA at position 39
5'F41A	5'CCAGCTGGTT <u>GCT</u> CGTCTCTCC 3'	PCR induced mutagenesis/ IL-4R α in AA at position 41
3'F41A	5'GGAGAGCAG <u>AGC</u> AACCAGCTGG 3'	PCR induced mutagenesis/ IL-4R α in AA at position 41
5'L42A	5'GCTGGTTTTT <u>GCG</u> CTCTCCGAAGC 3'	PCR induced mutagenesis/ IL-4R α in AA at position 42
3'L42A	5'GCTTCGGAGAG <u>CGC</u> AAAAACCAGC 3'	PCR induced mutagenesis/ IL-4R α in AA at position 42
5'L43A	5'CTGGTTTTTCT <u>GGC</u> CTCCGAAGCC 3'	PCR induced mutagenesis/ IL-4R α in AA at position 43
3'L43A	5'GGCTTCGGAG <u>GCC</u> CAGAAAAACCAG 3'	PCR induced mutagenesis/ IL-4R α in AA at position 43
WYH46	5'GCTCATGGAT <u>GCC</u> GTGGTCAGTGC 3'	PCR induced mutagenesis/ IL-4R α in AA at position 67
WYH47	5'GCACTGACCAC <u>GGC</u> ATCCATGAGC 3'	PCR induced mutagenesis/ IL-4R α in AA at position 67
5'V69A	5'GCTCATGGATGACGT <u>GCC</u> CAGTGC 3'	PCR induced mutagenesis/ IL-4R α in AA at position 69
3'V69A	5'GCACT <u>GGC</u> CACGTCATCCATGAGC 3'	PCR induced mutagenesis/ IL-4R α in AA at position 69
C4D72A 5	5'GTCAGTGCG <u>GCT</u> AACTATAACA 3'	PCR induced mutagenesis/ IL-4R α in AA at position 72
C4D72A 3	5'TGTATAGTT <u>AGC</u> CGCACTGAC 3'	PCR induced mutagenesis/ IL-4R α in AA at position 72
5'D72N	5'CGTGGTCAGTGCG <u>AATA</u> ACTATACACTGG 3'	PCR induced mutagenesis/ IL-4R α in AA at position 72
3'D72N	5'CCAGTGTATAGTT <u>ATT</u> CGCACTGACCACG 3'	PCR induced mutagenesis/ IL-4R α in AA at position 72
C4K91A 5	5'GGCTCCTTC <u>GCG</u> CCCAGCGAG 3'	PCR induced mutagenesis/ IL-4R α in AA at position 91
C4K91A 3	5'CTCGCTGGG <u>GCG</u> GAAGGAGCC 3'	PCR induced mutagenesis/ IL-4R α in AA at position 91
5'K91D	5'CTCCTTC <u>GAT</u> CCCAGCGAG 3'	PCR induced mutagenesis/ IL-4R α in AA at position 91
3'K91D	5'CTCGCTGGG <u>ATC</u> GAAGGAG 3'	PCR induced mutagenesis/ IL-4R α in AA at position 91
WYH60	5'CTTCAAGCCC <u>GCC</u> GAGGCATGTG 3'	PCR induced mutagenesis/ IL-4R α in AA at position 93
WYH61	5'CATATGCTC <u>GCG</u> GGGCTTGAAG 3'	PCR induced mutagenesis/ IL-4R α in AA at position 93
WYH31	5'CCTGACAAT <u>GCC</u> CTGTATAATCATC 3'	PCR induced mutagenesis/ IL-4R α in AA at position 127

2. Materials and Methods

Name	Sequence	Function
WYH32	5'GATGATTATACAGGGCATTGTCAGG 3'	PCR induced mutagenesis/ IL-4R α in AA at position 127
5'Y127F	5'CCCCCTGACAATTTCTGTATAATC 3'	PCR induced mutagenesis/ IL-4R α in AA at position 127
3'Y127F	5'GATTATACAGGAAATTGTCAGGGGG 3'	PCR induced mutagenesis/ IL-4R α in AA at position 127
5'Y183A	5'GCTCAGGCCGCTTAACACCACCTG 3'	PCR induced mutagenesis/ IL-4R α in AA at position 183
3'Y183A	5'CAGGTGGTGTTAGCGGCCTGAGC 3'	PCR induced mutagenesis/ IL-4R α in AA at position 183
5'Y183F	5'GCTCAGGCCTTTAACACCACCTGG 3'	PCR induced mutagenesis/ IL-4R α in AA at position 183
3'Y183F	5'CCAGGTGGTGTAAAGCCTGAGC 3'	PCR induced mutagenesis/ IL-4R α in AA at position 183
WYH37	5'CGCGGATCCATGAAGGTCTTGCAGGAGC 3'	an external primer, a BamHI restriction site, IL-4R α mutagenesis
WYH38	5'GCATAACCGATATATTCGGTCGCTGA 3'	an external wild type primer for amplifying IL-4R α
MF37	5'GGCGCATTCTGCCTTTGCG 3'	a sequencing primer- pAcGP67B
WYH39	5'CAGGAAAGGATCAGATCTGCAG 3'	a sequencing primer- pAcGP67B
5'R53A/IL4	5'CGACTGTCTTAGCGCAGTTCTACAGC 3'	PCR induced mutagenesis/ IL- 4 in AA at position 53
3'R53A/IL4	5'GCTGTAGAAGTGCCTAAGACAGTCG 3'	PCR induced mutagenesis/ IL-4 in AA at position 53
5'Y56A/IL4	5'TTAAGGCAGTTCGCGAGCCACCATGAGAAG GACA 3'	a cassette for mutagenesis in IL4 - AA at position 56
3'Y56A/IL4	5'CGCGTGTCTTCTCATGGTGGCTCGCGAACT GCC 3'	a cassette for mutagenesis in IL4 - AA at position 56
MF8	5'CGTTAAATCTATCACCGCAAG 3'	an external wild-type primer for amplifying IL-4
MF14	5'GTCATCACCGAAACGCGCGAG 3'	an external wild-type primer for amplifying IL-4
PWU22-5'	5'CAGGACTACTACGTTTTAACTGA 3'	a sequencing primer- R ^{TS} pRC109
PWU22-3'	5'CAGGATCGGTCGCTGAGGCTTGCA 3'	a sequencing primer- R ^{TS} pRC109

2.7 Microbiological Methods

2.7.1 Sterilization

Experiments dealing with bacteria were performed at sterilized conditions. Glassware and other experimental materials were sterilized at 180°C for 6 hours in a hot-air-cabinet (Heraeus, ST 5060). Buffers, media and plastic containers were autoclaved (Sterico Vapoclav Dampfsterilisator) at 121°C and 1.1 bar for 20 min. Solutions of temperature-unstable substances were sterilized by filtering through Millipore-Filter (DynaGard 0.22 μ m).

2.7.2 Culture Media

LB-medium: (Sambrook et al., 1989)	10g/l Bacto-Trypton, 5g/l Bacto-Yeast Extract, 10g/l NaCl pH7.5 with 0.1N NaOH adjusted
TB-medium: (Sambrook et al., 1989)	13.3g/l Bacto-Trypton, 26.6g/l Bacto-Yeast Extract, 4.4ml/l glycerin before use 10% sterilized 10x Phosphate buffer was added
10 x Phosphate buffer: (Sambrook et al., 1989)	0.17M KH ₂ PO ₄ , 0.72M K ₂ HPO ₄
5 x ENB-medium: (Sambrook et al., 1985)	40g/l Nutrient Broth, 25g/l Bacto-Peptone, 7.5g/l KH ₂ PO ₄ , 17.5g/l NaH ₂ PO ₄ , 25g/l NaCl
ENB-amp-plates	15 g agarose in 800 ml H ₂ O was autoclaved. When the agarose solution was cooled to 50°C, 200 ml 5 x ENB-medium, 2.5 ml 2M glucose, 0.5 ml thiamin solution in H ₂ O (10mg/ml) and 50 mg ampicillin in 2ml 1M TrisHCl buffer (pH 8.0) were added. After mixing, the agarose solution was filled into plates, cooled at RT and kept at 4°C

Ampicillin solution, 50 mg/ml in 1M TrisHCl pH 8.0, must be freshly prepared and added to final concentration of 50 µg/ml for all kinds of media.

2.7.3 Culturing of Bacteria

Glycerin stock-culture was spread over an agar plate and incubated at 30°C or 37°C overnight. A colony was picked up and incubated in 2 ml of medium at 30°C or 37°C for a day. This culture was further used for making larger culture.

2.7.4 Electrocompetent E.coli

2.7.4.1 Preparation of electrocompetent bacterial cells

E.coli from an agar plate or frozen stock were cultivated in 2 ml of TB-medium with ampicillin at 37°C for 8 h. From this culture was started 200 ml of a new culture, which was incubated and shook (200 rpm, Cetromat-R) overnight under the same conditions.

The overnight culture was centrifuged at 3500 rpm (Beckmann J2-21, JA-10 rotor), 4°C for 10 min. and then washed with 200 ml cold solution of 10% glycerin/H₂O (v/v). The suspension was consecutively centrifuged in the same way and resuspended in 100 ml, 50 ml, 20 ml and 2 ml of cold 10% glycerol solution. The final suspension was aliquoted in chilled Eppendorf tubes (40µl) and frozen in liquid Nitrogen. The competent cells were stored at -70°C.

2.7.4.2 Electrotransformation of competent E.coli

The electrocompetent E.coli were placed on ice and thawed out. 10-20 ng of DNA (in TE-buffer) were added and the suspension was mixed and transferred to a chilled 0.2 cm electroporation cuvette. Immediately after the pulse was applied (Biorad Gene PulserTM: 250 V, 25 mF and 200 W), 500 µl of LB-medium were added and the cuvette was vigorously shaken. The suspension was incubated at 30°C or 37°C for 30 min. For selection the bacterial material was placed in 2 ENB-amp-plates, which were kept at 30°C or 37°C overnight.

2.7.5 Storage of Bacterial Cultures

10 µl bacterial suspension was spread over an agar plate and incubated at 30°C or 37°C overnight until colonies appeared. Such a plate can be kept 4 to 6 weeks at 4°C.

For long-term bacterial storage, a single bacterial colony was cultivated in 50 ml of LB-medium with ampicillin at 30°C or 37°C until the suspension reached OD₅₅₀ of 1.5 - 1.7 (LKB Novaspec). The following centrifugation was carried out at 3000 rpm for 10 min. The pellet was resuspended in 2 ml of LB-medium/amp and mixed with 2ml of sterilized glycerol (87%). This culture can be kept at -20°C several years.

2.8 Molecular Biological Methods**2.8.1 Determination of the Concentration of Nucleic Acids**

The concentration of nucleic acids was measured by spectrophotometry in the absorption spectrum range 240-320 nm. (Kontron Uvikon 930 Spectrophotometer). Considering an extinction value of 1, the relation between A_{260} and the concentration is as follows:

Nucleic acids	Concentration
dsDNA	50 $\mu\text{g/ml}$
ssDNA	33 $\mu\text{g/ml}$
Oligonucleotide	20 $\mu\text{g/ml}$

The concentration of DNA can be roughly estimated by using an agarose gel electrophoresis. For amounts less than 200 ng, the fluorescence of the ethidium bromide, incorporated in the DNA fragments is proportional to the concentration of DNA. The intensity of the examined bands was compared to this of DNA standards with known concentrations.

2.8.2 Phenol Extraction of DNA

phenol solution: saturated phenol, neutralized with 1/50 Vol. 2.5M Tris-HCl pH8.0

To the DNA containing fraction was added the phenol solution (1:1 Vol). After 5 min of shaking, the sample was treated with (1/2 Vol.) chloroform/isoamyl alcohol solution (24:1), again shaken for 2 min and finally centrifuged for 2 min at 14000 rpm. The aqueous phase was transferred to a new tube.

2.8.3 Ethanol Precipitation of DNA

DNA solutions were precipitated by adding 1/10 Vol. 3M NaOAc pH 8.0 and 2.5 Vol. EtOH. The sample was thoroughly vortexed, incubated for 30 min at -20°C and centrifuged (15 min, 14000 rpm). The pellet was washed with 70% EtOH and dried under vacuum. The pellet was dissolved in desired volume sterile dH_2O or TE buffer.

2.8.4 DNA Molecular Standards

The following DNA molecular standards were used:

HMS: phage λ DNA, digested by HindIII

LMS: pBr322 plasmid DNA, digested by AluI

Table 2.2: DNA molecular standards

HMS		LMS	
bp	%	bp	%
23130	47.7	1608	21.2
9416	19.4	1201	15.9
6682	13.4	999	13.2
4361	9.0	711	9.4
2322	4.8	567	7.5
2027	4.2	517	6.8
564	1.2	396	5.2
125	0.3	360	4.8
		1222/219/214	9.6
		132/120/112	4.8
		76/65/30/27	2.6

2.8.5 DNA Agarose Gel Electrophoresis

(Hermann et al., 1980)

running buffer: 40mM Tris-acetate pH 8.2, 20mM NaOAc, 1M EDTA pH 5.0

EtBr: 5 mg/ml

5 x stop buffer: 15% Ficoll, 50mM EDTA, 0.5%SDS, 0.05% XC, 0.05% BPB in running buffer

DNA fragments with different length require different concentrations of the agarose for separation by gel electrophoresis (Table 2.3).

Table 2.3: DNA agarose gel electrophoresis

Length of DNA fragments [kbp]	Agarose concentration in %
5 – 60	0.3
1 – 20	0.6
0.8 – 10	0.7
0.4 – 7	1.0
0.2 – 4	1.5
0.1 – 3	2.0

The agarose was dissolved in running buffer by heating in a microwave oven and kept at 65°C. After adding of 1/1000 Vol. EtBr (final concentration 5 µg/ml), the agarose was poured into a horizontal gel-plate. A comb was put in the agarose and it was cooled down until the gel was formed.

The examined DNA was mixed with ¼ Vol. of 5 x stop buffer and heated at 65°C for 5 min. The DNA samples and 100 ng DNA molecular standard were loaded in parallel starts of the gel. The electrophoresis was performed in the electric field of 3 V/cm. The sample was visualized under UV light due to the incorporation of EtBr in DNA. The length of the DNA fragments was estimated by comparison with the bands of the standard.

2.8.6 Purification of DNA by Agarose Gel Electrophoresis

DNA fragments were purified from agarose gels using Nukleotrap™ kit (Macherey-Nagel).

A preparative agarose gel was run and the DNA fragment of interest was cut under a UV light panel. 330-350 mg of agarose gel containing DNA were transferred in an Eppendorf tube, where 300 µl of buffer T1 were added for each 100 mg from agarose material. This suspension together with 20µl of the glass beads “Nucleotrap” was incubated at 55°C for 10 min and meanwhile vortexed a few times. The sample was centrifuged for 30 sec at 13000 rpm and the supernatant was removed. This step was followed by consecutively washing the pellet twice with 500 µl of T2 buffer and twice with T3 buffer. After the pellet dried on air, it was resuspended in 50 µl of TE buffer pH 8.0 and incubated for 10 min at RT. The suspension solution was centrifuged 1min. at 13000 rpm and the DNA containing supernatant was then transferred to a clean Eppendorf tube. 2 µl of the DNA solution were analyzed on an agarose gel.

2.8.7 Site-directed Mutagenesis by PCR

(Higuchi et al., 1990)

apparatus:	DNA Thermal Cycler 480, Perkin Elmer
10 mM dNTPs	
Pfu polymerase	
10 x Cloned Pfu buffer:	200mM Tris-HCl pH 8.0, 20mM MgSO ₄ , 100mM KCl, 100mM (NH) ₄ SO ₄ , 1% Triton X-100, 1mg/ml nuclease-free BSA

2. Materials and Methods

Most of the mutations were generated by using a two-step polymerase chain reaction. The first step was performed in two different reactions - reaction 1a and reaction 1b. In reaction 1a (Table 2.4) the 5'-primer carries the mutation of interest and the 3'-primer is external (Table 2.1). The 3'-primer, which was used in reaction 1b, was mutated and complementary to the 5'-primer in reaction 1a. The 5'-primer in reaction 1b was external.

Table 2.4: PCR - reaction 1a and reaction 1b

	Reaction 1a	Reaction 1b
template	50 ng	50 ng
mutant primer	50 pmol (5'-primer)	50 pmol (3'-primer)
external primer	50 pmol (3'-primer)	50 pmol (5'-primer)
dNTPs	10 nmol	10 nmol
10 x Pfu polymerase buffer	5 μ l	5 μ l
Pfu polymerase	2.5 U	2.5 U
H ₂ O	to 50 μ l	to 50 μ l

The synthesized products from reaction 1a and 1b were analyzed by an agarose gel and directly used as a template during the second step of the PCR generated mutagenesis. This recombinant PCR was performed with the two external primers, used in the first step: the 3'-primer from reaction 1a and the 5'-primer from reaction 1b (Table 2.5).

Table 2.5: Second step of the PCR generated mutagenesis

	Reaction 2
reaction product 1a	2 μ l
reaction product 1b	2 μ l
5'-primer (from reaction 1b)	50 pmol
3'-primer (from reaction 1a)	50 pmol
dNTPs	10 nmol
10 x Pfu polymerase buffer	5 μ l
Pfu polymerase	2.5 U
H ₂ O	to 50 μ l

All reactions were performed in safe-lock Eppendorf tubes with the following program:

denaturation:	95°C	5 min.
25 cycles:	95°C	1 min.
	55°C	1 min.
	72°C	2 min.
	72°C	7 min.

The product, synthesized during the second step of the PCR, contains the mutation of choice. After visualization on an agarose gel, it was precipitated with EtOH and dissolved in 20 μ l of H₂O.

2.8.8 Site-directed Mutagenesis Using DNA Cassettes

This method was used for generation of mutations in the cDNA of IL-4. The cassette is synthetic double-stranded DNA, which contains a mutation of interest. Its ends are designed as restriction endonuclease cutting sites. In this way, it is possible using a ligation reaction to insert the cassette between the same cutting sites represented in the cDNA of IL-4.

2.8.9 Digestion of DNA

All restriction reactions were performed in the presence of recommended 10 x reaction buffer. For analytical purposes were digested 100-500 ng DNA in reaction volume of 10 μ l, using 1-10 U restriction endonuclease. The reaction mix was incubated for 1 h at 37°C and then 2-4 μ l were examined by agarose gel electrophoresis.

The reaction volume of a preparative digestion is dependent on the amount of the used DNA, which should not exceed 1 μ g/ml. It is necessary to consider that the standard enzyme solutions normally contain 50% glycerol. Some restriction endonucleases work non-specifically in the presence of too high glycerol concentrations (“star activity”). Because of this, the glycerol content in the reaction volume should not be more than 10%. Every kind of DNA, independent on the number of restriction sites, was digested with 1-5 U of restriction endonuclease per μ g DNA. (1 enzyme unit (U) is defined as the amount of the restriction endonuclease, which is able to digest 1 μ g of DNA for 1 h.) The incubation was done - if it is not mentioned otherwise - for 2 h at 37°C. The restriction reaction was stopped by adding ¼ volume 5 x stop buffer (15% ficoll, 0.5 % SDS, 50mM EDTA, 0.5 % BPB, 0.5% XB in 5 x tris-acetate buffer). A small aliquot was examined on an agarose gel. The rest of the DNA was purified by agarose gel electrophoresis, before it was used for ligation reaction.

tubes were inverted again, the samples were incubated for 15 min on ice. This turbid solution was centrifuged for 15 min at 14000 rpm. The clear supernatant was transferred to a fresh Eppendorf tube, avoiding floating precipitate. After precipitation with an equal volume of isopropanol, the DNA containing pellet was washed with 70% EtOH and dried under vacuum. The pellet was dissolved in 20 μ l of dH₂O. An aliquot of 2-5 μ l was used for restriction analysis.

2.8.11.2 PEG precipitation procedure

(Tartof and Hobbs, 1987)

solution 1 (GTE buffer):	50mM glucose, 10mM EDTA, 25mM Tris-HCl pH 8.0
solution 2:	1% SDS, 0.2M NaOH
solution 3:	3M KOAc pH4.8 (60 ml 5M KOAc with 11.5 ml acetic acid and 28.5 ml H ₂ O)
RNase solution:	10 mg/ml RNase A (DNase free)
PEG solution:	13% PEG ₈₀₀₀ autoclaved

The following procedure was used for preparation of plasmid DNA for sequencing.

Aliquots (1.4 ml) of overnight cultures were transferred to Eppendorf tubes and centrifuged at 14000 rpm in a microcentrifuge (Eppendorf Centrifuge 5415C). The supernatant was removed by aspiration and the bacterial pellet was resuspended in 200 μ l of solution 1. Then 300 μ l of solution 2 were added. The content of the tube was mixed by inversion and incubated for 5 min on ice. After this, 300 μ l of solution 3 were added, the content was mixed by inversion of the tubes and the sample was incubated again for 5 min on ice. Centrifugation at 14000 rpm for 15 min followed. The supernatant was carefully transferred in a fresh tube, avoiding floating precipitates. Solution of RNase A was added to a final concentration of 25 μ g/ml and the tubes were incubated for 30 min at 37°C. DNA was extracted using 400 μ l phenol/Tris and 400 μ l chloroform/isoamylalcohol (24:1). After centrifugation for 1 min at 14000 rpm, the aqueous phase was transferred to a fresh Eppendorf tube. DNA was precipitated with equal volume of isopropanol and washed with 70% EtOH. The dried pellet was dissolved in 32 μ l of H₂O and after 8 μ l of 4M NaCl and 40 μ l of autoclaved PEG₈₀₀₀ solution were added, the sample was thoroughly vortexed and placed on ice for 20 min. The following centrifugation was performed at 4°C, 14000 rpm, for 15 min in a fixed-angle rotor centrifuge (Biofuge A, Heraeus). The supernatant was carefully removed and the pellet was rinsed with 70% EtOH and dried under

vacuum. The DNA containing pellet was dissolved in 20 μ l of dH₂O. The so prepared DNA can be used for restriction analysis as well as for sequencing. The plasmid DNA was stored at -20°C.

2.8.11.3 Preparation of plasmid DNA with LiCl

solution 1:	50mM glucose, 10mM EDTA, 25mM Tris-HCl pH 8.0, 5mg/ml lysozyme
solution 2:	1% SDS, 0.2M NaOH
solution 3:	3M KOAc pH4.8 (60 ml 5M KOAc with 11.5 ml acetic acid and 28.5 ml H ₂ O)
solution 4:	5M LiCl
RNase solution:	10 mg/ml RNase A (DNase free)

The underwritten method is a simple way to prepare more plasmid DNA comparing to the described already PEG precipitation. The purity and the amount of the prepared DNA is sufficient for co-transfection in Sf9 cells.

Bacterial culture was started from a single colony in 2 ml of TB-medium/amp and incubated 8 h at 37°C. 10-20 μ l were transferred in 30-40 ml of fresh medium and cultivated at 37°C overnight. The bacterial suspension was transferred in a Falcon tissue culture tube and was spun down by centrifugation at 3000 rpm for 5 min (Megafuge1.0, Heraeus). The pellet was resuspended in 2 ml of solution 1 and after 50 μ l of RNase solution were added, the sample was mixed and placed on ice for 5-10 min. 3 ml of solution 2 were added, the content was thoroughly but gently mixed by inverting the tube and incubated for 5-10 min on ice. After this step, 2 ml of solution 3 were added and the tube was thoroughly but gently inverted until a homogeneous suspension was formed. The sample was incubated 5-10 min on ice, 6 ml of solution 4 (5M LiCl) were added and the content was mixed. After 5-10 min of incubation on ice, the sample was centrifuged for 15 min at 5500 rpm (Megafuge 1.0, Heraeus). The supernatant was further filtered through 2 layers of precision wiper paper and transferred to a new Falcon tissue culture tube. DNA was precipitated with an equal volume of isopropanol and after the pellet was rinsed with 70% EtOH, it was dried under vacuum. Then the pellet was resuspended in 500 μ l of dH₂O, transferred to a fresh Eppendorf tube and 50 μ l of RNase solution were added to the DNA solution. The sample was incubated for 30-60 min at 37°C. DNA was extracted with 400 μ l saturated phenol/tris and 400 μ l of chloroform/isoamylalcohol (24:1) solution. The aqueous phase was transferred to a new Eppendorf tube and 1/10 Vol. of 3M NaOAc and an equal volume of isopropanol were added to it. The sample was thoroughly vortexed, incubated at RT for 5 min and centrifuged at high speed

(14000 rpm) for 10 min. The pellet was briefly dried under vacuum and redissolved in 40 μ l of dH₂O. When the plasmid DNA was isolated to be used for co-transfection in Sf9 cells, the pellet from the last step was dried under sterile conditions and was dissolved in sterile dH₂O.

The concentration of the plasmid DNA was determined by spectrophotometry and the quality was examined by agarose gel electrophoresis.

2.8.12 DNA Sequencing

The DNA sequencing was performed by Wolfgang Haedelt, using an automatic DNA Sequencer (Applied Biosystems, Model 373A) and according to manufacturer's instructions.

The used method, according to Sanger, relies on the base-specific termination of the DNA chain elongation by random integration of labeled ddNTPs at the end of the chain. Four independent sequencing reactions were carried out for each analyzed DNA sample. Each reaction contained different chain-terminating ddNTP coupled to a corresponding fluorescent dye. After the end of PCR, the products of the four reactions were mixed together and analyzed on a 7 % polyacrylamide gel. Due to the different fluorescence, the single DNA fragments could be detected by an argon laser beam.

2.9 Protein Chemical Methods

2.9.1 Determination of the Protein Concentration

The concentration of a protein solution, when it is diluted to 0.1-0.5 mg/ml, can be measured by spectrophotometry at the absorption spectrum range 250-320 nm (Kontron Uvikon 930 Spectrophotometer). For calculation was used the absorbency value A at 280 nm. The concentration of IL-4 and IL-4BP per absorbency unit ($A_{280} = 1$) and the path length equal to 1 cm are shown in the Table 2.6.

Table 2.6: Molar absorbency factor and concentration of IL-4 and IL-4BP

Protein	Molar absorbency factor [$\text{mol}^{-1} \cdot \text{cm}^{-1}$]	Concentration per absorbency unit 1 [mg/ml]
IL-4	8610	1.7
IL-4BP	66930	0.357

2.9.2 Lyophilization of Proteins

The purified protein was divided into aliquots of 100 μ l each and then placed in an aluminum block and frozen at -70°C overnight. The frozen protein aliquots were then transferred to a Lyophilizator (Christ Lac-1), which was pre-cooled to -55°C and vacuum pumped to 0.02 bar overnight. KOH was kept in the lyophilization chamber as a dry reagent.

2.9.3 Molecular Weight Standard for Protein Samples

The molecular weight of the proteins was estimated by comparison with a protein standard marker, which was loaded parallel to the samples on a PAGE. This was used to identify the size of proteins, loaded on the gel. The characteristic bands of the protein standard and their molecular weights are presented in Table 2.7.

Table 2.7: Protein standard used for PAGE

Protein	Molecular weight [Da]
phosphorylase b	94000
albumin	67000
ovalbumin	43000
carboanhydrase	30000
trypsin-inhibitor	20100
lactalbunin	14400

2.9.4 SDS - Polyacrylamide Gel Electrophoresis

(Laemmli, U.K., 1970)

acrylamide solution:	30% acrylamide, 0.8% N,N' methylenbisacrylamide
4 x lower Tris:	1.5M Tris-HCl, 0.4% SDS, pH 8.8
4 x upper Tris	0.5M Tris-HCl, 0.4% SDS, pH 6.8
glycerol:	87% glycerol
TEMED	
APS solution:	40% APS
SDS running buffer:	25mM Tris-HCl pH 8.6, 190mM glycin, 0.15% SDS
SDS sample buffer:	62.5mM Tris-HCl pH 6.8, 2% SDS, 20% glycerol, 2% BPB, 2% β -mercaptoethanol

2. Materials and Methods

staining solution: 0.25% Coomassie Brilliant Blue R250 in destaining solution
destaining solution: 1 Vol. acetic acid, 1 Vol. isopropanol, 8 Vol. H₂O

In denaturing SDS-polyacrylamide gels the proteins were separated by their molecular weight. The electrophoresis was performed in a vertical gel electrophoresis system Mini-V 8.10 (Gibco BRL). Different acrylamide concentrations can be used for different gel preparations (Table 2.8) depending on the size of the separated proteins.

Table 2.8: Amount of the different components used for SDS-polyacrylamide gel electrophoresis

Solution	Stacking gel		Separating gel	
		7.5%	10%	12%
acrylamide solution	0.25 ml	1.25 ml	1.67 ml	2 ml
4 x lower Tris	-	1.25 ml	1.25 ml	1.25 ml
4 x upper Tris	0.62 ml	-	-	-
H ₂ O	1.6 ml	1.5 ml	1.1 ml	0.75 ml
87% glycerol	-	1 ml	1 ml	1 ml
TEMED	6 µl	5 µl	7 µl	7 µl
40% APS	6 µl	5 µl	7 µl	7 µl

The separating gel solution was decanted between two vertical glass-slabs (layer thickness 0.75 mm) with a Pasteur pipette to 2/3 of the glasses upper edge and then covered with a water layer. After polymerization, the water was poured out, the stacking gel solution was filled on the top and a comb was immediately inserted.

The protein samples and SDS sample buffer (1:1) were mixed and boiled at 100°C for 5 min. A microlitre syringe was used to place the protein solutions in the wells of the slab. For each well 0.5-2 µg of protein was loaded. In the first lane, parallel to the samples, was loaded the protein standard. Until the samples were concentrating, the gel was running at 100 V and for the separating part 150 V were used.

After the end of the electrophoresis, the gel was placed for 30 min in a coomassie solution for staining. The destaining was done overnight. The ready gel was kept 1 h in 20 % methanol and dried between two pieces of cellophane.

2.9.5 Concentration of Protein Samples by TCA

When the protein concentration was low, concentration by TCA was done before the sample was loaded on PAGE. To the protein sample, which had to be concentrated was added 1/9 Vol. of 5% TCA. After mixing, the protein solution was incubated for 20 min on ice and then centrifuged for

20 min at 14000 rpm (Eppendorf Centrifuge). The pellet was dissolved in desired volume of SDS sample buffer. When the solution had a yellow color, 1 µl of 2.5M Tris-HCl pH 8.0 was added until the color got blue.

2.9.6 Biotinylation of Proteins

For biotinylation were used protein solutions of purified IL-4BP in PBS. To 300 µl of such a solution 50 µl of 0.5M NaHCO₃, pH 8.5 were added. A solution of 1 µg EZ-LinkTM Sulfo-NHS-LC-Biotin (Pierce) in 300 µl DMSO was prepared. Biotin solution was added to the protein sample in such an amount that the protein and the biotin were in a molar ratio of 1:5. The sample was shortly vortexed and then incubated on ice for 3 h.

The biotinylated protein sample was separated from the free biotin by gel filtration through a column filled with Biogel P6DG. The column volume was about 14 ml and for elution was used PBS. The biotinylated protein was eluted after 4-5 ml flow through. The sample was divided into aliquots, which were kept at -20°C.

2.10 Immunological methods - Western Blot

2.10.1 Transfer of Proteins to a Nitrocellulose Membrane

(Gershoni and Palade, 1983)

Transfer buffer: 25mM Tris-HCl, 192 mM glycine, 20% methanol
Amidoschwarz: 0.1% (w/v) amidoschwarz 10-B, 45% methanol, 10% acetic acid
destaining solution: 1 Vol. acetic acid, 1 Vol. propanol, 8 Vol. H₂O
nitrocellulose membrane (Schleicher and Schmuell BA85)
Whatman paper

Western blotting was used to verify the expression of IL-4BP by Sf9 cells, after the second step of virus amplification.

First, the proteins were electrophoretically separated on a SDS polyacrylamide gel. 10 µl of virus supernatant were mixed with equal volume of protein sample buffer and after 5 min of boiling, the sample was loaded on a gel, parallel to a protein standard. As a negative control was used a sample of equal volume, which contained only the medium for Sf9 cells. The positive control was a sample of wild-type IL-4BP with known concentration. After the end of the electrophoresis, the

gel was rinsed shortly in transfer buffer. Then a paper-thin nitrocellulose membrane, which tenaciously binds most proteins, was carefully applied on the face of the gel, preventing the formation of air bubbles. The gel and its attached membrane were sandwiched between two pieces of Whatman paper, two porous pads and the plastic support was tightly fixed. The blotting apparatus (Blot Module Mini-V8.10), containing the gel and the membrane, was placed in an electrophoresis chamber in a way that the nitrocellulose membrane was toward the anode. The chamber was filled with transfer buffer and an electric field was applied (150 V) for 1 h. At this step, the proteins were driven out of the gel and transferred to the membrane.

After the blotting, the membrane was separated from the gel and the first lane, containing the protein standard was cut out and stained for 5 min in amidoschwarz solution. Then this part of the membrane was placed in destaining solution, washed in H₂O and dried.

All manipulations were carried out with gloves to prevent the transfer of foreign proteins to the membrane.

2.10.2 Detection of Western Blots by a Peroxidase Coupled Antibody

washing buffer:	10mM Tris-HCl pH 8.0, 150mM NaCl, 0.5% tween
blocking buffer:	3% BSA in washing buffer
luminol solution:	2.5 mM luminol (3-aminophthalhydrazid), 100mM Tris-HCl pH 8.5, 1% DMSO
enhancing solution:	90mM p-cumar acid in DMSO
primary antibody:	3 µg/ml X-14-38 (anti-IL-4BP monoclonal antibody) in blocking buffer
secondary antibody:	anti-mouse polyclonal antibody from goat, peroxidase coupled

In the next step, the membrane was soaked in a solution of the primary antibody, specific for IL-4BP. Only the band, which contained this protein, bound the antibody. To identify the band containing the protein of interest, the membrane was developed by a secondary antibody, coupled with POD.

After the blotting, the membrane was rinsed once for 5 min in washing buffer. Then it was incubated in blocking buffer for 30 min on a platform shaker to reduce the background of non-specific binding by blocking potential binding sites with irrelevant proteins. The blocking buffer was replaced by 5 ml solution of the primary antibody and the membrane was incubated at RT for at least 2 h with gentle agitation on a platform shaker. When the antibody solution was removed,

the membrane was rinsed 4 times in washing buffer (5 min between each change) at RT. From the final wash, the nitrocellulose membrane was transferred in 5 ml solution of the secondary antibody (0.5-5.0 µg/ml antibody in blocking buffer) and incubated for 1-3 h at RT with gentle agitation on a platform shaker. The reaction with the secondary antibody was stopped by rinsing the membrane 4 times in washing buffer (5 min between each change) at RT. For the developing solution in two separated tubes were added 2.5 ml of luminol solution and 11 µl of enhancing solution or 2.5 ml of 0.1M Tris pH 8.5 and 1 µl of 30% H₂O₂, respectively. Right before the development, the content of the two tubes was mixed. The development was completely carried out in a dark room. There the membrane was transferred into the developing solution and was incubated until luminescence was seen (usually not more than 30 sec). The nitrocellulose membrane was shortly dried, exposed to a X-ray film (Kodak X-100) for 30 sec to 1 min and then the film was developed.

2.11 Expression of Recombinant Proteins in E.coli

(Kato et al., 1985; Weigel et al., 1989)

2.11.1 Temperature Induced Protein Expression

medium: TB medium, 10 x phosphate buffer
antibiotic: ampicillin
TE buffer 10mM Tris-HCl, 1M EDTA pH 8.0
expression vector: R^{TS}pRC109, containing the insert of interest

Bacterial culture was started in 2 ml of TB-medium from a single colony and incubated for 8 h at 30°C. 20 µl of this suspension were used to start culture in 50 ml of fresh medium, which was incubated overnight at 30°C. In a flask (2 l) was prepared 800 ml TE-medium, containing ampicillin (50 µg/ml) and 1.6 ml from the overnight bacterial culture were added. This bacterial culture was grown at 30°C on a shaker (Braun Ceromat, 200 rpm) to early logarithmic phase with OD₅₅₀ of 0.5 (LKB Novaspec). The flask was then immediately moved to a rotatory water bath, where it was incubated for another 3 h at 42°C and shaken at 200 rpm. After this time, usually OD₅₅₀ of 1.2-1.5 was reached.

The bacterial cells were harvested by centrifugation for 10 min at 6000 rpm (Beckmann J2-21, JA-10 rotor). The pellet was resuspended and washed in 30 ml of TE buffer, pH 8.0. After the

bacterial suspension was centrifugated under the same conditions, the pellet was resuspended in 10 volumes of TE buffer (vol/wet mass) and frozen at -20°C.

2.11.2 Preparation of Inclusion Bodies

TE buffer was added to the thawed out cell suspension to about 50 volumes of wet mass. The bacterial cells were sonicated eight times (each time 30 sec sonication followed by 30 sec break) at 300 W by a sonicator (KLN System 585). During the sonication, the solution was kept in an ice bath. The suspension was centrifuged at 11000 rpm (Beckmann J2-21, JA-14 rotor) for 30 min at 4°C. The tight sediment was resuspended and washed once in 100 ml of TE buffer and then centrifuged under the same conditions for 20 min. The final pellet was resuspended in 10 volumes of TE buffer (vol/wet mass).

2.11.3 Denaturation and Renaturation of Proteins

GuHCl solution:	6M guanidine hydrochloride, 100mM Tris-HCl pH 8.0
PBS:	120mM NaCl, 2mM KCl, 3 mM NaH ₂ PO ₄ pH 4.8, 7mM Na ₂ HPO ₄ pH 8.0
TE buffer:	10mM Tris-HCl, 1mM EDTA, pH 8.0
acetic acid:	4M acetic acid pH 5.0

To the suspension, containing inclusion bodies slowly were added 3 volumes of 6 M guanidine hydrochloride solution and 0.1% (by volume) 2-mercaptoethanol. The mixture was stirred for 30 min at RT and then centrifuged at 11000 rpm (Beckmann J2, JA-10 rotor) for 15 min at 4°C. 4 volumes H₂O were added drop by drop to the supernatant. The sample was centrifugated at 11000 rpm for 20 min at 4°C. The supernatant was dialysed against 20 volumes of PBS pH 7.4 for 16-20 h at 4°C. The cloudy suspension first was adjusted to pH 5.0, using 4 M acetic acid and then was centrifuged at 11000 rpm (Beckmann JA-14 rotor) for 20 min at 4°C. The protein containing supernatant was further purified by ion exchange chromatography.

2.12 Expression of Recombinant Proteins in Sf9 cells

2.12.1 General Handling Techniques

2.12.1.1 Insect cell culture media

Insect - Express medium (BioWhittaker)

SF - 1 medium (BioConcept)

Sf - 900 II Serum-Free Medium (Gibco BRL)

Pluronic F68 for ICM - 10% (BioConcept)

Lipid Ethanol solution for ICM (BioConcept)

L - Glutamine (Seromed)

FCS (Gibco BRL)

All of these media provide basic nutrients for Sf9 cells and have a pH of approximately 6.2. Insect-Express medium does not require additional supplements and was completed only with 5% of FCS. The rest of the mentioned mediums were supplemented as shown in Table 2.9.

Table 2.9: Insect cell culture media and required supplements

Medium	Lipid mix	Pluronic	L-glutamine	FCS
Insect-Express 1000 ml	-	-	-	50 ml
SF-1 950 ml	1 ml	10 ml	25 ml	50 ml
SF-900 SFM II 980 ml	1 ml	10 ml	10 ml	50 ml

2.12.1.2 Cultivation of Sf9 cells

To prevent bacterial or yeast contamination, all experiments dealing with Sf9 cells were performed at sterile conditions. Glass pipettes, plastic materials and solutions were sterilized. Flasks and tubes, containing cells were opened only in a laminar flow hood (LaminAir HB 2448S, Heraeus).

Old medium was exchanged with fresh every second day, since the healthy Sf9 cells double every 18-24 h. The culture was incubated at 27°C in incubators (Heraeus, Memmert).

2.12.1.3 Staining and counting of Sf9 cells

trypan blue 0.4% (w/v) solution in PBS

The trypan blue exclusion method was used to count the proportion of viable cells and their concentration in the suspension. Since the exclusion of the stain is a selectively working definition for viability, the dead cells appear as blue spots, when observed with an inverse microscope.

A small aliquot of cells was mixed with trypan blue solution at a ratio of 1:1 and kept at RT for 1 min. Apart of this, the suspension was placed in a Neubauer's chamber and observed with an inverse microscope. The viable cells in 16 different squares were counted. To calculate the cell density (cells/ml), the sum of cells counted within those squares has to be multiplied by 10^4 .

2.12.1.4 Long-term cell storage

freezing medium: 90% culture medium and 10% DMSO, freshly filtered through
 22 μm filter

cryovials: 2.0 ml, sterile (Nalgene)

Sf9 cells can be stored for long periods of time by freezing in liquid nitrogen. Sf9 cells from a healthy, log-phase culture were spun down at 2500 rpm (Megafuge 1.0, Heraeus) for 10 min. After the supernatant was decanted, the cell pellet was kept on ice and resuspended in such a volume of freezing medium, that the final cell density was 4×10^6 . The cell suspension was aliquoted (1 ml) into freezing vials. To freeze the cells slowly, the vials were placed at -20°C for 1 h and then kept at -80°C overnight. The next day the cells were transferred to liquid nitrogen. A week or two after the cells were frozen, one vial was thawed to check for cell viability and contamination.

The frozen cells were quickly thawed by gentle agitation in a 37°C water bath. Then, they were transferred to a centrifuge tube (Falcon) and 25 ml of fresh medium were added. The cells were spun down by centrifugation at 1000 rpm (Megafuge 1.0, Heraeus) for 5 min. The pellet was resuspended in 40 ml of fresh medium and centrifuged again at the same conditions. After the supernatant was removed, the cells were resuspended in 10 ml of medium and the suspension was seeded in a 25 cm^2 culture flask, which was incubated at 27°C . After 12-24 h the old medium was replaced with fresh and the culture was incubated at 27°C as long as the cells needed to get

confluent. Then they were transferred to a bigger flask (75 cm²) and the medium was exchanged with fresh.

2.12.1.5 Monolayer culture

tissue culture flasks: 25 cm² (Falcon)
 75 cm² (Falcon)
 175 cm² (Falcon)

Insect cells grow well both in suspension and as monolayer cultures and can be transferred from one to the other with minimal adaptation.

Sf9 cells from a monolayer culture were subcultured when they were 80-90% confluent. After the culture was examined for contaminations and cells floating in the medium, the old medium was discarded and the cells were washed from the surface of the flask by gentle pipetting using 10 ml of fresh medium. A small aliquot of this suspension was stained with trypan blue. The cells were examined and counted with an inverse microscope. The suspension was diluted and the cells were seeded in a new flask with a density of 7.0×10^4 - 1.0×10^5 cells/cm² in a final volume of 5 ml (for 25 cm² flask), 15 ml (for 75 cm² flask) or 35 ml (for 175 cm² flask). A culture prepared with such cell density was ready for next passage in 2-3 days. The flasks were incubated in a humidified incubator at 27°C.

2.12.1.6 Suspension culture

plastic roller bottles: 2 l (Greiner)

Continuous propagation of Sf9 cells in suspension for more than a few passages resulted in decreased cell viability and growth rate. That was the reason, that the stock cultures were passaged as monolayer and used then to seed suspension cultures when it was required.

Usually, 2-3 confluent 175 cm² flasks were used to start one bottle of a suspension culture. After the cells were counted, they were inoculated in a plastic roller bottle with a density of 0.8×10^5 - 1.0×10^6 cells/ml in a total volume of 80-100 ml. The bottle was incubated at 27°C in an incubator, where it was slowly rolled (5 rpm). When cells from the suspension attached to the wall of the bottle and the cell density reached $3-4 \times 10^6$ cells/ml, fresh medium was added to the

culture. In a roller bottle were incubated maximum 200 ml of cell suspension and the cell density was controlled to be not more than 4.5×10^6 cells/ml.

2.12.2 Generation of Recombinant Baculoviruses

2.12.2.1 The Baculovirus expression system

Baculoviruses belong to a diverse group of large double-stranded DNA viruses that infect different insects as their natural hosts (Matthews, R.E.F., 1982). The Baculovirus genome is replicated and transcribed in the nuclei of infected host cells where the large Baculovirus DNA (between 80 and 120 kbp) is packaged into rod-shaped nucleocapsids. Since the size of this nucleocapsids is flexible, recombinant Baculovirus particles can accumulate large amounts of foreign DNA.

One of the most commonly used Baculoviruses for expression vector work is *Autographa californica* nuclear polyhedrosis virus (AcNPV). Infectious AcNPV particles enter susceptible insect cells by endocytosis or fusion and viral DNA is uncoated in the nucleus. DNA replication starts 6 h post-infection. The virus infection cycle can be divided into two different phases: early and late. During the early phase, the infected insect cell releases extracellular virus particles by budding off from the cell membrane of infected cells. During the late phase of the infection cycle, occluded virus particles are assembled inside the nucleus. The occluded viruses are embedded in a homogenous matrix made predominantly of a single protein, the polyhedrin protein. That is why, during the late phase of infection, the polyhedrin protein accumulates to very high levels. Although the polyhedrin protein seems to be one of the most abundant proteins in infected insect cells, it is not essential for the Baculovirus life cycle in tissue culture. Cloning of a gene of interest under the control of the polyhedrin promoter, leads to high expression levels of the recombinant protein. This fact defines the Baculovirus expression vector system as one of the most powerful available systems for eukaryotic expression of recombinant proteins.

2.12.2.2 Co-transfection of BaculoGold DNA and a transfer vector into insect cells

The Baculovirus genome is too large to directly insert foreign genes easily. Hence the foreign gene has to be cloned first in a transfer vector, which later is co-transfected with AcNPV DNA into Sf9 cells.

2. Materials and Methods

For co-transfection was used BaculoGold DNA (Pharming), which is a modified AcNPV Baculovirus DNA, containing a lethal deletion and does not code for viable virus. Co-transfection of BaculoGold DNA with a complementing Baculovirus Transfer Vector rescues the lethal deletion. The foreign gene has to be cloned into a transfer vector that contains flanking sequences, which are homologous to the Baculovirus genome. After co-transfection, recombination takes place within the insect cells between the homologous regions in the transfer vector and the BaculoGold DNA. Recombinant virus produces recombinant protein and also infects additional insect cells, thereby resulting in additional recombinant virus.

As a transfer vector was used pAcGP67B, where the gene of interest was cloned under the control of the strong Baculovirus polyhedrin promoter. It also contains gp67 signal sequence upstream of a multiple cloning site, which is one of the most effective Baculovirus-encoded signal sequences for protein secretion. The signal peptide mediates the forced secretion of the recombinant protein, even if it is normally not secreted. During transport across the cell membrane, the signal peptide is cleaved and the native protein can be purified from the infection supernatant. The vector has an E.coli origin of replication, which allows to be amplified in bacteria. It was prepared for co-transfection by LiCl purification method (see 2.7.11.3).

Co-transfection was performed using BaculoGold transfection kit (Pharming). The following materials were required:

confluent monolayer culture of Sf9 cells

BaculoGold transfection kit:	linearized BaculoGold Baculovirus DNA
	transfection buffer A
	transfection buffer B
	AcNPV wild-type high titer stock solution

purified recombinant Baculovirus transfer vector (pAcGP67B)

FCS

6-well tissue-culture plate

Confluent Sf9 cells were counted and diluted with medium containing 5% FCS to a cell density of 7×10^5 cells/ml. In each well of a 6-well tissue culture plate, 1 ml of this cell suspension was seeded and 1 ml of fresh medium was added. The plate was incubated shortly at 27°C until the cells attached firmly to the bottom.

In a sterile Eppendorf tube in a laminar hood, 1 µg of the pure recombinant transfer vector was mixed with 0.25 µg (2.5 µl) of BaculoGold DNA. After 5 min of incubation at RT, 500 µl of transfection buffer B were added to the co-transfection mixture. To prepare the positive control,

25 µl of AcPNV wild-type high titer stock solution were added to 1.5 ml of medium. The old medium from the cells in the experimental co-transfection well was aspirated and replaced with 500 µl of transfection buffer A. The medium in the positive control well was replaced with the mixture containing wild-type AcNPV. In the negative control well the medium was aspirated and 1.5 ml of fresh medium were added. Nothing else was added to this well. Drop-by-drop, in the experimental co-transfection well was added the earlier prepared solution containing BaculoGold DNA and Baculovirus transfer vector. After every 3-5 drops, the plate was gently rocked back and forth to mix the drops with the medium. During this procedure, a fine calcium phosphate/DNA precipitate with white color was formed. The plate was incubated for 4 h at 27°C and then the medium from the experimental and the positive control wells was aspirated. The cells there were washed with 1.5 ml of fresh medium, which then was removed. Again 1.5 ml of fresh medium was added to each of these wells. The plate was placed in a incubator and kept at 27°C for 5 days.

After 5 days the cells in the three wells were examined for signs of infection. The supernatant from the experimental co-transfection well was collected and centrifuged at 2500 rpm (Biofuge A, Heraeus) for 5 min. The supernatant was stored at 4°C in the dark and later was used for plaque purification.

2.12.2.3 Generating pure virus stocks by plaque purification

The principle of the following method is to infect cells with extremely low numbers of infectious particles, so that only isolated cells become infected. An overlay of agarose keeps the cells stable and limits the spread of virus. When the originally infected cell produces virus and eventually lyses, only the immediate neighboring cells become infected. Each group of infected cells is referred to as a plaque. Uninfected cells are dispersed throughout the culture, surrounding the plaques. After several infection cycles, the infected cells in the center of the plaques begin to lyse and the peripheral infected cells remain surrounded by uninfected cells. All the virus particles in a plaque derive from a single infectious particle. Therefore, clonal virus populations may be purified by isolating individual plaques.

confluent monolayer Sf9 culture

FCS

Insect Express Medium (2 x) (BioWhittaker)

agarose solution: 1.8% SeaPlaque Agarose (BioZym) dissolved in H₂O, autoclaved and kept at 65°C

MTT solution: 1 mg/ml MTT dissolved in H₂O, filtered through 22 µl filter
6-well tissue culture plate

The cells were counted and diluted to a cell density of 1.2×10^6 cells/ml. In each well was seeded 1 ml of cell suspension and 1 ml of fresh medium was added. The plate was kept 10-15 min at 27°C on a level surface to allow the cells to spread evenly over the bottom. Serial dilutions of the viral transfection supernatant in fresh medium were made, as it follows:

$$3 \times 10^{-1}, 1 \times 10^{-1}, 1 \times 10^{-2}, 1 \times 10^{-3} \text{ and } 1 \times 10^{-4}.$$

All dilutions were performed in a total volume of 1 ml in sterile Eppendorf tubes. The medium was aspirated and replaced with the virus in oculum. One well was used for negative control and there only fresh medium was added. The plate was incubated at 27°C for 1 h. For each plate was prepared a solution containing 5 ml of agarose solution, 4.5 ml of Insect Express Medium (2x), and 500 µl of FCS, which was kept fluid at 40°C. The virus dilutions were aspirated and the cells were overlaid with an agarose containing solution (1 ml/well). The plate was kept on a leveled surface until agarose hardened (about 20 min). The plate was incubated in a humid atmosphere at 27°C until visible plaques developed (usually 5-6 days).

To better visualize the plaques, the cells were stained with solution of MTT. To each well was applied 1 ml of it and the plate was incubated for 1 h at RT. After this time, the plaques were seen as small white points on a violet background.

2.12.3 Amplification of Virus Stocks

The generation of a pure high titer virus stock involved the preparation of a stock starting from a single infectious unit. During the virus amplification, the following steps were performed to increase the volume and the titer of the virus stock.

2.12.3.1 Virus amplification from a single virus plaque

The plaques were picked from wells containing not more than 20 single plaques. To pick up the plaques, a sterile micropipette tip was used. Each single plaque was placed in a sterile Eppendorf tube containing 1 ml of medium and was incubated for 1 h at 27°C. In a 6-well tissue-culture plate was seeded 1 ml/well Sf9 cells from confluent culture with a cell density of $1.2-1.5 \times 10^6$ cells/ml and 1 ml of fresh medium was added to each well. After the cells attached to the bottom,

the medium was replaced with plaque containing solutions. In the negative control well, 1 ml of fresh medium was added. The plate was incubated for 1 h at 27°C and then 1 ml of fresh medium was added to each well.

After 3 days of incubation at 27°C, the supernatant from the different virus clones was collected and centrifuged at 2500 rpm (Biofuge A, Heraeus) for 5 min. This amplifying step was repeated once more using 500 µl of each virus stock mixed with 500 µl of fresh medium. After the second amplification, the virus clones were tested for protein expression by Western blotting (see 2.9). The virus clone, which showed the best expression level, was chosen for further amplification.

2.12.3.2 Virus amplification in a small volume scale

In a 175 cm² tissue-culture flask were seeded Sf9 cells with a density of 1.6-2.0 x 10⁵ cells/cm² in a total volume of 35 ml. After the cells attached to the bottom, the medium was aspirated and cells were infected with 1 ml of the virus supernatant collected after the second amplification step. Additionally, 10 ml of fresh medium were added and the flask was incubated for 1 h at 27°C. Then 24 ml of fresh medium were added to the flask. After 3 days of incubation at 27°C, the virus supernatant was collected and centrifuged (Megafuge 1.0, Heraeus) at 2500 rpm for 5 min.

2.12.3.3 Virus amplification in a large volume scale

5 ml from the virus supernatant collected after the described amplification step were used to infect Sf9 cells in a roller bottle (Greiner). 95 ml of suspension culture from Sf9 cells with cell density 1.5 x 10⁶ cells/ml were transferred to a fresh plastic roller bottle and then the virus stock was added. After 3 days of incubation at 27°C, the supernatant was centrifuged at 2500 rpm (Megafuge 1.0, Heraeus) for 5 min and was used for determination of virus titer.

2.12.3.4 Determination of virus titer by plaque assay

The titer of a virus stock is the concentration of infectious virus particles in that stock. It was determined by a plaque assay. Plaque assay of a virus stock involves essentially the same protocol as plaque purification. Because each plaque derives from a single infectious unit,

counting the number of plaques formed by different dilutions of a virus stock allows determining the concentration of infectious units in the stock. Viral titers determined in this manner are expressed in plaque-forming units/ml (pfu/ml). For practical purposes, the virus stock titered by plaque assay was diluted as it follows:

$$1 \times 10^{-4}, 1 \times 10^{-5}, 1 \times 10^{-6}, 1 \times 10^{-7} \text{ and } 1 \times 10^{-8}.$$

2.12.3.5 Virus storage

(Jarvis, D.L. et al., 1994)

Working stocks of recombinant viruses were stored at 4°C in tissue-culture medium containing 5% of FCS. Infected cells and cell debris were removed from the virus stock by centrifugation at 1000 x g for 5 min. The stocks were stored in the dark, because the viruses are extremely light sensitive.

For long-term storage, aliquots of the virus stock were frozen in polypropylene cryovials at -80°C without any cryoprotectant. Before freezing, FCS was added to 10%. Virus stocks were retitrated before use after prolonged storage.

2.12.4 Protein Expression

After the virus titer was determined, the high titer virus stock was used for protein expression. 200 ml of suspension culture with cell density 1.5×10^6 cells/ml, were transferred to a fresh plastic roller bottle. The cells were infected with such an amount of high titer virus stock, that the multiplicity of the infection (infectious virus units/cell) was between 3 and 5. The bottle was rolled (5 rpm) at 27°C. Aliquots were examined under a microscope and depending on the number of infected cells, the expression was done for 4 or 5 days. The suspension was centrifuged at 3000 rpm for 10 min. The protein containing supernatant was frozen and stored at -20°C.

2.13 Purification of Recombinant Proteins

2.13.1 Purification of Proteins Expressed in E.coli

2.13.1.1 Protein purification by ion exchange chromatography

buffer A:	25mM NH ₄ OAc, pH 5.0
buffer B:	25mM NH ₄ OAc, 1M NaCl, pH 5.0
column:	3 x 10 cm (Biorad)
ion exchanger:	CM-Sepharose fast flow
pump:	LKB 2232 Microperpex S Peristaltic Pump
detector:	LKB 2238 Uvicord, LKB 2210 Recorder
collector:	ISCO Retriever II

CM-Sepharose fast flow (Pharmacia) was equilibrated with 4 M NH₄OAc, pH 5.0 and washed several times with 25 mM NH₄OAc, pH 5.0 by a funnel. The so prepared ion exchanger was packed in a column (5-10 ml) and washed with solution A, until the elute reached pH 5.0. The protein containing solution was slowly loaded (ca. 250 ml/h) into the column. This was followed by rinsing with five column volumes of solution A. The elution of proteins was performed by a 60 ml linear salt gradient from 0 to 0.5 M NaCl/25 mM NH₄OAc pH 5.0 with a flow rate ca.0.5 ml/min. The elute peak was detected with an absorbance device at 280 nm and recorded. The described procedure was performed in a 4°C room. The collected fractions (2 ml each) were measured at 280 nm (Konto Uvikon 930 Spectrophotometer), using solution A as a blank. Further, the fractions (10 µl from each) were examined on a SDS-polyacrylamide gel. The fractions, which contained pure protein in a sufficient amount were combined and later purified additionally by the use of RP-HPLC.

2.13.1.2 Protein purification by RP-HPLC

controller:	LKB 2152 HPLC Controller
pump:	LKB 2150 HPLC Pump
detector:	Merk Hitachi 655A Variable Wavelength UV Monitor
recorder:	LKB 2210
superrac:	LKB 2210

2. Materials and Methods

acetonitrile: acetonitrile (Roth, HPLC Grade), filtered through a 22 μm filter
TFA: 0.1% TFA (Merck) in H_2O , filtered through a 22 μm filter
protein stock buffer: 12.5 ml of 4 x upper Tris-HCl, 20 ml of 10% SDS, 47.5 ml of H_2O , 30 ml of glycerol mix

The protein containing fractions, collected during the ion exchange chromatography, were centrifuged at 3000 rpm for 15 min at 4°C. The supernatant was injected into a Vydac C4 HPLC column (250 x 4.6 mm or 250 x 8 mm), equilibrated with 0.1% TFA. The protein was eluted by acetonitrile gradient from 0 to 100%. The elution was controlled automatically by the presented programs (Table 2.10).

Table 2.10: Acetonitrile gradient and retention time, used for analytical and preparative RP-HPLC

	Acetonitrile [%]	Retention time [min]
Analytical RP-HPLC	0 – 35	15
	35 – 45	40
	45 – 100	15
	100 – 100	10
Preparative RP-HPLC	0 – 30	5
	30 – 50	45
	50 – 100	10
	100 – 100	10
	100 – 0	10

The flow rate was 0.7 ml/min for the column (250 x 4.6 mm) and 2 ml/min for the column (250 x 8 mm). The protein concentration of the collected fractions was measured at the absorption spectrum range 250-320 nm (Kontron Uvikon 930 Spectrophotometer). An aliquot (10 μl) from every fraction was mixed with 30 μl of protein buffer and 5 μl from this solution was analyzed by SDS-polyacrylamide gel electrophoresis. The fractions with the highest amount of pure protein were combined, aliquoted and lyophilized.

In addition to the SDS-PAGE, the protein purity was also examined by analytical RP-HPLC, performed with the use of the small column (250 x 4.6 mm). The procedure followed the described details for preparative RP-HPLC, except that only 100 μg of protein were required for analysis and the detection sensitivity was set at 0.08.

2.13.2 Purification of Proteins Expressed in Sf9 Cells

2.13.2.1 Affinity chromatography using IL-4 as a ligand

PBS:	120mM NaCl, 2mM KCl, 3mM NaH ₂ PO ₄ , pH 7.4
eluent:	4M MgCl ₂
affinity adsorbent:	IL-4, immobilised to Sepharose gel
pre-column:	1 x10 cm column (Biorad)
filling for pre-column:	CM Sepharose fast flow (Pharmacia)

The affinity matrix (2 ml) was packed in a sterile Pasteur pipette. The so prepared affinity column was washed with 10 volumes of PBS and stored at 4°C. The filling for the pre-column (CM Sepharose fast flow) was washed several times with 20 x PBS, using a funnel. The gel was stored under 20 x PBS at 4°C. Immediately before the purification step, 2-3 ml were used to fill the pre-column, which was washed with 10 volumes of PBS.

The protein containing supernatant was thawed out and centrifuged at 2500 rpm (Megafuge 1.0, Heraeus) for 10 min to eliminate the precipitate, resulting from freezing. After the affinity column and the pre-column were connected, the protein material was loaded in a way that it passed slowly (about 100 ml/h) first through the pre-column. The two columns were disconnected and the affinity column was washed with 10 column volumes (20 ml) of PBS. During the elution, which was performed with 4 M MgCl₂, 5-6 protein fractions were collected (each 1.5 ml). The described procedure was carried out at 4°C. The protein concentration was measured at the absorption spectrum range 250-320 nm (Kontron Uvikon 930 Spectrophotometer). The quality of the protein was analyzed by an SDS-PAGE, where 15 µl of every fraction were loaded. The fractions containing the highest amount of pure protein were combined.

The pre-column could be used only once, and then had to be cleaned and refilled with fresh CM Sepharose. After elution, the affinity column was washed with 20 ml of PBS and recovered in this way for the next protein purification. It was stored at 4°C under PBS.

2.13.2.2 Affinity chromatography using X14/38 as a ligand

PBS:	120mM NaCl, 2mM KCl, 3mM NaH ₂ PO ₄ , pH 7.4
eluent:	4M MgCl ₂
affinity adsorbent:	X-14-38, bond to Sepharose gel

pre-column: 1 x10 cm column (Biorad)
filling for pre-column: CM Sepharose fast flow (Pharmacia)

X14/38 is an anti-IL-4BP monoclonal antibody, which was used as a ligand for the purification of low-affinity IL-4BP variants that could not be purified by the method described in above.

The procedure is essentially the same as described in 2.12.2.1. The main difference was, that the protein containing supernatant was loaded very slowly (usually overnight) onto the columns.

2.13.2.3 Dialysis

After the purification by an affinity column, the fractions containing the highest amount of pure IL-4BP, were combined and dialyzed in order to reduce the high salt concentration. The protein solution was placed in a semi-permeable dialysis tubing (type 20/32, Roth) made of cellulose acetate. The dialysis was performed in 2 l of PBS, which was stirred at 4°C overnight. At the next day, the buffer was exchanged with fresh and the dialysis repeated one more night. To prevent contamination with foreign proteins, the tubing was touched only through gloves.

2.13.2.4 Concentration of proteins by ultrafiltration

ultrafilter: YM10 = 10000 MW (Amicon)
apparatus: stirred cell covering range 1-10 ml (Amicon 8010)

During ultrafiltration, water and other small molecules were driven out of the protein solution through a semi-permeable membrane by a transmembrane force, such as high pressure.

The new membrane was washed according to the manufacturer's instructions and stored under 30% ethanol at 4°C. Before use, the filter was washed with dH₂O. The system was assembled and the membrane was placed with the glossy side toward the solution. It was rinsed by filtering a few ml of PBS at 3.5 atm. PBS was replaced by the dialyzed protein solution (10-15 ml) and pressure of 4 atm was applied until the protein sample reached a volume of 1-1.5 ml. The ultrafilter was rinsed in dH₂O and stored under 30% ethanol solution at 4°C. The protein concentration was measured at the absorption spectrum range 250-320 nm. Aliquots of 350 µl were frozen at -20°C and further biotinylated.

2.14 Analysis of Protein-Protein Interactions by BIAcore Technology

The analysis of kinetic and thermodynamic data of protein-protein interactions between the extracellular domain of IL-4 receptor (IL-4BP) and its mutated variants with the ligand (IL-4) was performed with a BIAcore 2000 (Pharmacia). BIAcore 2000 is an instrument, which measures bio-molecular interactions in real time without labeling of the interactants and allows detailed investigation of the reaction kinetics by analysis of the resultant signals (Karlsson, R. & Fealt, A., 1997).

For this purpose, one interactant (here IL-4BP or its variants) is immobilized on the surface of a sensor chip and a solution containing the other binding partner (IL-4) flows continuously over the chip. The sensor chip consists of a glass slide coated with a thin gold film to which is attached, by an inert linker layer, a dextran matrix onto which the mentioned interactant can be immobilized using well-defined chemistry. The sensor chip forms one wall of a micro-flow cell where its matrix covered side comes into contact with the solution containing the second interactant. This system uses the detection principle of surface plasmon resonance. During the interaction, light passing a prism is focused onto the gold surface of the sensor chip through the glass, and reflected light is monitored. Evanescent wave photons produced by the incident polarized light interact with free oscillating electrons (plasmons) in the gold surface. Resonance occurs at a critical angle of the incident light, and light energy is transferred to electrons in the metal film surface, causing a minima in the reflected light. This angle depends on the refractive index at, or close to the metal surface opposite to where the light is focused. By measuring small changes in refractive index, the instrument monitors the change in mass as a ligand binds to, or dissociates from, its binding partner. Data are presented as sensograms that show the change in resonance units (RU) versus time. For proteins, which have a refractive index increment of approximately 0.18, a signal of 1000 RU is equivalent to a surface concentration of 1 ng/mm^2 (Stenberg, E. et al., 1990).

Association is monitored when a sample is injected and binding occurs to the immobilized interactant. After sample injection, buffer alone flows over the sensor surface and dissociation parameters can be recorded. At the end of the experiment, the surface can be regenerated using suitable reagents to remove remaining bound analyte without denaturing the immobilized reaction partner and the chip can be used for a new cycle of measurements (Nice, E.C. & Catimel, B., 1999)

2.14.1 Immobilization of Proteins by Streptavidin-Biotin Coupling

After streptavidin was covalently immobilized onto the surface of a sensor chip, the biotinylated protein was bound to the prepared matrix.

- sensor chip: CM5
- EDC: 50mM N-Ethyl-N'-(dimethylaminopropyl) carbodiimide
- NHS: 200mM N-Hydroxysuccinimide
- HBS buffer: 10mM HEPES pH 7.4, 150mM NaCl, 3.4 mM EDTA,
0.005% Surfactant P20
- streptavidin solution: 100µg/ml streptavidin in 10mM NaOAc, pH 4.5
- regeneration buffer: 100mM HOAc, 1M NaCl, pH 3.0

The immobilization and preparation of a sensor chip was carried out according to the manufacturer’s instructions (BIAcore Handbook, 1995). The immobilization of streptavidin was run automatically following the program shown in Table 2.11.

Table 2.11: Immobilization of streptavidin by amine coupling

Immobilization procedure	
continuously flow buffer HBS	flow rate 5 µl/min
EDC/NHS (50 mM/200 mM)	35 µl (7 min)
streptavidin (100 µg/ml)	35 µl (7 min)
1 M ethanolamine-HCl	35 µl (7 min)

The concentration of biotinylated proteins used for immobilization was usually 0.1 µg/ml.

2.14.2 Measuring and Evaluation of Protein-Protein Interactions

A typical sensogram recorded with BIAcore 2000 is characterized by the following three phases:

- 1) Association phase - when the sample is injected; increases in the signal correspond to binding to the immobilized interactant.
- 2) The signal reaches a constant plateau when equilibrium between association and dissociation is reached.
- 3) Dissociation phase - occurs when buffer alone flows over the sensor surface. The decrease in signal reflects dissociation of analyte from the surface-bound complex.

Kinetic rate constants can be derived from the association and dissociation phases of the sensogram. The height of the plateau represents the thermodynamic affinity of binding.

The program BIAevaluation 2.0 was used to calculate the kinetic and thermodynamic constants. The theoretical equations, which describe the kinetics and equilibrium of interactions in real-time BIA, are listed in Appendix 1.

2.14.3 Assessment of the Energetic Effects of Introduced Mutations

Substitution of a residue, which is direct or indirect involved in binding is followed by a change in the binding energy of the protein-protein complex. The equilibrium dissociation constants determined by experiments performed with the BIAcore 2000 analytical system were used to calculate the loss of binding free energy ($\Delta\Delta G$) characterizing the mutated variants:

$$\Delta\Delta G = R \cdot T \cdot \ln (K_d \text{ mut} / K_d \text{ wt})$$

where R is the gas constant, T is the absolute temperature, $K_d \text{ mut}$ is the equilibrium dissociation constant for the mutant variant, $K_d \text{ wt}$ is the equilibrium dissociation constant for the wild-type interaction.

The total change in binding free energy (ΔG) for the interaction of IL-4 and IL-4BP was calculated according to the formula:

$$\Delta G = -R \cdot T \cdot \ln (1/K_d)$$

where R is the gas constant, T is the absolute temperature, K_d is the equilibrium dissociation constant for the IL4/IL-4BP interaction.

3. Results

3.1 Preparation of Recombinant IL-4BP and Its Variants

In the framework of the present project was analyzed the effect of amino acid substitutions within the α -chain of the human IL-4 receptor on the kinetics of the interaction with IL-4. Earlier, it was shown that the separately expressed 207-residue ectodomain of the α -chain (IL-4BP) forms a 1:1 complex with IL-4 and exhibits the same binding affinity as the entire receptor α -chain (Hoffman et al., 1995; Shen et al., 1996). Based on these results, the selection of the amino acids subjected to mutagenesis was restricted to the mentioned domain.

Table 3.1: IL-4BP variants designed by site-specific mutagenesis.

IL-4BP Variant	IL-4BP Loops	
Y13A	A-B	L1
Y13F	A-B	L1
L39A	C-C'	L2
F41A	C-C'	L2
L42A	C-C'	L2
L43A	C-C'	L2
D66A	E-F	L3
D67A	E-F	L3
V69A	E-F	L3
D72A	E-F	L3
D72N	E-F	L3
K91A	G-A	L4
K91D	G-A	L4
S93A	G-A	L4
D125A	B-C	L5
N126A	B-C	L5
Y127A	B-C	L5
Y127F	B-C	L5
L128A	B-C	L5
Y183A	F-G	L6
Y183F	F-G	L6

All variants of IL-4BP, which were constructed by specific substitutions of a single amino acid, are shown in Table 3.1. Variants D66A, D67A, V69A, D125A, N126A, Y127A and Y128A were expressed and purified by Dr. Yonghong Wang and further examined by the author. The study was accomplished by analyses of variants containing two independent mutations (Table 3.2).

Table 3.2: A list of the IL-4BP double mutants. The contact clusters are defined according Hage et al., 1999.

Variant	Contact cluster		
	I	II	III
Y13F/L39A	Y13	L39	D67
Y13F/F41A	Y13	F41	
Y13F/D67A	Y13		
Y13F/V69A	Y13	V69	
Y13F/D72N	Y13	D72	
Y13F/Y127A	Y13	Y127	
Y13F/Y183F	Y13	Y183	
D72N/L39A		D72	L39
D72N/F41A		D72	F41
D72N/D67A		D72	D67
D72N/V69A		D72	V69
D72N/Y127A	Y127	D72	
D72N/Y183F	Y183	D72	

The proteins representing IL-4BP and its variants, without any exceptions, were recombinantly expressed in an eukaryotic expression system (Baculovirus expression system). Since in the human IL-4BP six sites of potential N-linked glycosylation are present, the expression of functionally active recombinant proteins requires eukaryotic conditions. Therefore, was chosen the Baculovirus expression system that offers the advantage to express high levels of soluble proteins in which post-translational modifications are performed.

The kinetics of the binding of IL-4 to the IL-4BP variants was measured by means of the BIAcore system after the receptor variants were immobilized on the biosensor matrix. This method requires high purity and homogeneity of the examined samples because this is the only way to determine the exact concentration of the recombinant IL-4BP variants. The variants that had relatively higher affinity to IL-4 were purified by affinity chromatography exploring IL-4 as a ligand. For the rest of the proteins a chromatographic step using anti-IL-4BP antibody was performed. Both procedures resulted in highly pure protein fractions, which could be used for BIAcore measurements without any necessity of further purification.

3.1.1 Cloning of IL-4BP and Its Variants in the Baculovirus Transfer Vector pAcGP67B

The cDNA representing the first 207 residues of mature human IL-4 receptor α chain, extracellular domain was mutated by recombinant PCR. As a template was used the vector pRPR9IL4FD (C. Söder, based on vector R^{TS}pRC109, McCarthy et al., 1985, Appendix 2). It contains an IL-4BP cDNA modified at position C182A, in which the free cysteine is substituted in order to prevent the formation of disulfide bridges. The complete nucleotide and amino acid sequence of hIL-4BP is shown in Figure 3.1.

```

      Y A F K V L Q E P T C V S D Y M S I S T
5' CTATGCATTTAAGGTCTTGCAGGAGCCACCTGCGTCTCCGACTACATGAGCATCTCTAC 3'
      10      20      30      40      50      60
3' GATACGTA AATTC CAGAACGTCCTCGGGTGGACGCAGAGGCTGATGTACTCGTAGAGATG 5'

      C E W K M N G P T N C S T E L R L L Y Q
5' TTGCGAGTGGAAGATGAATGGTCCCACCAATTGCAGCACCCGAGCTCCGCCTGTTGTACCA 3'
      70      80      90      100     110     120
3' AACGCTCACCTTCTACTTACCAGGGTGGTTAACGTCGTGGCTCGAGGCGGACAACATGGT 5'

      L V F L L S E A H T C I P E N N G G A G
5' GCTGGTTTTTCTGCTCTCCGAAGCCACACGTGTATCCCTGAGAACAACGGAGGCGCGGG 3'
      130     140     150     160     170     180
3' CGACCAAAAAGACGAGAGGCTTCGGGTGTGCACATAGGGACTCTTGTTGCCTCCGCGCC 5'

      C V C H L L M D D V V S A D N Y T L D L
5' GTGCGTGTGCCACCTGCTCATGGATGACGTGGTCAGTGCGGATAACTATACTACTGGACCT 3'
      190     200     210     220     230     240
3' CACGCACACGGTGGACGAGTACCTACTGCACCAGTCACGCCTATTGATATGTGACCTGGA 5'

      W A G Q Q L L W K G S F K P S E H V K P
5' GTGGGCTGGGCAGCAGCTGCTGTGGAAGGGCTCCTTCAAGCCCAGCGAGCATGTGAAACC 3'
      250     260     270     280     290     300
3' CACCCGACCCGTCGTCGACGACACCTTCCCGAGGAAGTTCGGGTGCTCGTACACTTTGG 5'

      R A P G N L T V H T N V S D T L L L T W
5' CAGGGCCCCAGGAAACCTGACAGTTCACACCAATGTCTCCGACACTCTGCTGCTGACCTG 3'
      310     320     330     340     350     360
3' GTCCCGGGGTCCTTTGGACTGTCAAGTGTGGTTACAGAGGCTGTGAGACGACGACTGGAC 5'

      S N P Y P P D N Y L Y N H L T Y A V N I
5' GAGCAACCCGTATCCCCCTGACAATTACCTGTATAATCATCTCACCTATGCAGTCAACAT 3'
      370     380     390     400     410     420
3' CTCGTTGGGCATAGGGGACTGTTAATGGACATATTAGTAGAGTGGATACGTCAGTTGTA 5'

      W S E N D P A D F R I Y N V T Y L E P S
5' TTGGAGTGA A A C G A C C C G G C A G A T T T C A G A A T C T A T A A C G T G A C C T A C C T A G A A C C C T C 3'
      430     440     450     460     470     480
3' AACCTCACTTTTGGCTGGGCCGTCTAAAGTCTTAGATATTGCACTGGATGGATCTTGGGAG 5'

```

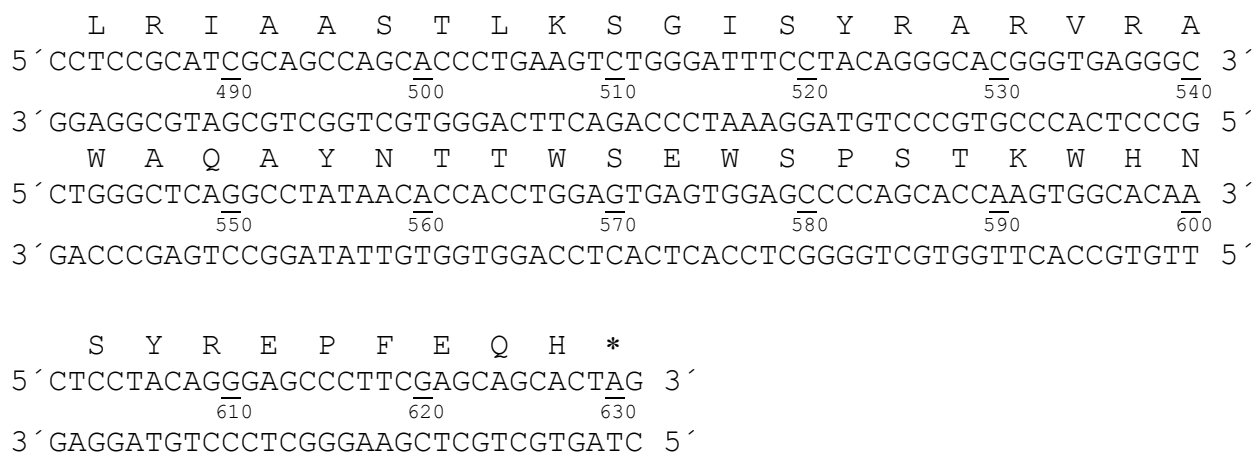


Figure 3.1: Nucleotide and amino acid sequence of hIL-4BP cDNA.

The PCR reactions were divided into two steps. During the first step (PCR 1) two fragments (PCR1a and PCR1b) were separately synthesized and a mutation of interest was introduced with the help of mutant primers containing one mismatch codon. For variants which were constructed by a substitution of a single amino acid, as a template in this reaction was used the wild-type cDNA. To produce variants in which two different amino acids were mutated, as a template was used a plasmid of hIL-4BP containing already one modified site and applying the described PCR techniques a second mutation was created. The length of the fragments differed for the particular variants depending on the exact location of the introduced mutation (Figure 3.2).

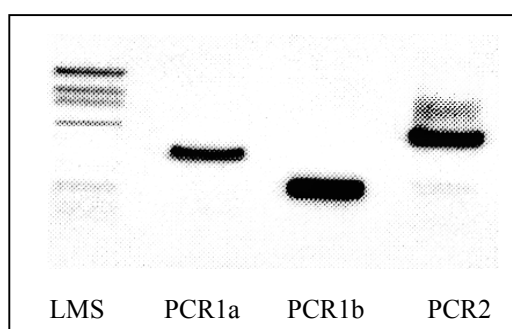


Figure 3.2: Reaction products from PCR 1 and PCR 2 of IL-4BP.

The fragments from PCR 1 (20-30 ng) were used as a template in PCR 2. Since the external primers specific for PCR 2 were in large excess compared to the amount of primers left from PCR 1a and PCR 1b, the purity of the reaction product was ensured. One of the external primers

in this step introduces a BamHI restriction site (WYH37) and the other (WYH38) contains a wild-type sequence. The product of PCR 2 has the length of 682 bp for all mutants in this method and yielded 1-3 µg DNA.

After the reaction mixture from PCR 2 was precipitated in a volume of 30 µl, and then digested by BamHI. The restriction product containing the mutated IL-4BP cDNA has a length of 635 bp. This fragment was isolated and purified exploring an agarose gel electrophoresis and glass milk elution. It was inserted into the baculovirus transfer vector pAcGP67B cut by BamHI (Appendix 3). The plasmid carrying the mutated IL-4BP (Figure 3.3) was then used for electrotransformation of competent *E.coli* (JM 103 recA⁻ or JM 109).

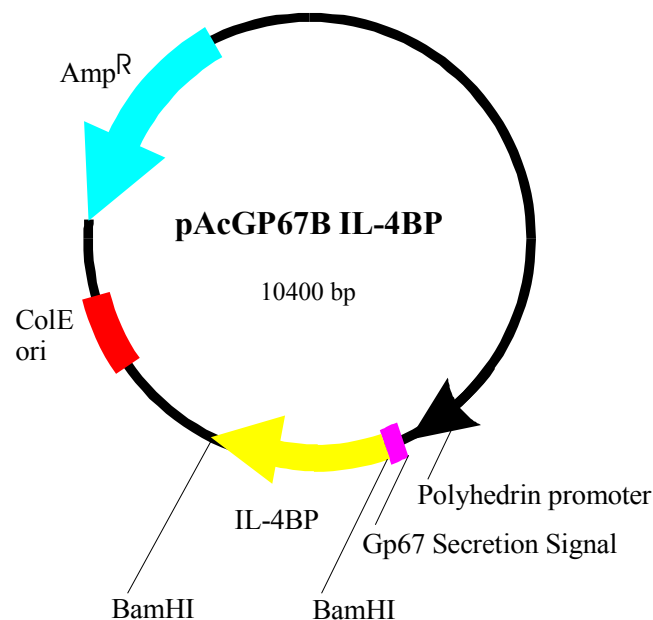
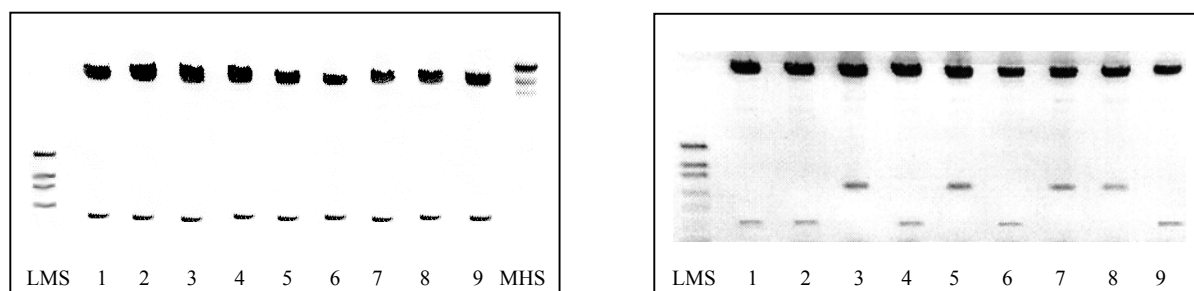


Figure 3.3: Baculovirus transfer vector pAcGP67B with cloned IL-4BP.

The first selection of plasmid-containing *E.coli* was performed by plating the transformation cell suspension on ampicillin agar plates. Since the plasmid contains an ampicillin resistance gene, only bacterial cells, which carry the plasmid pAcGP67B/IL-4BP, would be able to form colonies. The selection procedure was completed by analytical restriction endonuclease digestion. For this were prepared plasmid DNAs from several individual clones at analytical scale. The intact circular plasmids were digested first with BamHI to confirm the presence of IL-4BP in the plasmid. The positive clones showed a band of 635 bp after the restriction reaction, which was visualized on a 1 % agarose gel (Figure 3.4a). Only in few plasmid samples an IL-4BP insert was

not found. Most likely the reason that bacterial clones, which do not carry IL-4BP, grew up over agar plates, is not completed dephosphorylation of vector ends. Since only one cutting enzyme was used during cloning, the positive plasmid samples were analyzed by a second restriction reaction with EcoRV and SacI. The products from this reaction give information about the orientation of the inserted IL-4BP fragment within the plasmid pAcGP67B. The cutting site of SacI is unique and located asymmetrically within the cDNA sequence of IL-4BP. Therefore plasmids which inserted the IL-4BP cDNA parallel to the direction of transcription, showed after such restriction reaction a shorter fragment of 320 bp, and those of them which inserted it in the opposite direction were characterized by a fragment of 800 bp (Figure 3.4b). Usually, equal number of bacterial colonies representing both kinds of plasmids was detected, as it was theoretically expected.



a) Analytical restriction with BamHI. Lines 1 to 9 represent positive clones.

b) Analytical restriction with EcoRV and SacI. Lines 1,2,4,6 and 9 represent positive clones. Lines 3, 5, 7 and 8 represent clones which inserted the modified cDNA but in the “wrong” direction.

Figure 3.4: Analytical restriction of pAcGP67B containing the modified IL-4BP cDNA.

Plasmid DNA was isolated from clones, which were positive after all selection steps. Such preparations were used for sequence analyses and therefore another purification procedure was used which increased the amount and the quality of purified DNA (see 2.7.11.2). Sequencing was performed with 5'- and 3'- external primers (MF37 and WYH39). The sequence analysis confirmed the presence of the introduced mutation in all samples. No other mutations in the DNA sequence were detected. After the mutation was verified by sequencing, the mutant plasmid DNA was prepared at large scale for storage and following co-transfection (see 2.7.11.3). With the used method usually 20 to 30 mg of plasmid DNA were obtained from 40 ml of bacterial culture.

3.1.2 Co-transfection into SF9 Insect Cells and Amplification of the Recombinant Virus

The first step necessary to construct recombinant Baculoviruses was co-transfection of the transfer vector pAcGP67B containing mutated IL-4BP cDNA and BaculoGold DNA into SF9 insect cells. BaculoGold DNA is a modified AcNPV Baculovirus DNA, which contains a lethal deletion and does not code for viable virus. Co-transfection of the BaculoGold DNA with a complementing Baculovirus Transfer Vector, such as pAcGP67B, rescues the lethal deletion by homologous recombination. Since only the recombinant BaculoGold produces viable virus, a recombination frequency of 99 % is expected. To purify the stock of generated recombinant viruses during co-transfection, plaque purification was performed. The virus stock after co-transfection showed titer between 5×10^7 and 5×10^8 pfu/ml. Since each plaque represents a single virus, several individual plaques were randomly picked up and used to generate clonal virus populations. Usually, the plaques were picked up from plates corresponding to a viral dilution of $1:10^{-7}$ or $1:10^{-6}$. All clonal virus populations were separately amplified in two steps. A Western blot was performed with the virus supernatants to verify the protein production (Figure 3.5). The examined clones were compared to a sample of purified IL-4BP with known concentration. As expected, 100 % recombination efficiency was achieved during co-transfection and in all tested supernatants expression of IL-4BP was detected. The virus clone, which showed the largest amount of recombinant IL-4BP (clone 7), was selected for further amplification.

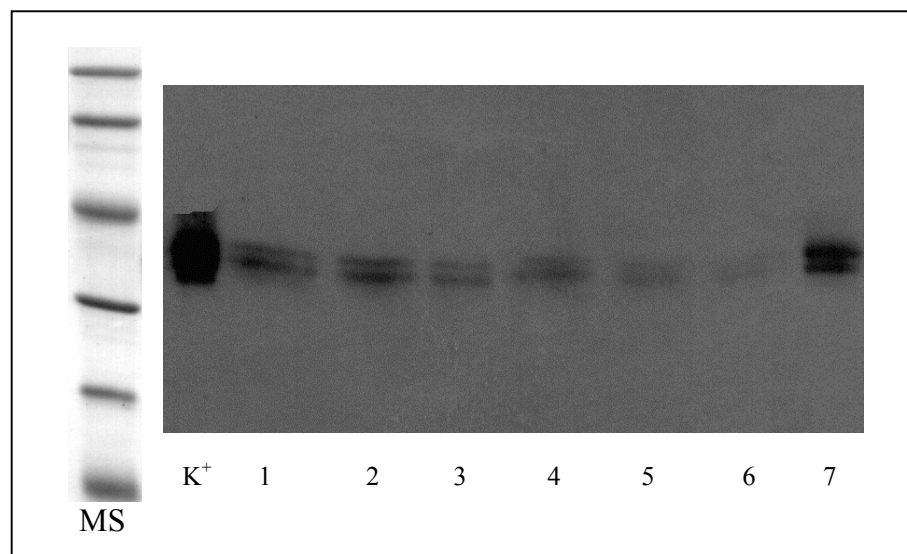


Figure 3.5: Western blot analysis of virus supernatants after the second virus amplification. MS, molecular standard; K⁺, positive control (40 ng); lines 1 to 7, examined recombinant virus clones. Clone 7 was chosen for further amplification.

Two additional steps of virus amplification were performed to produce a larger stock of recombinant virus with a high titer. Using a plaque assay the viral titer was determined to vary between 3×10^7 to 2×10^8 pfu/ml (Table 3.3). An aliquot was frozen for long-term storage and the rest was used to infect SF9 cells for expression of recombinant protein.

3.1.3 Expression and Purification of Recombinant IL-4BP and Its Variants

Recombinant proteins were expressed into SF9 insect cells after infection with high titer virus stock. For optimal protein production the MOI was estimated to be 5. The infected cells were incubated at 27°C for 3, 4, and 5 days and the protein content in the supernatant was examined. After the fourth day the level of expressed proteins did not increase and therefore 4 days were established as the optimal incubation time. Protein expression was performed in serum-free and serum-containing insect culture medium. The presence of serum increased the cell viability and respectively the amount of expressed protein. Since it did not interfere with the purification procedure, serum was kept in the expression medium. Under these conditions, the expression of recombinant IL-4BP and its variants from SF9 cells yielded 2-7 mg protein per liter of insect cell suspension (Table 3.3).

The modified cDNAs were cloned downstream of the gp67 signal sequence in the transfer vector, which ensured that the recombinant proteins were expressed as gp67 signal peptide fusion proteins. The signal peptide mediates the forced secretion of recombinant proteins. During the transport across the cell membrane, the signal peptide is cleaved. Therefore the mature recombinant proteins could be purified from the infection supernatant, which was collected at the end of the incubation period.

3.1.3.1 Purification of IL-4BP and its variants by IL-4 affinity column

The purification of IL-4BP and most of its mutated variants explored the high-affinity binding ($K_d \approx 100$ pM) of IL-4 to its receptor (Shen, 1996). A column, containing IL-4–Sepharose 6B gel was prepared and used for affinity chromatography. After the expression step, the clarified culture supernatant was passed over the affinity matrix and washed with PBS to clean the column from non-specifically bound proteins. The specifically bound IL-4BP and variants were eluted with 4 M $MgCl_2$. The protein amount and purity of the collected fractions were analyzed on a SDS-PAGE (Figure 3.6).

Table 3.3: Virus titer and protein expression of IL-4BP and its variants

Variant	Virus titer [pfu/ml]	Expressed protein [mg/l cell suspension]	Column used for purification
IL-4BP	1.8×10^8	7.0	IL-4
Y13A	5.6×10^7	4.0	Ab
Y13F	7.0×10^7	5.5	IL-4
L39A	1.0×10^8	4.0	IL-4
F41A	1.1×10^8	4.5	IL-4
L42A	2.2×10^8	7.5	IL-4
L43A	2.3×10^8	6.5	IL-4
D66A	1.5×10^8	3.0	IL-4
D67A	2.0×10^8	3.0	IL-4
V69A	1.5×10^8	3.0	IL-4
D72A	1.4×10^8	3.5	Ab
D72N	1.5×10^8	3.5	Ab
K91A	2.3×10^7	4.5	IL-4
K91D	1.5×10^8	4.0	IL-4
S93A	2.5×10^7	4.5	IL-4
D125A	4.0×10^7	3.5	IL-4
N126A	2.3×10^8	3.5	IL-4
Y127A	6.0×10^7	2.0	IL-4
Y127F	8.0×10^7	6.0	IL-4
L128A	2.3×10^8	2.0	IL-4
Y183A	1.3×10^8	3.5	Ab
Y183F	7.0×10^7	4.5	IL-4
Y13F/L39A	4.0×10^7	2.5	Ab
Y13F/F41A	2.2×10^8	3.5	Ab
Y13F/D67A	5.5×10^7	3.0	Ab
Y13F/V69A	3.8×10^7	2.5	Ab
Y13F/D72N	8.0×10^7	3.5	Ab
Y13F/Y127A	2.2×10^7	3.5	Ab
Y13F/Y183F	5.2×10^7	3.5	Ab
D72N/L39A	7.9×10^7	2.5	Ab
D72N/F41A	8.0×10^7	3.5	Ab
D72N/D67A	6.0×10^7	3.0	Ab
D72N/V69A	4.3×10^7	3.5	Ab
D72N/Y127A	6.7×10^7	2.5	Ab
D72N/Y183F	9.0×10^7	3.0	Ab

Usually, the first 3 to 4 fractions showed concentrations of pure protein in the range of 100 – 400 $\mu\text{g/ml}$ and in the rest of the fractions the protein was either of an inadequate quality either of an insignificant quantity. The best fractions were collected together, dialyzed against PBS and concentrated by ultrafiltration to a total volume of 1.5 ml. The amount of protein in the concentrated samples was determined by spectrophotometry and the purity was examined on a SDS-PAGE. No difference was found between the quality of protein samples expressed in the presence of FCS or in FCS-free culture medium.

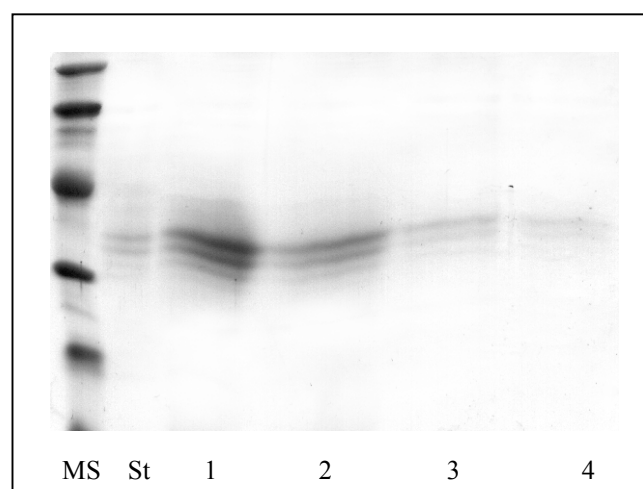


Figure 3.6: Fractions after purification via IL-4 affinity column (variant F41A). MS, molecular standard; St, standard of IL-4BP (1 μg); lines 1, 2, 3, 4, fractions 1 to 4, respectively.

IL-4BP and its variants produced in SF9 insect cells are extensively glycosylated. Accordingly, on SDS gels they migrate as two bands with apparent molecular masses of 35 kDa and 32.5 kDa. Respectively, variant N73A where a potential N-glycosylation site was modified exhibited only one band, corresponding to 32.5 kDa (Figure 3.7).

Using the IL-4 affinity column successfully were purified IL-4BP, most variants included in the alanine screening (L39A, F41A, L42A, L43A, D66A, D67A, V69A, N73A, K91A, S93A, D125A, N126A, Y127A, and L128A), variants in which the original tyrosine amino acid was exchanged by phenylalanine (Y13F, Y127F, and Y183F) and variant K91D (Table 3.3, Figure 3.7). The total amount of pure protein varied between 200 μg and 1 mg. A correlation between the protein amount and purity on the one side, and the subsequently determined binding affinity on the other, was observed for the variants purified by an IL-4 affinity column. Mutated variants

that later showed a similar K_d to this which characterizes the interaction between IL-4 and IL-4BP in BIAcore measurements, were yielded in larger amount and with better quality than the variants which exhibited greater values of K_d .

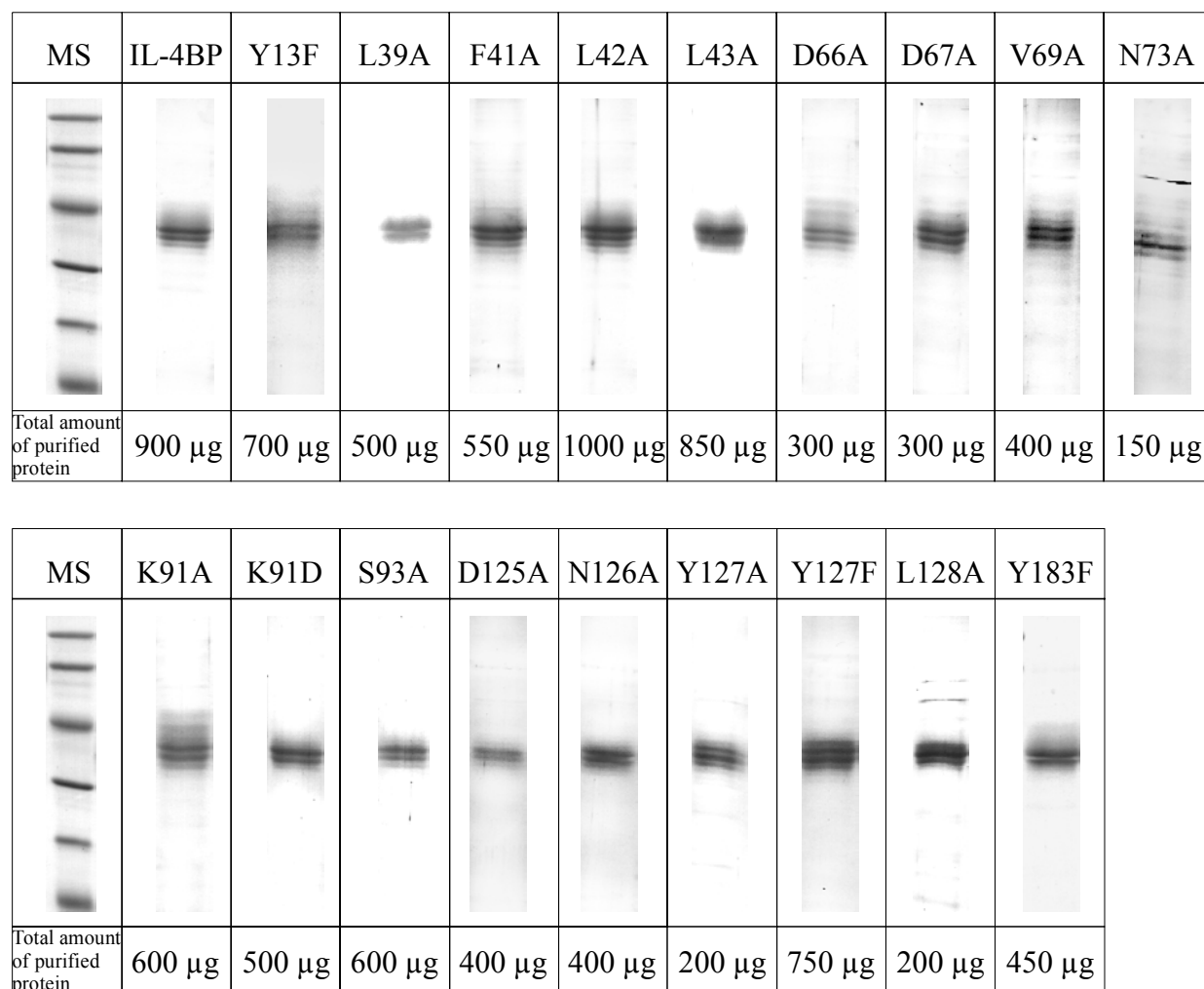


Figure 3.7: Variants purified by an IL-4 containing affinity column.

Figure 3.8 shows the result of the purification of variant D72A via IL-4 affinity column in comparison to IL-4BP, which was prepared in parallel. Since it was the first variant for which the purification step did not give a useful protein and the Western blot showed lower levels of expression, contamination in the virus clone was considered and a new viral stock was prepared. A Western blot after subcloning revealed that the newly generated viral clones expressed the recombinant protein in amounts comparable to all other variants, which were already successfully purified. Despite the convincing expression demonstrated by Western blot, the second attempt for

purification through an IL-4 affinity column failed again. Significant amount of recombinant protein was found in the flow-through fraction, which indicated that the column failed to bind specifically variant D72A.

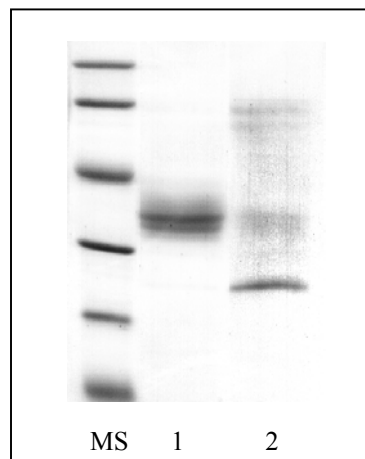


Figure 3.8: Purification of variant D72A via IL-4 affinity column. Line 1 represents IL-4BP and line 2, variant D72A. Both samples were loaded after dialysis and concentration.

Those experiments led to the conclusion that the purification problems did not concern expression levels, rather the affinity of variant D72A to IL-4 and respectively to the affinity column. Since D72 was suggested to be one of the most prominent amino acids implicated in the interaction with IL-4, the alanine substitution at this position was considered to affect the functional epitope to such an extent that the binding properties of variant D72A were altered completely. Therefore to exam the contribution of D72 in the receptor ligand interaction, an alternative variant was designed. In the additional variant the aspartic acid at position 72 was replaced by asparagine, which is a more conservative substitution and was expected to influence the binding affinity to IL-4 to a minor degree. Surprisingly, variant D72N was not able to bind to the IL-4 affinity column and demonstrated already during the purification procedure lower binding affinity to IL-4 than anticipated. At a later stage of the study, similar purification problems occurred also with variant Y13A and all double mutants included in the study. This was the first indication that the variants mentioned above would demonstrate extremely low binding affinity to IL-4 during BIAcore measurements.

The purification of variant Y183A through IL-4 affinity column resulted in larger amount of protein compared to D72A and D72N. Although the sample was determined to contain a fraction

that migrated on a SDS-PAGE as IL-4BP, generally the purity was of inadequate quality. Since the interaction between variant Y183A and IL-4 was characterized by $K_d \approx 60$ nM, such a constant value seems to settle the affinity limits for purification of IL-4BP variants by the IL-4 affinity column.

3.1.3.2 Purification of IL-4BP variants through Antibody column

All IL-4BP variants, which could not be purified through the IL-4 affinity column, in spite of these negative results, demonstrated an intensive signal when they were examined by Western blot. As an example, Figure 3.9 represents the protein expression of variants Y13A, D72A, D72N, and Y183A, in SF9 insect cells. For detection was used the monoclonal Ab X14/38, against the extracellular domain of IL-4R. Those results suggested that despite the introduced mutation, the mAb X14/38 still recognizes the modified proteins. Obviously, two different and independent epitopes within the IL-4BP molecule are responsible for the high-affinity interaction with IL-4 and the recognition events with the used mAb. Therefore, even when the affinity to IL-4 was affected due to a mutation introduced in the IL-4-binding epitope, the anti-IL-4BP mAb X14/38 was still able to recognize specifically the IL-4BP modified forms.

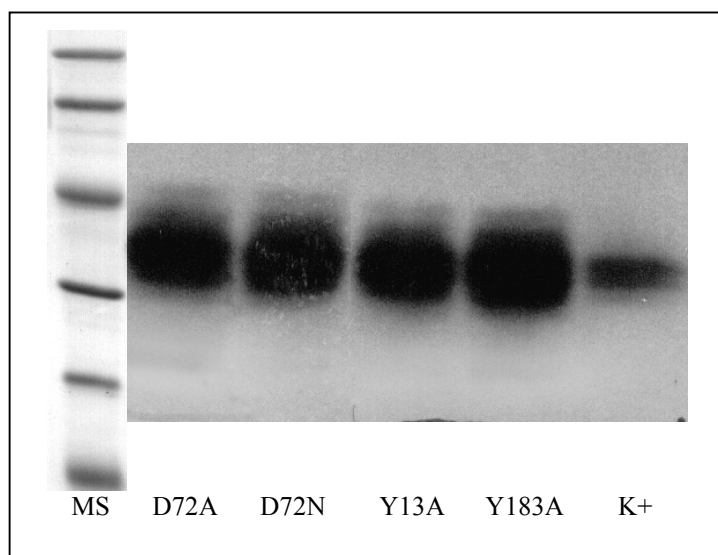


Figure 3.9: A Western blot of some IL-4BP variants, which could not be purified using the IL-4 affinity column, demonstrated intensive signals after detection with the mAb X14/38.

Based on these conclusions, the mAb was used to prepare a column for purification of those IL-4BP variants, which failed to be purified by the use of the IL-4 affinity column. To examine the qualities of the new column and to find a suitable purification procedure, it was tested by purification of IL-4BP. At first, conditions similar to these already established for the IL-4 affinity column were tested. After expression in SF9 cells, the clarified supernatant was applied to the column. A washing step with 10 column volumes of PBS was performed. The protein was eluted with 4 M MgCl₂ and the first 10 collected fractions were examined on a SDS-PAGE. Fractions 1 to 4 showed IL-4BP which purity was comparable to the IL-4BP sample purified by the IL-4 affinity column. These fractions were combined and the procedure was completed by dialysis against PBS and concentration by ultrafiltration. In the analyzed fractions no traces of the mAb X-14-38 released from the column were found. The Ab containing column was washed with 20 volumes of PBS and a following purification of IL-4BP was performed to verify whether the column was able to regenerate or not. The collected fractions from the second purification were examined spectrophotometrically and on a SDS-PAGE. Both analyses confirmed that the column recovered fully and could be successfully used more than once. Experiments with different column flow rates indicated that the sample had to be applied slower than to the IL-4 column. A flow rate of 0.5 ml/min was established as optimal.

Purification following the described procedure was performed with the variants that failed to be purified via IL-4 affinity column. In all experiments the first 3 to 4 eluted fractions contained a pure protein, which on a SDS-PAGE migrated in parallel to IL-4BP (Figure 3.10).

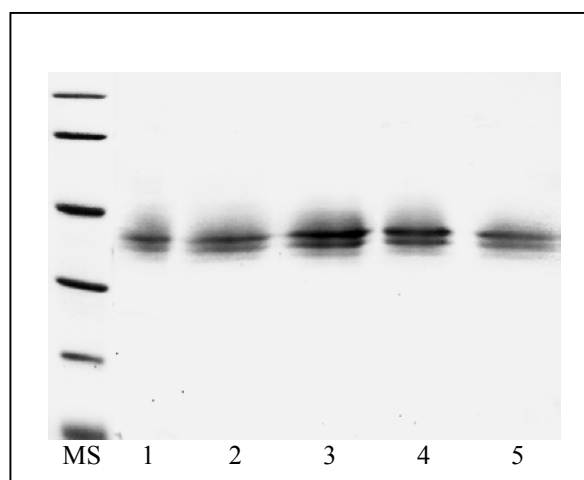


Figure 3.10: Purification of variant D72A through an Ab column. Line 1 represents a control of IL-4BP, lines 2 to 5 correspond to fractions 1, 2, 3, and 4 of D72A, collected during the purification.

Generally, the protein concentration was lower than in the corresponding fractions for variants purified by the IL-4 column and varied between 50 and 200 $\mu\text{g/ml}$. The flow-through was examined and residual protein was found there. This suggested that the lower protein concentration resulted from a low capacity of the Ab column, rather than from low expression levels. However, the column capacity was not optimized, since the amount of pure proteins was sufficient for the following experiments.

The Ab containing column was used to purify variants Y13A, D72A, D72N, Y183A, Y13F/L39A, Y13F/F41A, Y13F/D67A, Y13F/V69A, Y13F/Y127A, Y13F/Y183F, D72N/L39A, D72N/F41A, D72N/D67A, D72N/V69A, D72N/Y127A, D72N/Y183F, and Y13F/D72N (Table 3.3, Figure 3.11).

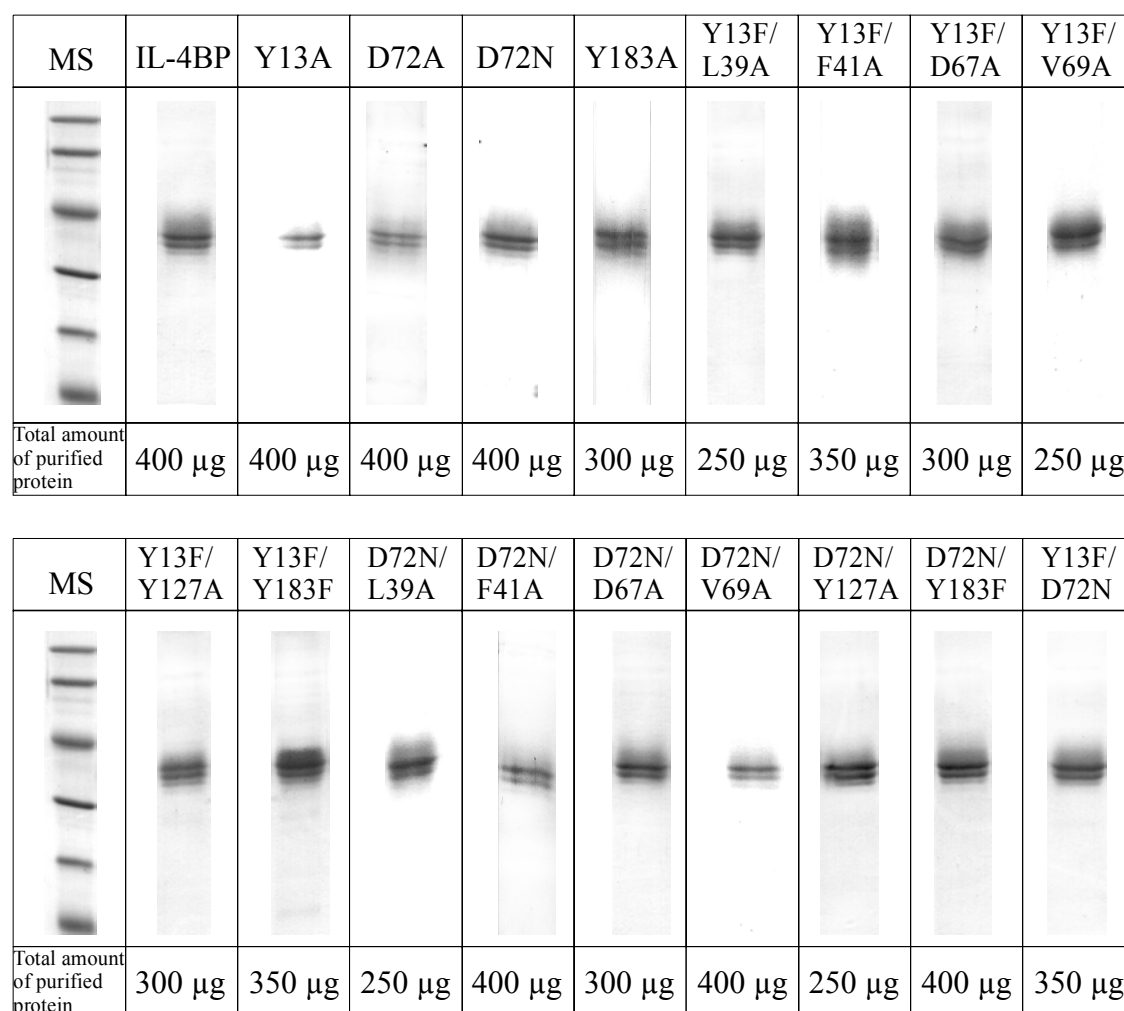


Figure 3.11: A full collection of proteins purified by a column containing a mAb against IL-4BP (X14/38).

None of them failed to be purified, confirming that the substituted amino acids are located out of the epitope recognized by X14/38. Accordingly, independent on the kind of introduced mutation and its modifying effect on the measured binding affinity, all analyzed protein samples showed similar purity. There was no correlation between the protein quantity and the extent to which a mutation affected the binding properties.

In summary, an alternative procedure for purification of IL-4BP and its variants through an Ab containing column was established. The new purification method is simple for accomplishment and very similar to the methods for purification required by the IL-4 column. That makes possible the simultaneous and reversal use of both columns for more effective purification.

3.1.4 Biotinylation of IL-4BP Recombinant Variants

The IL-4BP recombinant variants purified by affinity chromatography or antibody column were biotinylated following the procedure described in 2.9.6. The biotinylated protein samples were further purified using gel filtration. During the purification step around 50-60 % of the protein was lost. Therefore the biotinylated proteins were in a final concentration range between 20 and 70 $\mu\text{g/ml}$ and the total protein amount varied between 30 and 80 μg . For each variant was prepared a dilution with protein concentration of 1 $\mu\text{g/ml}$, which was further used in biosensor experiments.

3.2 Preparation of Recombinant IL-4 Variants

Although a collection of different IL-4 variants was previously analyzed, within the framework of the presented project two more amino acids of IL-4 were substituted by alanine. The crystal structure of the complex between the human IL-4 and IL-4BP suggested a contribution of R53 and Y56 to possible contacts with the receptor part. Both amino acids are located on helix B of IL-4 and are part of the second discrete cluster of *trans*-interacting residues within the binding epitope (Hage et al., 1999).

3.2.1 Cloning of IL-4 Mutant Variants

The cDNA of IL-4 was inserted into the expression vector R^{TS}pRC109 under the control of the right λ -phage promoter (Figure 3.12; Appendix 4). The regulation of the transcription was performed through the temperature sensitive repressor cI185, which is also encoded by this expression plasmid.

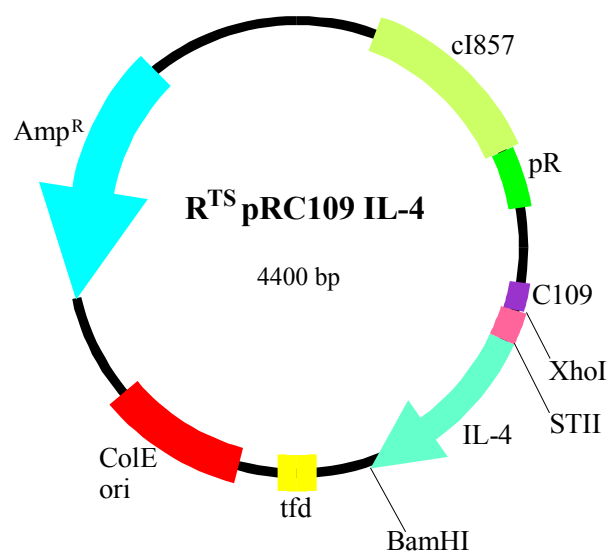


Figure 3.12: Schematic diagram of expression vector R^{TS}pRC109/IL-4.

The variant Y56A was generated by cassette mutagenesis. A synthetic doublestranded DNA cassette which carried the mutation of interest was inserted between engineered restriction

endonuclease cutting sites of AflIII and MluI. The complete nucleotide and amino acid sequence of hIL-4 cDNA with the restriction sites of both endonucleases is shown in Figure 3.13.

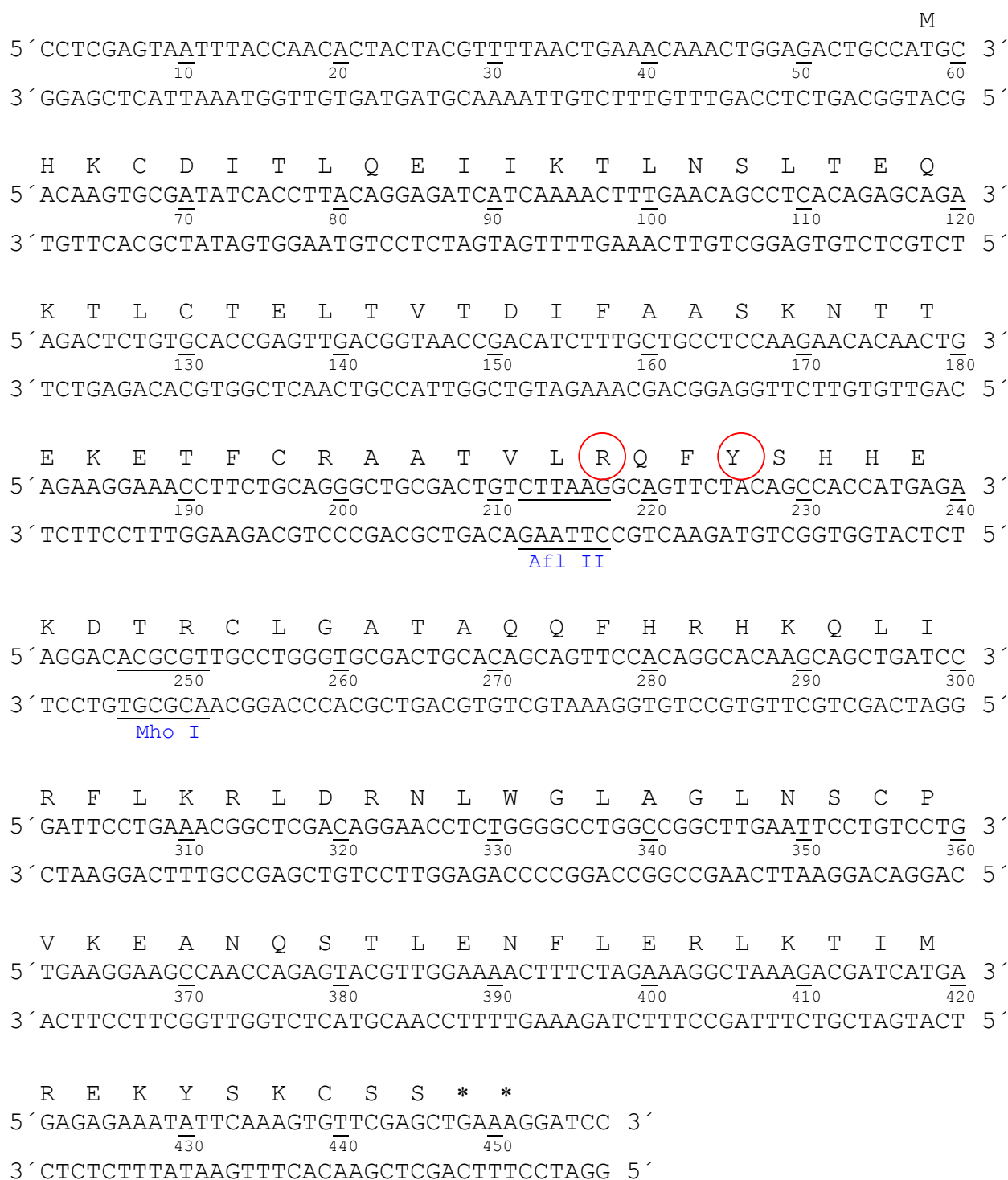


Figure 3.13: Nucleotide and amino acid sequence of the hIL-4 cDNA. The modified residues are encircled. The endonuclease restriction sites of Afl II and Mlu I were used for cassette mutagenesis.

Both complementary oligonucleotides were first phosphorylated, hybridized and then ligated into the vector, which was cut, by AflIII and MluI. E.coli cells (JM109) were transformed with the plasmid R^{TS}pRC109IL-4Y56A by electroporation.

Since there were not available any suitable endonuclease restriction sites which could be used to mutate R53, the site-directed mutagenesis of the variant R53A was accomplished by means of PCR technology. Similarly to the approach used to mutate IL-4BP, a two-step PCR was performed. The products resulting from the first step (PCR 1a and PCR 1b), when the mutation was introduced by internal primers, had lengths of 455 bp and 629 bp, respectively. They were used as a template for PCR 2. During this reaction, with the help of two external primers, a product of 1057 bp was synthesized (Figure 3.14).

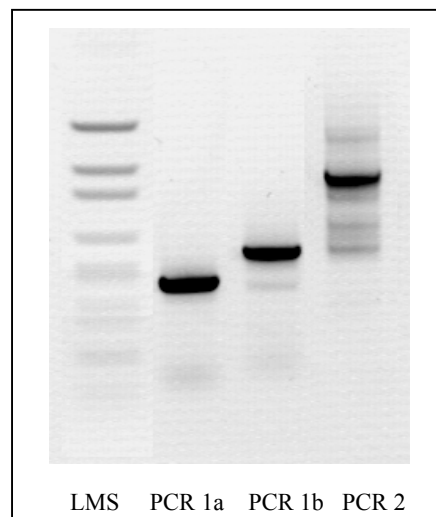


Figure 3.14: Amplification products from the PCR induced mutagenesis of variant R53A.

The PCR 2 reaction product was precipitated and then cut with restriction enzymes XhoI and BamHI to produce 3 fragments with the length of 230 bp, 450 bp, and 380 bp. The digestion mixture was separated by an agarose electrophoresis and the 450 bp fragment containing the mutated IL-4 cDNA was isolated and purified from the gel. The pure fragment was used in a ligation reaction with the XhoI/BamHI digested expression vector R^{TS}pRC109. Electrocompetent E.Coli (JM 109) were transformed with the recombinant plasmid.

The transformed E.Coli were plated on selective ampicillin containing medium. Plasmid DNAs from a few bacterial colonies representing both variants were isolated for analytical application. The intact circular plasmids were digested with restriction enzymes XhoI and BamHI to confirm the presence of the insert. All analyzed plasmid samples after separation on an agarose gel,

showed the 450 bp fragment representing the hIL-4 cDNA. In addition, the exact DNA sequence and the presence of the mutation were verified by DNA sequencing with 5'- and 3'- external primer.

3.2.2 Expression and Purification of IL-4 Variants

For expression of IL-4 variants, E.coli was cultivated until reaching early logarithm phase with OD₅₅₀ of 0.5-0.6 and then induced by heating at 42°C and incubated for 3 h. Under these conditions, the recombinant IL-4 variants were expressed as insoluble aggregate form (inclusion bodies) in the cell cytoplasm. The amounts of bacterial cells and inclusion bodies for both variants, which were obtained from 1 liter of E.coli culture, are compared in Table 3.4.

Table 3.4: The yields at different steps of preparation of recombinant proteins for the IL-4 variants.

Variant	Cells	Inclusion bodies	Protein [mg]	
	[g]	[g]	(after CM-Sepharose)	(after HPLC)
	(per 1 liter of E.Coli culture)			
R53A	3.1	1.3	1.6	0.6
Y56A	3.8	1.7	1.7	0.9

The inclusion bodies were completely dissolved in 6 M guanidine hydrochloride (GuHCl), pH 8.0. To reduce the disulfide bonds between cysteine residues and to accomplish the protein denaturation, 0.1% of β -mercaptoethanol was added. The renaturation of the protein to its native form was achieved by slow dialysis in PBS.

Since the pI of hIL-4 is 10.5 (Callard, R. & Gearing A, 1994) the refolded proteins were applied to a CM-Sepharose matrix at pH 5.0. During this cation-exchange chromatography, the acidic and neutral contaminating proteins, which comprised most of the impurities, could not bind to the column and therefore the IL-4 variants were effectively separated. The bound proteins were eluted using a linear salt gradient from 0 M NaCl to 0.5 M NaCl. Only a limited amount of basic contaminating proteins overlapped with the IL-4 pick (Figure 3.15). After this step, the purity of the IL-4 variants reached over 90%.

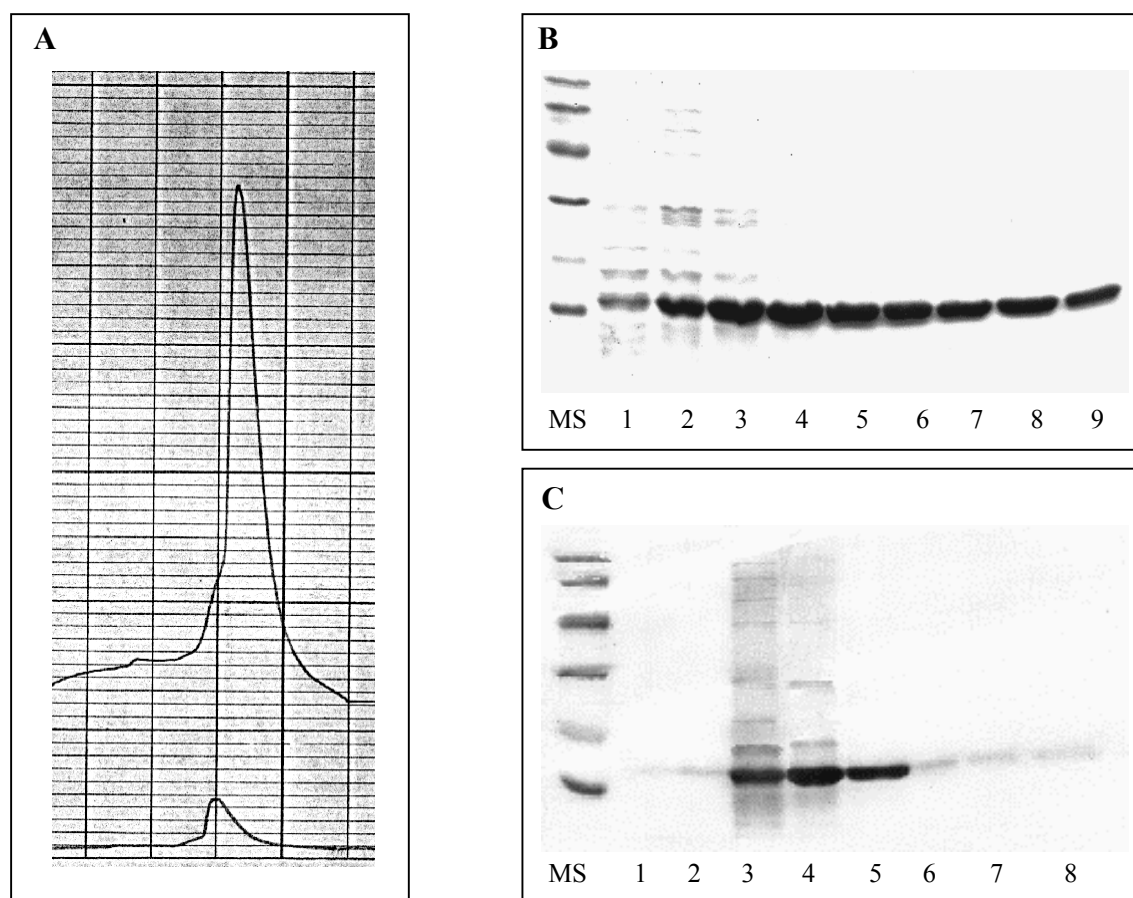


Figure 3.15: Purification of the IL-4 variants through CM-Sepharose column. (A) The elution chart of variant Y56A. (B) SDS-PAGE analysis of collected fractions for variant R53A. The fractions represented here by lines 3, 4, 5, 6, 7, and 8 were selected for following purification. (C) SDS-PAGE of the fractions collected during the purification of the variant Y56A. The fractions represented by lines 4 and 5 were further purified. MS, molecular standard.

Further, the protein purification was accomplished by reversed phase HPLC. Based on hydrophobic interactions, the protein bound to the chromatography matrix and then elution with increasing concentration of acetonitrile was performed (Figure 3.16 A). The IL-4 variants were eluted at around 40% of acetonitrile. Both variants were successfully purified, suggesting that neither the protein refolding neither the protein stability were disrupted by the individual mutations. The collected fractions during HPLC were monitored by SDS-PAGE, which revealed high purity of the obtained protein (Figure 3.16 C, D). In addition, the purity and the refolding quality of the proteins were examined by analytical RP-HPLC performed in a small column with detective sensitivity of 0.08. Both variants showed only a single sharp peak confirming the high homogeneity of the analyzed samples (Figure 3.16 B). The highly purified proteins were divided into aliquots lyophilized and in this way stored for following experiments.

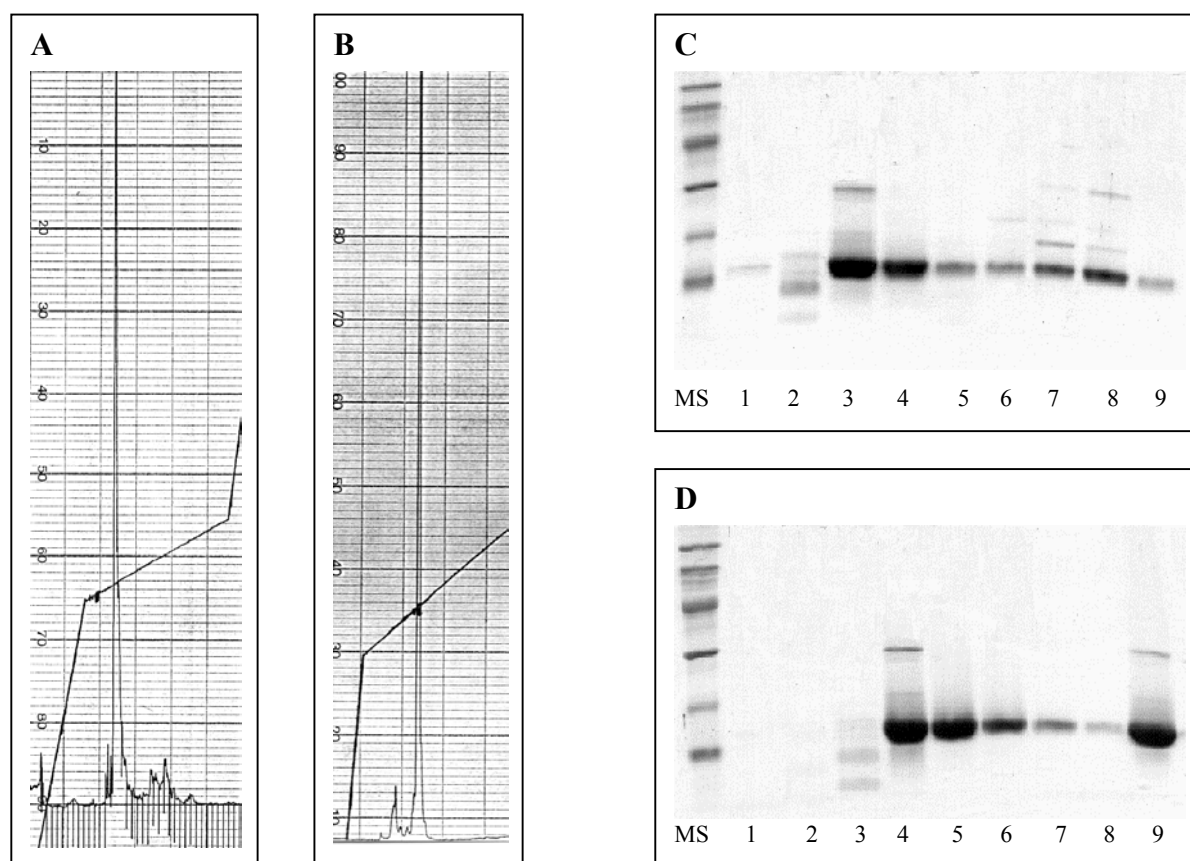


Figure 3.16: HPLC purification step of the IL-4 variants. (A) The elution chart of the variant Y56A. (B) Analytical HPLC of variant Y56A. (C) SDS-PAGE of variant R53A. The fraction represented by line 3 was chosen for further applications. (D) SDS-PAGE of the fractions collected for variant Y56A. The fractions represented by lines 4 and 5 were combined (line 9) and used in following experiments. MS, molecular standard.

3.3 Kinetic Analysis of the Interaction of IL-4 with the IL-4BP Variants Using BIAcore Technology

The purified IL-4BP and its variants were used in a biomolecular examination to determine both, the kinetic and equilibrium binding constants characterizing the interaction with the ligand. This comprehensive analysis was carried out to assess the roles of the mutated side chains in modulating the affinity and kinetics of binding.

A biosensor technology that relies upon surface plasmon resonance to measure changes in refractive index upon ligand binding to an immobilized receptor was explored to record binding curves and to evaluate the kinetic parameters of the interaction. The evaluation methods are described in 2.13.2.

3.3.1 Immobilization of the Biotinylated IL-4BP and its Variants on the Sensor Chips

Among the several available immobilization techniques, the amine coupling and streptavidin-biotin coupling had been chosen to immobilize IL-4BP and its mutated variants on sensor chips. Earlier experiments have proven that this method offered a higher ligand binding capacity of the chip, considering the certain amount of immobilized receptors (Shen et al., 1996). The reason for this seems to be the nonspecific nature of the amine coupling technique and stereo obstacle, which gives rise to association perturbation of IL-4 to IL-4BP. Therefore the streptavidin-biotin coupling was used as a standard immobilization method in this study.

First, the four cells of a sensor chip CM5 were coated with streptavidin employing the amine coupling procedure as described in 2.13.1 (Figure 3.17). Thereafter, the matrix of flow cells 2, 3 and 4 was loaded separately with different IL-4BP variants, which earlier were randomly biotinylated (Figure 3.18). No receptor was loaded onto flow cell 1. It was used to record a background sensogram that was subtracted during the evaluation from the sample sensograms in flow cells 2, 3 and 4.

Experimental conditions connected with different density of the immobilized receptor were tested. Usually, in the beginning the variants were loaded on the chip with a density of approximately 150 RU. Since the streptavidin-biotin interaction has an extremely high affinity ($\sim 10^{15} \text{ M}^{-1}$) (BIAcore Handbook, 1995) the chips could be repeatedly regenerated and the amount of the immobilized receptor could be increased. For low affinity variants more receptor was added to the chip until a density of 200, 400 or 500 RU was reached (Table 3.5).

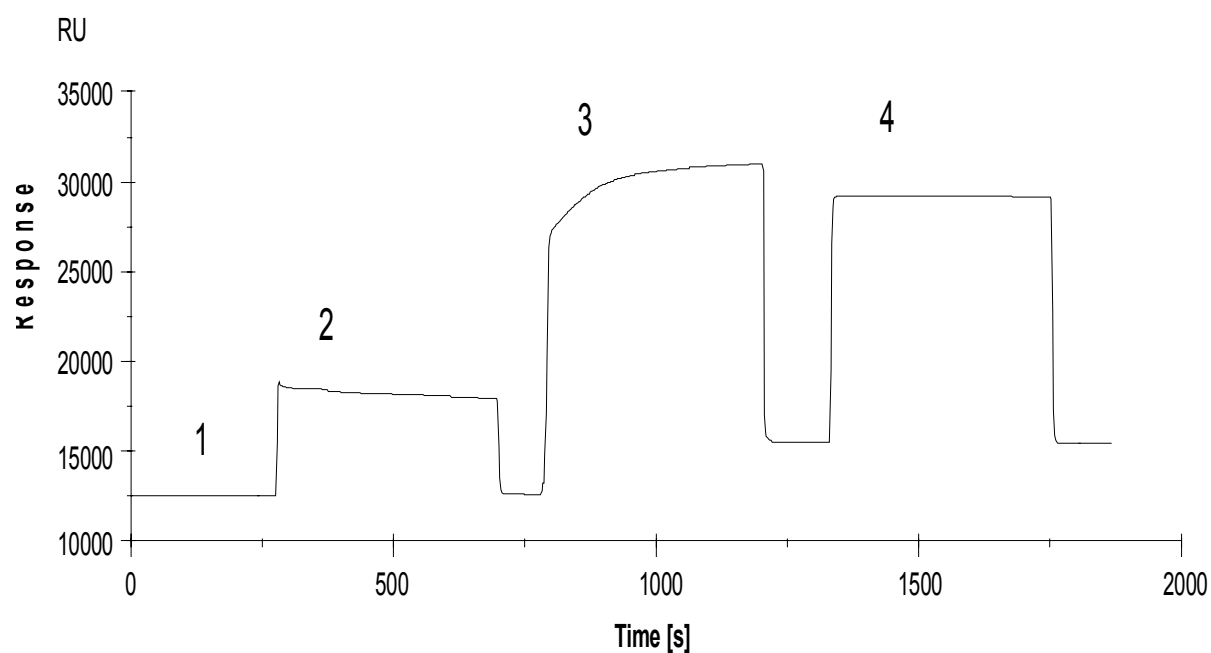


Figure 3.17: Sensogram showing the immobilization of streptavidin on a sensor chip CM5 by using standard amine coupling. (1) Baseline signal for the unmodified sensor chip treated with continuous flow buffer HBS (5 $\mu\text{l}/\text{min}$). (2) Injection of 35 μl of NHS/EDC for 7 min. to activate the dextran matrix. (3) 7 min. injection of 35 μl of streptavidin (50 $\mu\text{g}/\text{ml}$). (4) Injection of 35 μl of ethanolamine hydrochloride (1 M) to deactivate the matrix and remove non-covalently bound streptavidin.

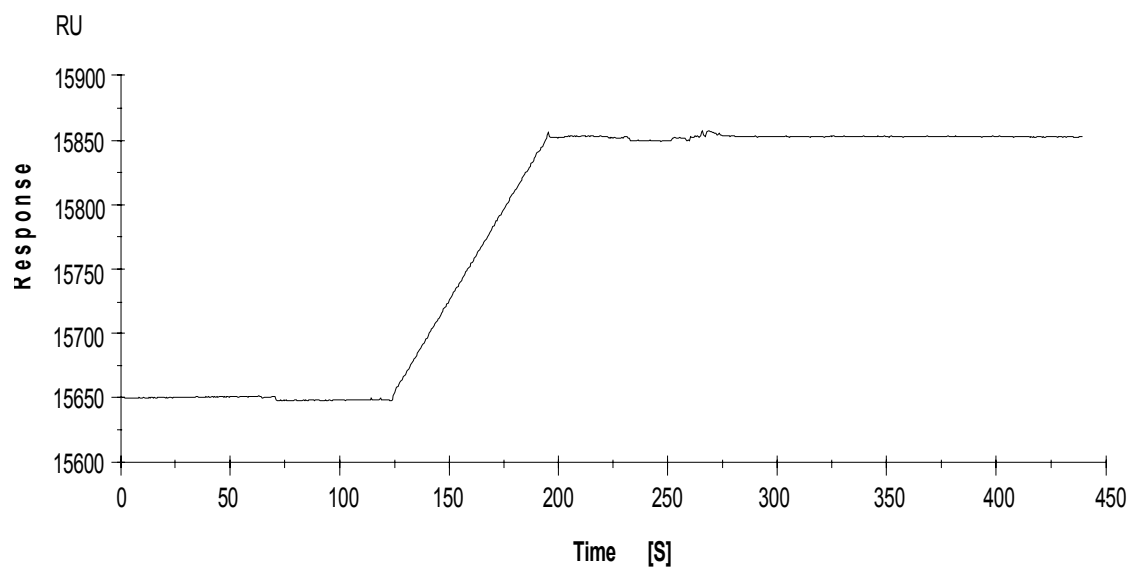


Figure 3.18: Immobilization of an IL-4BP variant on a streptavidin chip. The protein was manually injected into the chip and the injection was stopped at 200 RU.

Table 3.5: Amount of the immobilized receptor at the biosensor matrix for IL-4BP and the different variants

Receptor variant	Immobilized protein		
	[g]	[M]	Rel. Resp. [RU]
IL-4BP	4.0×10^{-10}	6.6×10^{-11}	79
Y13A	5.4×10^{-9}	3.3×10^{-10}	243
Y13F	2.8×10^{-10}	6.7×10^{-11}	89
L39A	2.8×10^{-10}	6.7×10^{-11}	103
F41A	6.4×10^{-10}	6.7×10^{-11}	151
L42A	5.6×10^{-10}	6.7×10^{-11}	151
L43A	7.4×10^{-10}	6.7×10^{-11}	148
D66A	7.0×10^{-10}	1.6×10^{-10}	163
D67A	6.7×10^{-10}	1.1×10^{-10}	157
V69A	3.4×10^{-9}	3.3×10^{-10}	503
D72A	6.4×10^{-10}	1.8×10^{-10}	225
D72N	6.1×10^{-10}	1.7×10^{-10}	223
K91A	5.6×10^{-10}	6.6×10^{-11}	154
K91D	1.6×10^{-9}	6.6×10^{-11}	145
S93A	8.4×10^{-10}	6.6×10^{-11}	152
D125A	5.6×10^{-10}	6.6×10^{-11}	152
N126A	7.0×10^{-10}	1.7×10^{-10}	156
Y127A	2.3×10^{-9}	2.9×10^{-10}	505
Y127F	2.4×10^{-10}	6.6×10^{-11}	102
L128A	4.0×10^{-10}	1.7×10^{-10}	154
Y183A	9.4×10^{-10}	6.7×10^{-11}	152
Y183F	3.6×10^{-10}	6.6×10^{-11}	94
Y13F/L39A	2.0×10^{-10}	3.3×10^{-10}	128
Y13F/F41A	7.0×10^{-10}	2.6×10^{-10}	97
Y13F/D67A	4.0×10^{-10}	3.3×10^{-10}	136
Y13F/V69A	7.0×10^{-10}	1.7×10^{-10}	216
Y13F/D72N	8.0×10^{-9}	1.3×10^{-10}	423
Y13F/Y127A	6.0×10^{-10}	1.8×10^{-10}	225
Y13F/Y183F	7.0×10^{-10}	1.9×10^{-10}	248
D72N/L39A	1.0×10^{-9}	1.7×10^{-10}	417
D72N/F41A	1.1×10^{-9}	1.7×10^{-10}	400
D72N/D67A	1.3×10^{-9}	1.7×10^{-10}	394
D72N/V69A	1.1×10^{-9}	1.7×10^{-10}	413
D72N/Y127A	1.2×10^{-9}	1.7×10^{-10}	410
D72N/Y183F	9.5×10^{-9}	1.8×10^{-10}	407

3.3.2 Kinetics of the Interaction of IL-4 and IL-4BP

Although the kinetics of binding of IL-4 to IL-4BP was investigated in a earlier study (Shen et al., 1996), similar measurement was performed again as a control basis of estimation the changes in binding affinity of the mutated variants. Experiments were performed with IL-4 concentrations of 2.5, 5.0 and 7.5 nM (Figure 3.19). The sensograms, which recorded the interaction of IL-4 and IL-4BP at different IL-4 concentrations, showed the typical model of extremely fast association and slow dissociation, observed earlier.

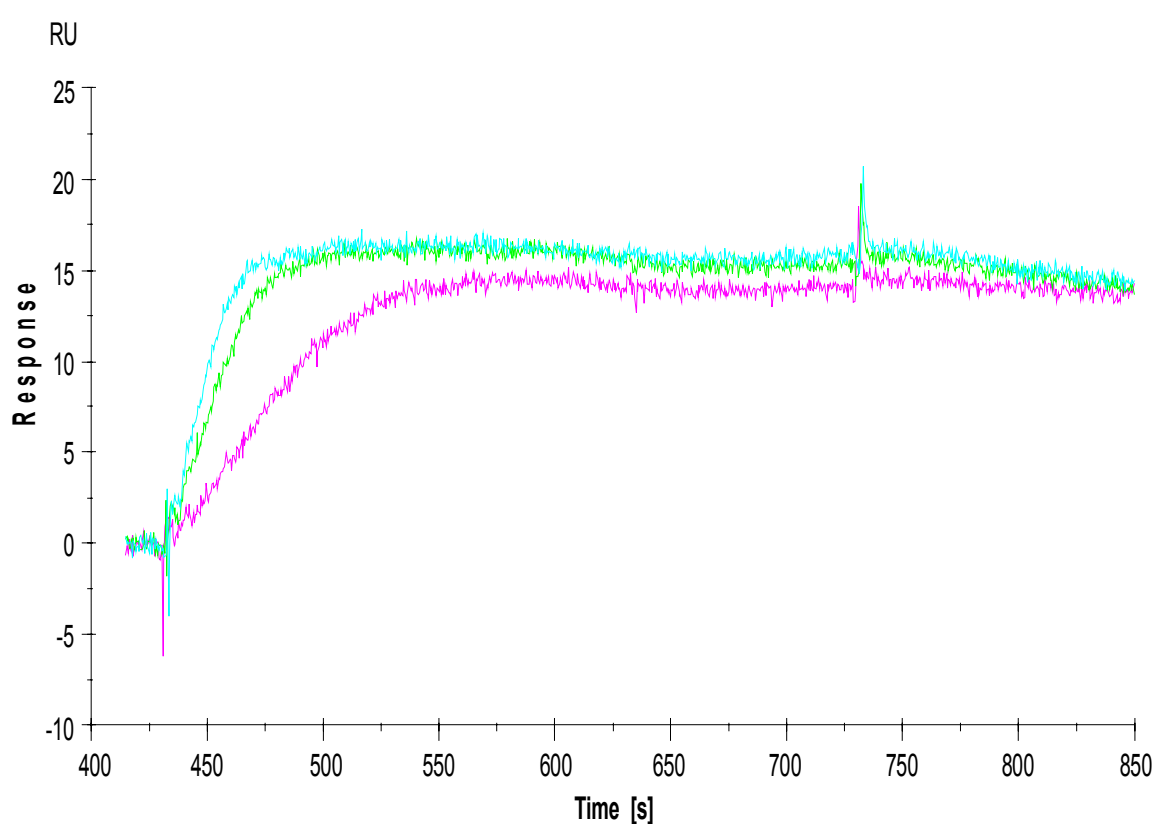


Figure 3.19: Overlay of sensograms showing the binding of IL-4 to the immobilized IL-4BP. IL-4 at concentrations of 2.5, 5.0 and 7.5 nM was applied.

Both, the association and dissociation phases were evaluated with BIAevaluation software to yield the association (k_{on}) and dissociation (k_{off}) rate constants, respectively (Figure 3.20). Due to the very fast association that in the beginning was diffusion controlled, only a small window (5 RU) could be evaluated for calculation of the association rate constant before attaining equilibrium. Based on this, the association rate constant was determined to be $k_{on}=1.3 \times 10^7 \text{ M}^{-1} \text{ s}^{-1}$. The dissociation phase commenced when the perfusion with IL-4 was exchanged to a perfusion

with buffer alone. An exponential dissociation of the complex occurred only during a short initial period of 10 s. This part of the sensogram was used to evaluate the dissociation rate constant as $k_{\text{off}} = 1.0 \times 10^{-3} \text{ s}^{-1}$.

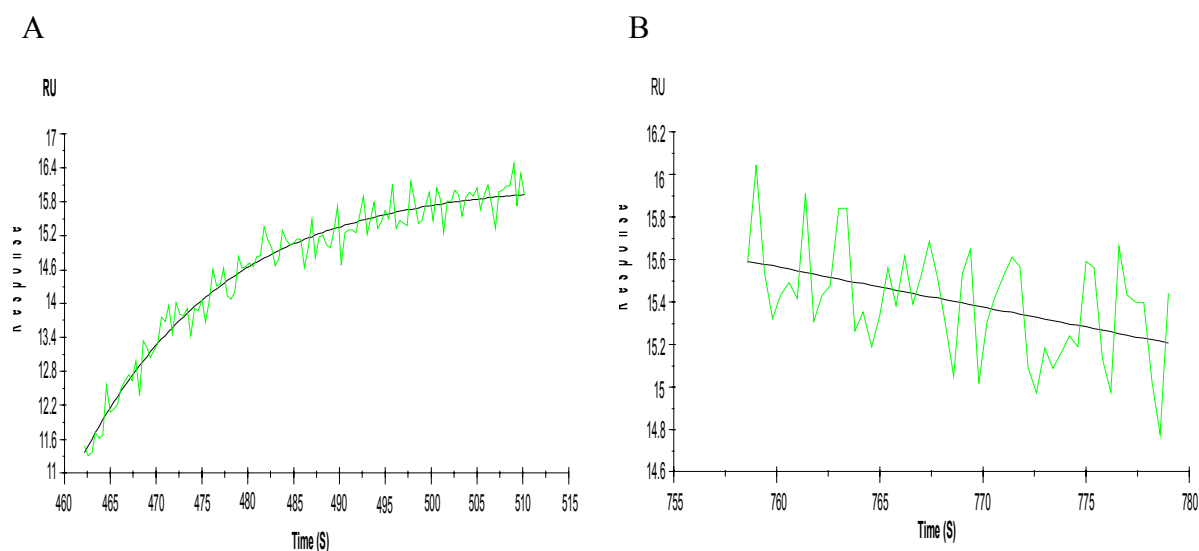


Figure 3.20: Association (A) and dissociation (B) plots of the recorded interaction of IL-4 and IL-4BP.

The constant phase of the sensogram represents the equilibrium level between the IL-4 dissociation and association reached at a defined IL-4 concentration. Usually, this part is evaluated for calculation of the equilibrium dissociation constant K_d . However, this was not possible during the present analysis because of technical reasons. The low K_d characterizing the IL-4/IL-4BP interaction would have required such low concentrations of IL-4 which could not be handled with the used technical device. Therefore, the equilibrium dissociation constant K_d was determined from the ratio of the association and dissociation constants ($k_{\text{off}}/k_{\text{on}}$) to be 77 pM.

The results of the kinetic analysis were not only reproducible in the frame of the presented experiments, but they are also comparable with the findings of all previous studies dealing with this interaction. The association rate constant fits in completely with the earlier established range of $1.3\text{-}1.8 \times 10^7 \text{ M}^{-1}\text{s}^{-1}$. Previously, the dissociation rate constant was evaluated as $k_{\text{off}} = 1.5\text{-}2.1 \times 10^{-3} \text{ s}^{-1}$. The value of the equilibrium dissociation constant calculated here is as well comparable to the K_d of 58-160 pM, determined earlier (Shen et al., 1996; Wang et al., 1997).

3.3.3 Effects of Site-Specific Perturbations in IL-4BP on the Interaction with IL-4

Initially, the amino acids from IL-4BP which were submitted to site-directed mutagenesis, were selected using the structural alignment between the receptor sequences including human and mouse IL-4BP, hGHbp (human growth hormone- binding protein), human and mouse IL-2 β and γ_c (Bamborough et al., 1994). Furthermore, the set of amino acids of interest was extended based on the results obtained from the crystal structure of the complex between IL-4 and IL-4BP (Hage et al., 1999). With the purpose of establishing the structure-function correlation, as targets for mutagenesis were identified residues involved in polar and hydrophobic interactions in the complex. Basically, all amino acids of interest were included in an alanine scanning mutational analysis. In order to define the results from the alanine scan more accurately, it was necessary to replace additionally a few tyrosine residues, involved in potentially important contacts with the ligand, by phenylalanine.

3.3.3.1 Kinetics of the binding of IL-4 to the alanine variants of IL-4BP

The rationale behind alanine scanning mutagenesis is that all interactions of a side chain except for the C β are eliminated (Lau & Fersht, 1987; Cunningham & Wells, 1989). This strategy assumes that the alanine substitution eliminates interaction without introducing new properties. The contribution of the deleted groups relative to the alanine residue is assessed from the difference between the properties of the wild-type relative to the alanine mutant. Free energies of binding are used to quantify the effect of the alanine substitution at any given site (Di Cera, 1998).

To assess the effect of the introduced mutation on the binding of IL-4 to the IL-4BP, every single variant was immobilized to a sensor chip as mentioned above (Table 3.5). Sensograms recorded at different concentrations of IL-4 were evaluated for the kinetic constants (Table 3.6). Based on the results from the BIAcore measurements the alanine variants assessed in the frame of this study could be classified into 3 main groups, according to the extent to which the mutation affects the functional properties of the IL-4BP molecule.

1. Variants L42A, L43A, D66A, K91A, S93A, D125A, N126A, and L128A showed a pattern of binding very similar to this observed during the interaction of IL-4 and the wild-type IL-4BP. As the sensograms revealed (Figure 3.21 - A and B), these variants rapidly associate when perfusion with IL-4 is committed and slowly dissociate when it is changed to perfusion with buffer alone. IL-4 was applied in concentrations of 2.5, 5 and 7.5 nM. Under such conditions it was possible to

evaluate both the association and the dissociation phase for all variants from this group (Figure 3.22). The alanine substitution in variant K91A merely did not have any effect on the association. Variants L42A, L43A, D66A, D125A, and L128A showed association rate constants which were only slightly altered due to the present mutation (Table 3.6). The on-rates of variants S93A and N126A were found to be negligible faster than that of IL-4BP.

Table 3.6: Kinetic constants for binding of IL-4 to IL-4BP and its variants included in the alanine screening.

Receptor variant	n	k_{on} (SE)		k_{off} (SE)		K_d [M]	
		[$\times 10^6 M^{-1} s^{-1}$]		[$\times 10^{-3} s^{-1}$]		K_d (kin.)	K_d (equilib.)
IL-4BP	3	13	(0.8)	1.0	(0.3)	7.7×10^{-11}	
Y13A	18	ND		ND		ND	7.9×10^{-7}
L39A	15	4.9	(0.7)	42	(7.8)	8.6×10^{-9}	1.6×10^{-8}
F41A	9	5.6	(0.7)	29	(3.4)	5.2×10^{-9}	8.8×10^{-9}
L42A	3	12	(0.8)	1.5	(0.4)	1.2×10^{-10}	
L43A	3	12	(0.8)	3.1	(0.4)	2.6×10^{-10}	
D66A	3	11	(0.6)	6.0	(0.4)	5.6×10^{-10}	
D67A	9	3.1	(0.2)	32	(1.2)	1.0×10^{-8}	9.3×10^{-9}
V69A	9	6.3	(0.8)	26	(0.9)	4.1×10^{-9}	6.1×10^{-9}
D72A	18	ND		ND		ND	2.0×10^{-7}
D72N	18	ND		ND		ND	2.7×10^{-7}
K91A	3	13	(2.2)	4.3	(0.4)	3.2×10^{-10}	
K91D	9	4.8	(0.6)	12	(0.3)	2.5×10^{-9}	1.9×10^{-9}
S93A	3	17	(0.9)	2.6	(0.5)	1.5×10^{-10}	
D125A	18	9.4	(0.5)	7.3	(0.6)	7.8×10^{-10}	
N126A	9	14	(0.6)	6.8	(0.4)	4.7×10^{-10}	
Y127A	18	4.5	(0.2)	19	(0.3)	4.3×10^{-9}	6.2×10^{-9}
L128A	18	7.5	(0.4)	11	(1.3)	1.5×10^{-9}	
Y183A	18	ND		ND		ND	6.2×10^{-8}

n: number of measurements.

SE: Standard error.

K_d (kin.): K_d calculated from kinetic data.

K_d (equilib.): K_d calculated from steady state binding data. The mean standard error for this value over all variants was 9 %.

ND: the values could not be accurately determined because they exceeded the limitations of the instrument.

No large changes in the dissociation rate constant were observed in the above-mentioned set of alanine variants. The off-rate constant increased in variant L128A 12-fold and this was the fastest recorded dissociation constant among all variants from this group. Variants D66A, D125A and N126A showed a 6-7-fold increase of the dissociation rate constant. A 3-4-fold higher off-rate was found in variants L43A and K91A. A marginal increase in k_{off} occurred in IL-4BP variants L42A and S93A.

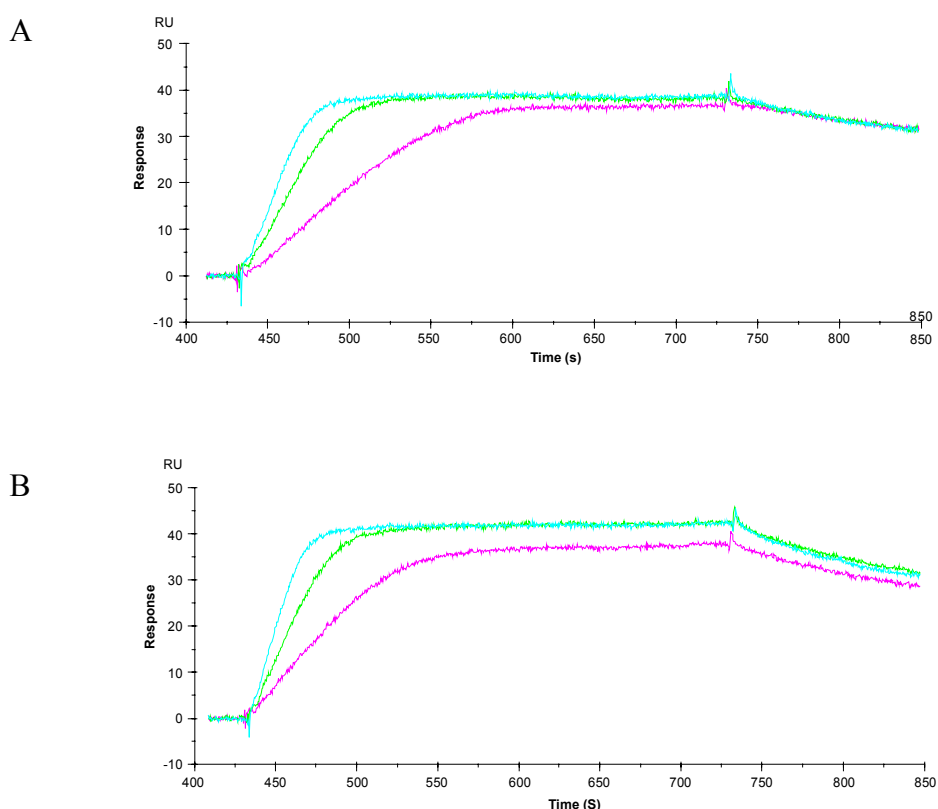


Figure 3.21: Overlay of sensograms of IL-4BP variants included in the alanine screening. (A) L42A, (B) K91A

Unfortunately, it was not possible for any of those variants to evaluate the part of the sensograms representing the equilibrium level between ligand association and dissociation. Similar to the interaction of IL-4 and the wild-type IL-4BP, the binding of IL-4 to the variants is characterized by such low equilibrium dissociation constants that would require concentrations of the ligand under the limit, which the technical device is able to process. Therefore, the equilibrium dissociation constants for the variants included in the first group were calculated from the ratio of the on- and off-rates (Table 3.6). Regarding K_d , the most considerable difference showed variants L128A and D125A, whose binding affinity dropped down 20- and 10-fold, respectively

compared to the wild-type. The effect is due to the relatively high ratios of k_{off} , which were recorded for both mutant forms. Marginal increases in K_d , 2 to 7-fold, were observed for variants L43A, D66A, K91A, and N126A. The equilibrium dissociation constant of variants L42A and S93A was almost not altered in comparison to the wild-type receptor (Table 3.7).

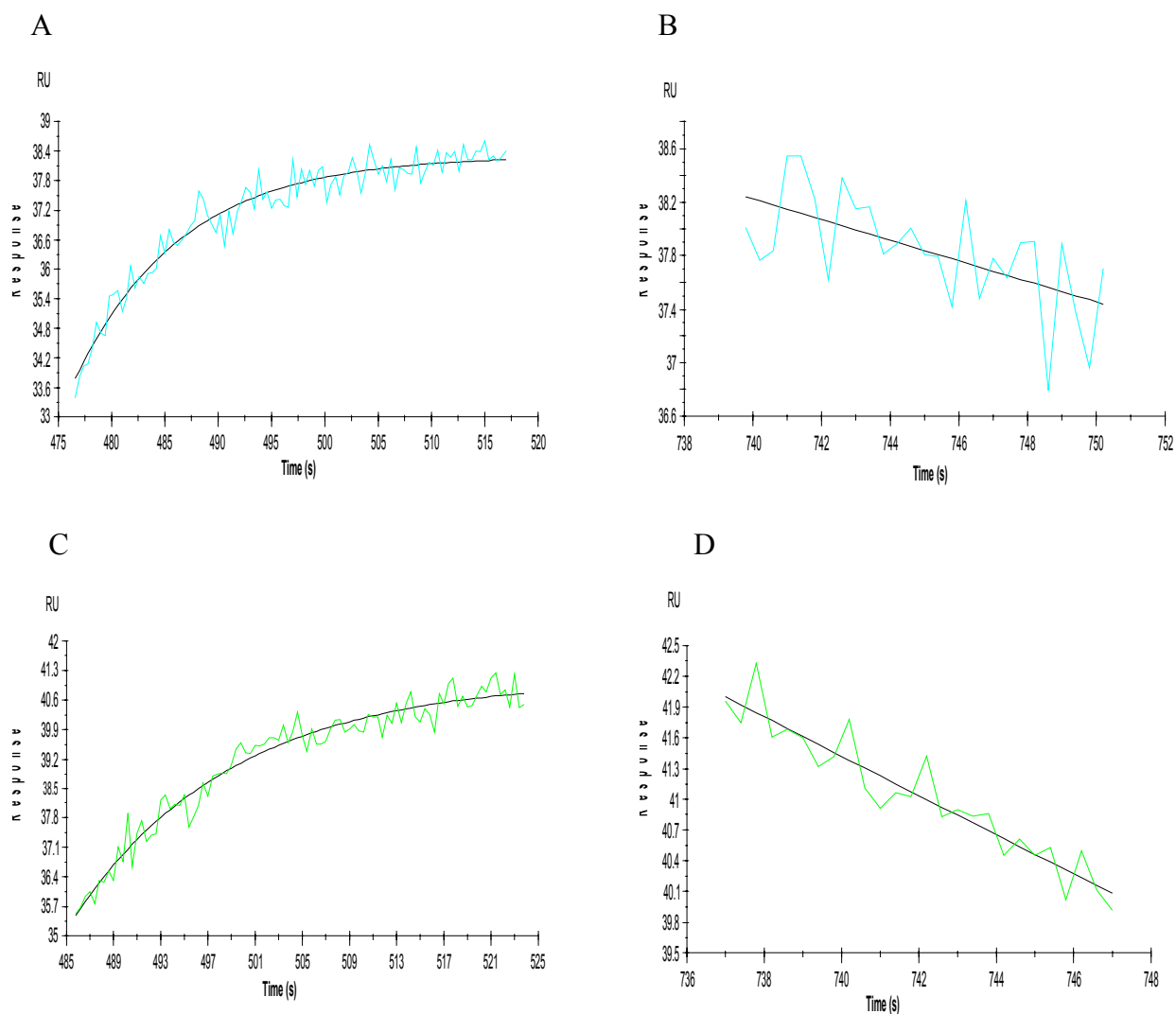


Figure 3.22: Plots representing the association (A, C) and the dissociation (B, D) phase of variants with high affinity to IL-4. (A) and (B), L42A; (C) and (D), K91A.

Based on the models of the complex between IL-4 and IL-4BP, K91 was suggested to stabilize this complex by forming an ion pair with the IL-4 residue E9 (Bamborough et al., 1994). Therefore, K91 was a residue of particular interest, and additionally to the alanine substitution it was subjected to a charge conversion. The positive charge was exchanged with negative by replacing the original lysine residue with aspartic acid. Although a dramatic effect was expected,

the charge variant K91D exhibited simply 30-fold decrease in binding affinity. The kinetic constants were as well only slightly affected after the negative charge was introduced. Both the results from the analyses of the alanine and the charge variant did not support an important implication of K91 in contacts to amino acids from IL-4.

The described features define the alanine variants included in the first group as not highly affected due to the introduced amino acid substitution. Alanine substitution at the particular positions neither caused large changes of the kinetic constants, nor brought the binding affinity drastically down. Generally, the mutated variants retained relatively high binding affinity to IL-4. Thus, even if the analyzed amino acids influence the interaction to some extent, they are not main binding determinants of the receptor part.

2. The alanine variants L39A, F41A, D67A, V69A, and Y127A represent a different model of binding to IL-4. As the sensograms recorded (Figure 3.23), the association phase is still a rapid process. In contrast to the above-mentioned IL-4BP variants, the dissociation phase occurred to be much faster. Since lower binding affinity was expected after the preliminary analysis, the BIAcore measurements were performed with wider concentration range of the ligand. The IL-4 concentration was increased to over 100 nM in some cases. Within such a concentration range it was still possible to obtain plots from the association and dissociation phase and to evaluate the kinetic constants (Figure 3.24 A, B, D and E).

The evaluated on-rates for all variants are merely slightly lower than the on-rate for IL-4BP (Table 3.6). Variant D67A exhibited a 4-fold decreased association rate constant. 2 to 3-fold lower k_{on} compared to the wild-type interaction characterized the rest of the variants. In contrast, the complex dissociation was considerably accelerated in all examined receptor mutants. The largest effect in this respect was recorded for variant L39A, which off-rate constant increased over 40-fold compared to the wild-type receptor. In two further alanine mutants, F41A and D67A, k_{off} was found to be 30-fold faster. The variant V69A showed a dissociation rate constant that was 25-fold faster. The alanine substitution in variant Y127A resulted in a relatively modest effect of 20-fold increase in the off-rate constant.

The relatively low binding affinity of the alanine variants included in this group allowed an independent determination of the dissociation equilibrium constants by evaluating the receptors saturation levels obtained at different IL-4 concentrations (Figure 3.24 C and F). The K_d values derived from the equilibrium phase are in good agreement with the K_d values calculated from the kinetic constants (Table 3.6). A more than 210-fold reduced binding affinity characterizes the variant L39A. Over 100-fold decreased the binding affinity for variants F41A and D67A. Both, variants V69A and Y127A exhibited 80-fold faster K_d than the IL-4BP (Table 3.7).

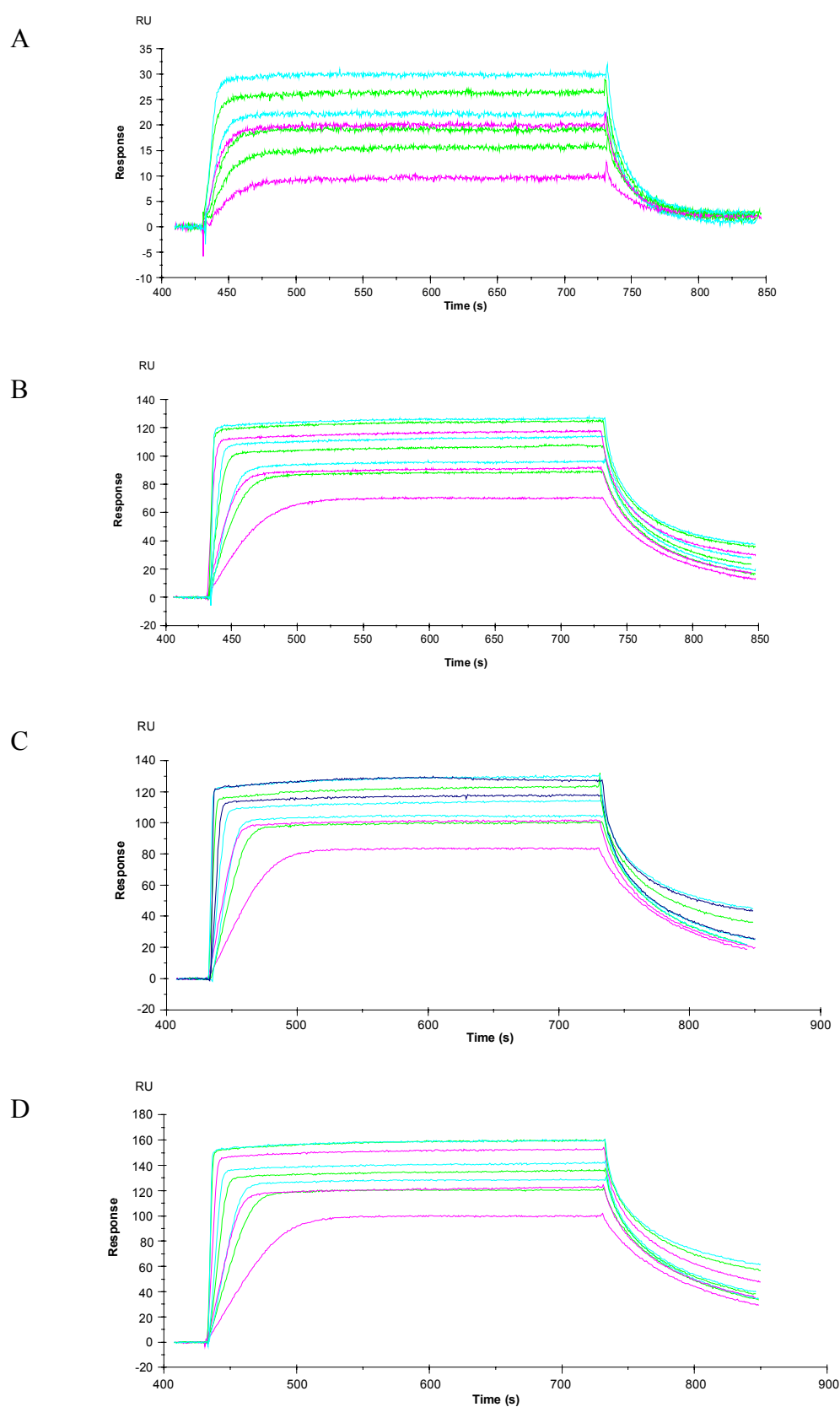


Figure 3.23: Sensograms which recorded the binding of IL-4 to the IL-4BP mutants F41A (A), D67A (B), V69A (C), and Y127A (D).

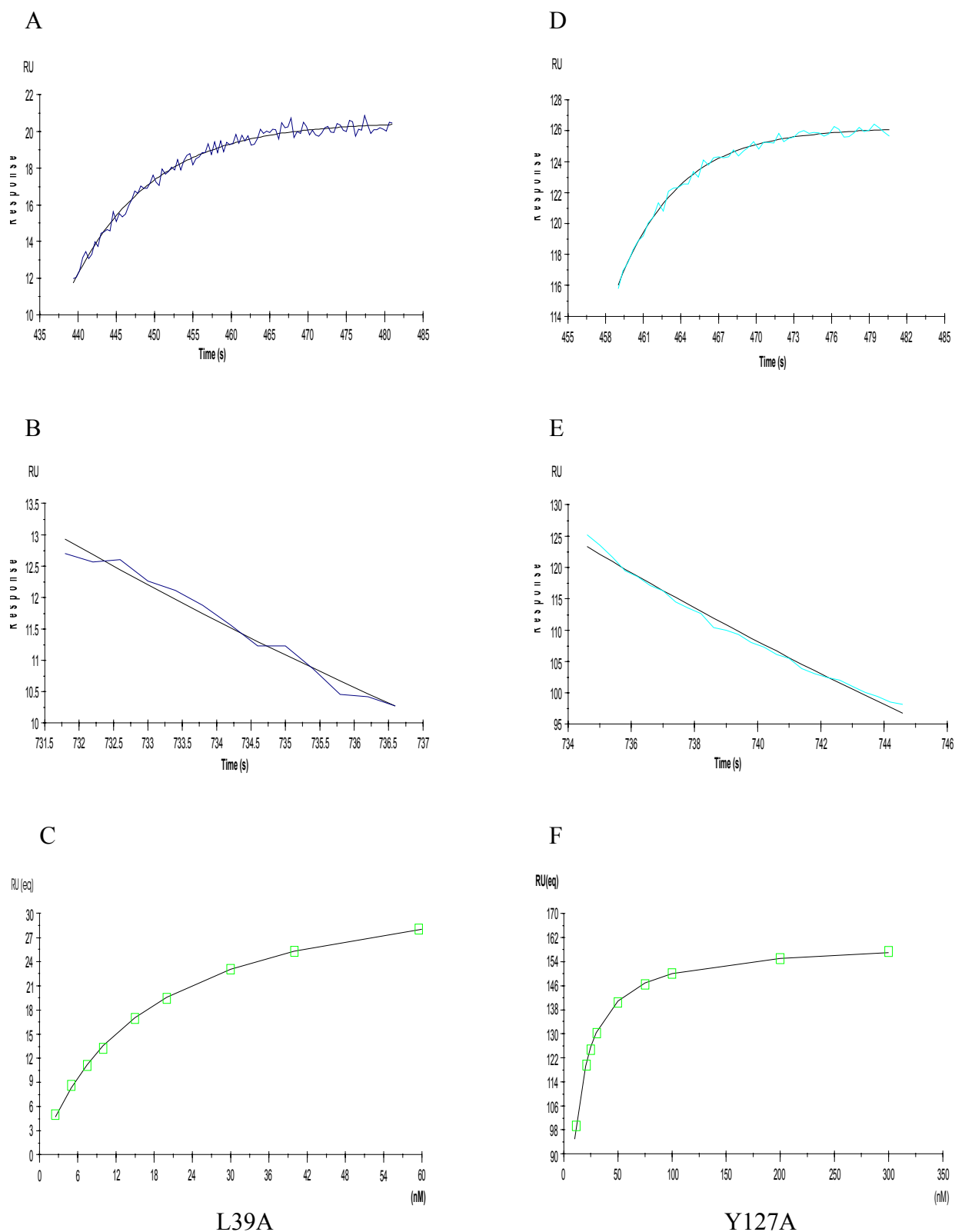


Figure 3.24: Plots for variants L39A and Y127A representing association (A and D), dissociation (C and F), and equilibrium phases (C and F).

Generally, alanine substitution at the mentioned sites is followed by severely affected receptor binding properties, suggesting an important function of the replaced amino acids in forming contacts within the complex with IL-4. However, the effect is still limited and does not imply that the particular residues are the main contact determinants in the receptor molecule.

3. Compared to the wild-type the alanine mutants D72A, Y13A, and Y183A revealed the most significant changes, as demonstrated by the overlay of the corresponding sensograms (Figure 3.25 A, B, and D). The three variants still associated rapidly with IL-4, but they as well dissociated extremely fast when buffer alone was applied. Due to the low binding affinity, it was necessary to increase the amount of the immobilized receptor on the chip, which for the variants D72A and Y13A exceeded 200 RU (Table 3.5). In addition, the IL-4 concentration was also increased during the experiments until it reached 750 nM.

The high ligand concentration caused such rapid association phase that could not be evaluated to calculate the association rate constant. The alanine substitution enhanced the dissociation phase to such an extent that it was impossible to estimate the dissociation rate constant. Therefore, as presented in table 3.6, the kinetic constants for those variants are not available.

The presented data for the equilibrium dissociation constant K_d was obtained by the evaluation of the equilibrium phase (Figure 3.26). By far the most affected variant occurred to be Y13A. The interaction of IL-4 and Y13A was characterized by over 10000-fold decreased binding affinity. Sensitive to the alanine substitution was also variant D72A which binding affinity dropped down 2600-fold. Although the variant Y183A showed a less remarkable effect, it still demonstrated large changes in K_d (Table 3.7). The variant decreased its binding affinity to IL-4 800-fold. The observed extreme changes in K_d give a reliable explanation to the fact that particularly these variants could not be successfully isolated and purified by an affinity column containing IL-4.

The strong effect of the alanine substitution on the binding affinity indicates that the replaced amino acids provide the largest contribution from the receptor side to the stabilization of the complex. However, it has to be considered that if the introduced alanine residues would cause structural perturbation in the receptor molecule, the observed effect would rather be structural than functional. To assess the exact functional role of the examined residues in the interaction and the character of the contacts in which they are implicated, additional experiments were performed.

Furthermore, a mutational variant D72N was analyzed. Originally, the variant was constructed as more conservative than D72A and was expected to retain the high binding affinity to IL-4. As already mentioned, D72N could not be purified using the IL-4 affinity column, and this was the first indication that it was strongly affected due to the amino acid substitution. The overlay of the

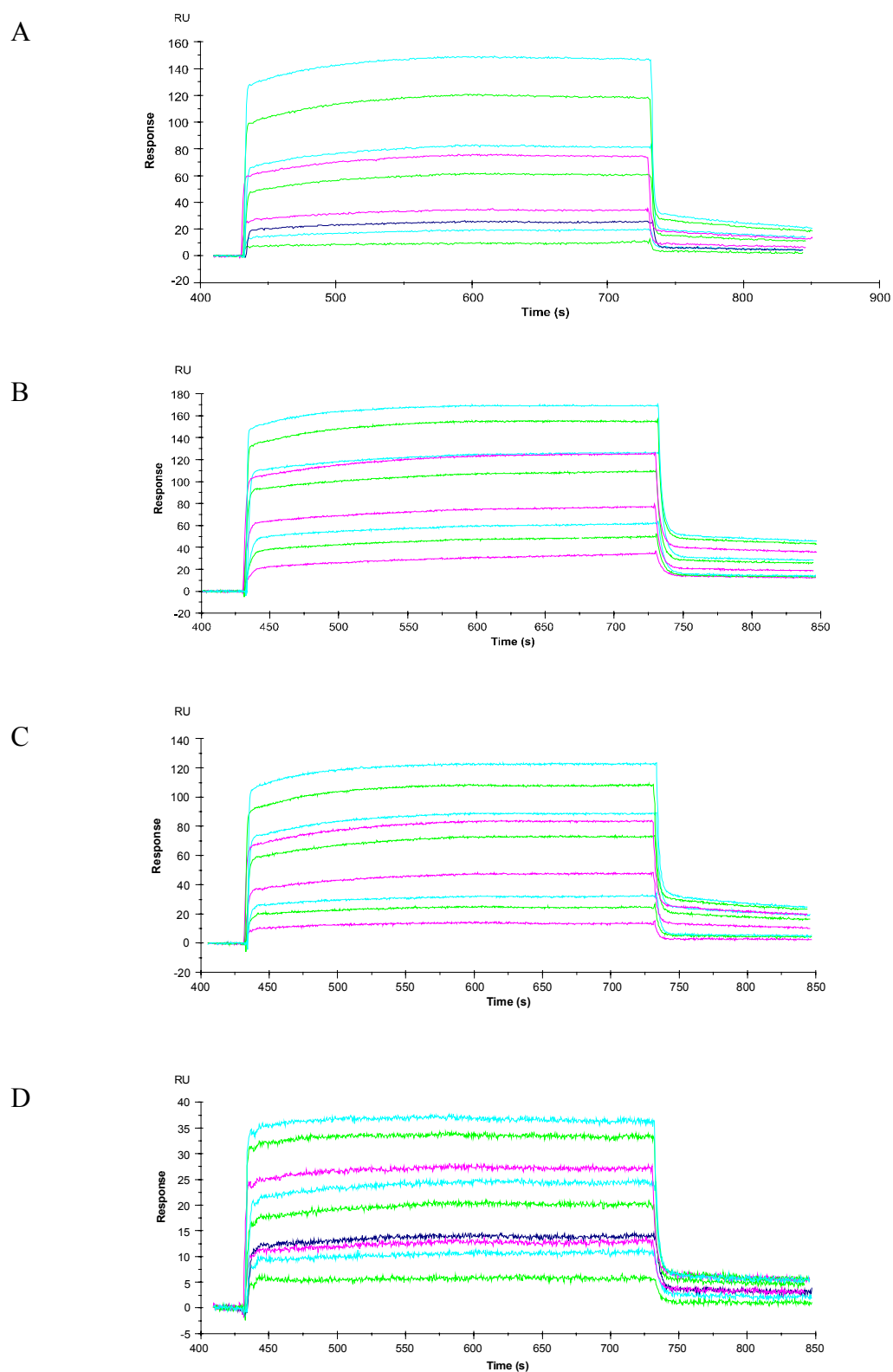


Figure 3.25: Overlay of sensograms representing the interaction of IL-4 and the low affinity variants of IL-4BP: Y13A (A), D72A (B), D72N (C), and Y183F (D).

sensograms which recorded the interaction supported this suggestion (Figure 3.25 C). The kinetic constants could not be calculated and the equilibrium phase was used to evaluate the equilibrium dissociation constant K_d (Figure 3.26 B). Similar to the corresponding D72A, the variant D72N revealed largely altered K_d (Table 3.6). Moreover, D72N was characterized by slightly lower binding affinity than D72A.

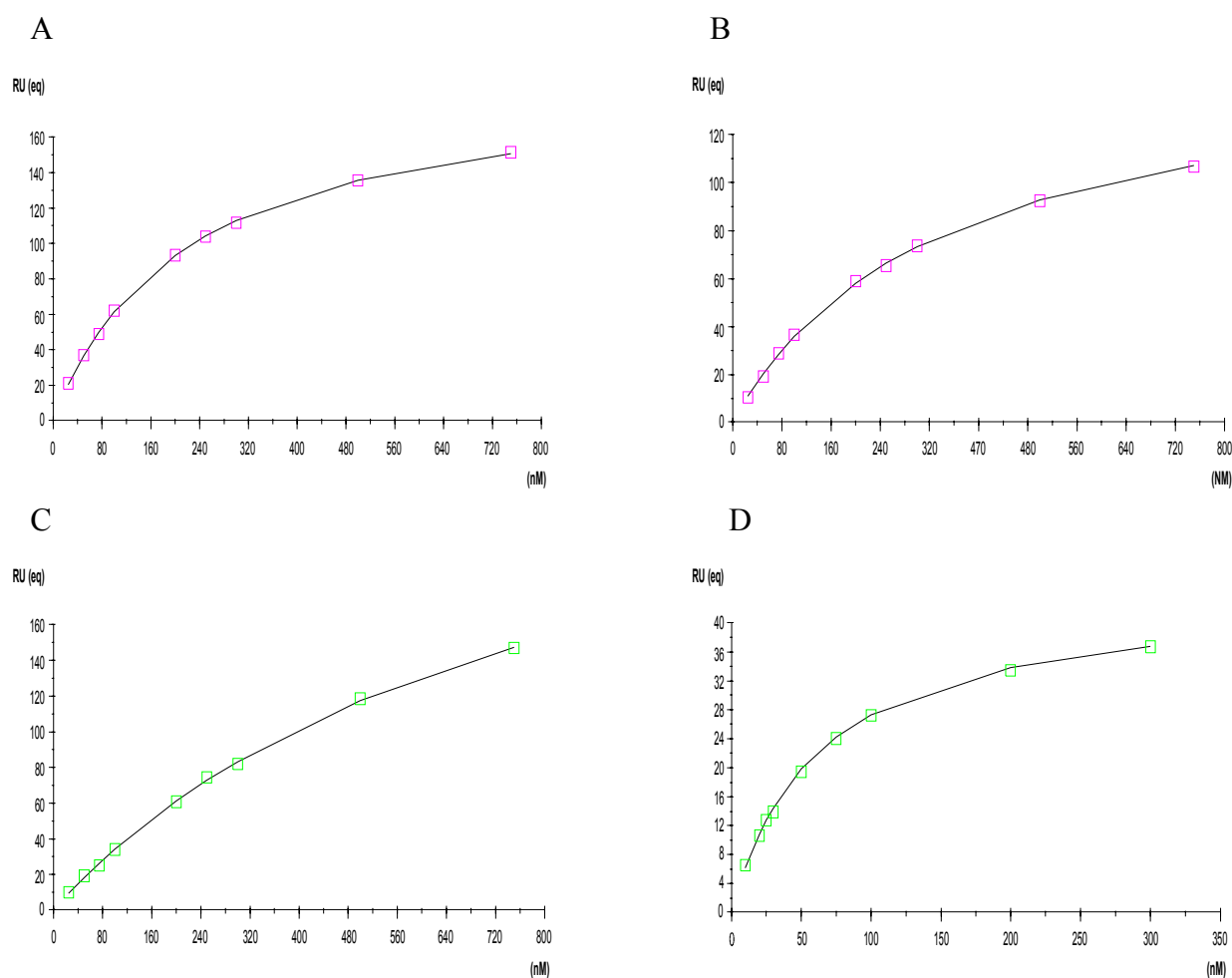


Figure 3.26: Equilibrium phase. Variants D72A (A), D72N (B), Y13A (C), Y183A (D).

The analysis of variant D72N was of particular significance since the original amino acid and the replacing are structurally very similar, implying that the observed effects as to both D72A and D72N were caused by functional alterations, but not structural. In addition, the low binding affinity of D72N indicates that D72 takes part in the interaction due to the charge of its side chain. Thus, the obtained results confirm the functional importance of the aspartic acid at position

72 in forming ion pairs within the complex, and define it as one of the main binding determinants in the IL-4BP.

The analyses of the alanine variants and one additional mutant (K91D) performed by BIAcore system demonstrate that the rate constant of association between IL-4 and IL-4BP is remarkably insensitive to amino acid substitutions. The examined residues did not apparently determine the velocity of the complex formation to an appreciable degree. Loss of charge generally did not affect the on-rates except in a case of variant D67A. Unfortunately, it was not possible to obtain neither association nor dissociation rate constants for the variants which exhibited the largest changes regarding binding affinity and therefore to figure out whether the charge of D72 contributes to the rapid association phase. As far as off-rates could be calculated, they showed more significant changes, which were followed by a corresponding decrease in the binding affinity of the particular variants. Generally, no correlation was noticed between the side chains that had the most affected on- and off-rate. Among the amino acids that showed significant effect on the dissociation rate constant after alanine substitutions are some large hydrophobic side chains as well as charged residues. That suggests that electrostatic interactions in parallel with hydrophobic contacts stabilize the complex between IL-4 and IL-4BP.

3.3.3.2 Thermodynamic aspects of the interaction between IL-4 and the IL-4BP variants included in the alanine scanning mutagenesis

The introduction of a mutation in the system requires determining the energetic consequences of the substitution made. The information about the energetic alteration caused by an amino acid substitution indicates how exactly and to which extent the exchanged residue contributes to the binding properties of the receptor and its importance for the stability of the complex with the ligand. As an estimation of the effect of the site-directed mutation on the binding process often is used the change of binding energy relative to the wild-type protein ($\Delta\Delta G$), which in fact measures the linkage between the functional properties of the examined molecule and the mutation. Therefore, when the contact determinants are defined the data about $\Delta\Delta G$ is considered as follows. When $\Delta\Delta G > 0$, the mutation is assumed to reduce the complex stability, whereas enhanced stability are reflected by $\Delta\Delta G < 0$, and no effect is considered when $\Delta\Delta G = 0$ (Di Cera, 1998).

The total change in binding free energy (ΔG) for the interaction of IL-4 and IL-4BP is 13.8 kcal/mol, as it was calculated from the corresponding equilibrium dissociation constant of 77 pmol estimated within the present study. The loss of binding energy in the alanine variants ($\Delta\Delta G$)

was calculated according to the change in the dissociation constant K_d relative to the wild-type interaction (Table 3.7). The K_d values obtained from the equilibrium phase of the biosensor experiments were used where it was possible. For variants which retained high binding affinity and the equilibrium dissociation constant could not be directly evaluated were used the K_d ratios from kinetic measurements.

Table 3.7: Relative K_d and loss of binding free energy of the IL-4BP variants included in the alanine mutational analysis.

Receptor variant	Relative K_d (Mut/Wild-type)	$\Delta\Delta G$ [kcal/mol]
Y13A	10300	5.5
L39A	210	3.2
F41A	110	2.8
L42A	1.6	0.3
L43A	3.3	0.7
D66A	7.2	1.2
D67A	120	2.8
V69A	80	2.6
D72A	2600	4.7
K91A	4.2	0.8
S93A	2	0.4
D125A	10	1.4
N126A	6.1	1.1
Y127A	80	2.6
L128A	20	1.7
Y183A	800	4.0

The most significant loss of binding free energy after alanine substitution was observed for Y13. The alanine mutant contributes 5.5 kcal/mol, which accounts for 40 % of the total binding energy. The most important polar residue in the functional epitope is D72, which provides over 33 % (4.7 kcal/mol) to the total binding energy. Another tyrosine residue, at position 183, also makes a large apparent contribution with loss of free binding energy of 4 kcal/mol during the alanine scan. The sum of the reductions in free energy caused only by the alanine substitutions at these particular positions already exceeds the total binding energy for the complex with IL-4. Five

additional residues included in the study, L39, F41, D67, V69, and Y127, produced a loss of 2.5 to 3.5 kcal/mol each after they were replaced by alanine residues. The summed contribution of these amino acids is comparable with the total binding energy characterizing the complex. Lesser contributions demonstrated D66, D125, N126, and L128 when they were replaced by alanine (1 to 2.1 kcal/mol). The rest of the examined amino acid side chains showed negligible energetic contribution (under 1 kcal/mol). No one of the alanine variants showed a negative value for $\Delta\Delta G$, suggesting that all analyzed residues directly or indirectly stabilize the complex.

The energetic contribution of single amino acid side chains from IL-4BP to the high-affinity interaction with the ligand, according to the results obtained from the alanine scanning mutagenesis, is indicated in the space-filling IL-4 BP model presented in Figure 3.27. The largest contribution was established for Y13, D72, and Y183 (colored in red) surrounded by residues of less importance. The mixed character of the functionally important amino acids suggests a mixed character of the contacts with IL-4, in contrast to the other well-studied receptor-ligand system of hGH, where two tryptophan residues form a central hydrophobic patch (Clackson & Wells, 1995; Clackson et al., 1998). Furthermore, the present model is in agreement with the crystal structure of the complex with IL-4, which proposed a mosaic binding interface (Hage et al., 1999). Mutations of amino acids from cluster I and II clearly affected the dissociation rate constant. They resulted in a greater loss of free binding energy supporting the idea that the residues from those clusters have the main role for the stability of the complex with IL-4. The three tyrosine residues Y13, Y127, and Y183, with properties for forming hydrogen bonds, have shown a significant energetic contribution which implies their central role within the first cluster. The primary contact residue in the second cluster seems to be D72, surrounded by the hydrophobic side chains of L39, F41, and V69, which also have an important energetic contribution. In contrast, the mutation analysis of residues within cluster III indicates that they have less energetic contribution and therefore confirms their minor functional role for complex stability. Their binding affinity is altered mainly due to slower association phases (especially for D67) which determines the amino acids from this cluster as k_{on} determinants.

The sum of the apparent binding free energy contributions for the amino acids included in the alanine mutational analysis accounts for 35.8 kcal/mol. This value considerably exceeds the calculated binding free energy for the complex. The high cumulative loss might indicate that some of the examined mutations are not completely independent, but interact with each other directly or indirectly. Furthermore, the additivity could be broken down if a mutation causes a change in the mechanism or rate-limiting step of the reaction. Another possibility is that some of the main binding determinants contribute to more than one single contact. A large loss of binding free energy in particular variants, and thereby in the total sum, might be explained also with great

structural perturbations due to the alanine substitution. Such effects would be rather structural than functional. This does not seem to be the case for D72, since the variant D72N, which struct-

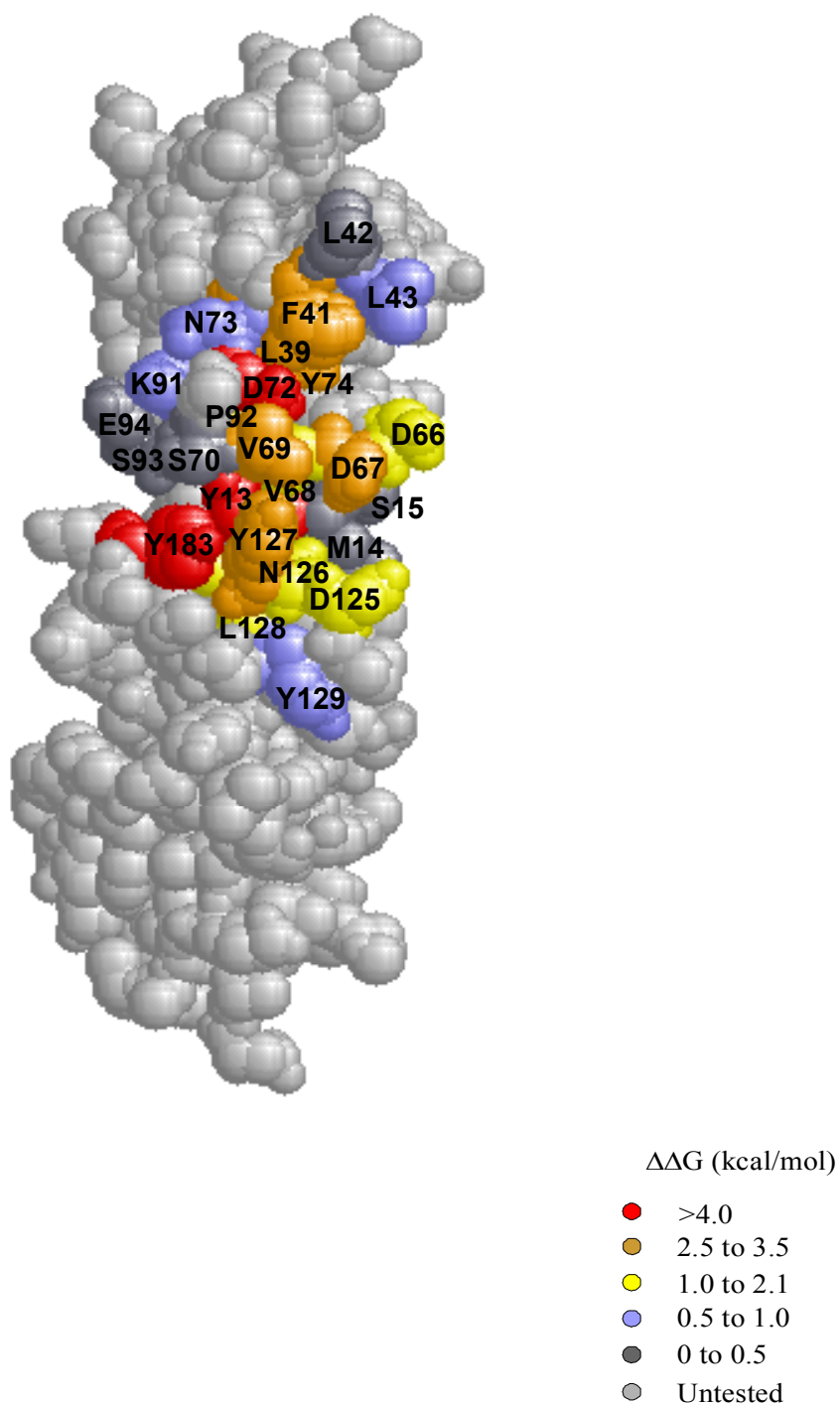


Figure 3.27: Loss of binding free energy of residues from IL-4BP due to alanine substitution. Residues have been color-coded as indicated to denote their apparent contributions to the loss of binding free energy, as determined by alanine scanning mutagenesis. Data from a previous study have been used for residues M14, S15, V68, S70, N73, Y74, P92, E94, and Y129.

urally should be highly similar to the wild-type protein demonstrated as well a large loss of binding free energy as D72A. However, structural consequences from the replacement of Y13 and Y183 by alanine could not be ignored.

3.3.3.3 Analysis of the binding of IL-4 to the IL-4BP tyrosine variants

The three phenylalanine side chains which indicated the largest contribution to the loss of binding free energy during the alanine scan (Y13, Y127, and Y183) were replaced by tyrosine residues. Due to the conservative substitution, these variants were expected to be structurally very similar to the wild-type receptor, however without properties to form hydrogen bonds. Therefore the tyrosine variants were used to find out whether structural changes were the reason for the significant energetic alterations in the corresponding alanine mutant forms, or the effect was caused only because of disrupted binding contacts.

The IL-4BP variants Y13F, Y127F and Y183F were expressed in SF9 insect cells following the described procedure (see 2.11). They were easily purified by an IL-4 affinity column, which was the first indication that they would retain much higher affinity to IL-4 than the parallel alanine variants. Furthermore, this expectation was confirmed by the BIAcore analyses. The sensograms (Figure 3.28) revealed a different pattern of interaction compared to the observed within the alanine scan. Variant Y127F showed a model of interaction very similar to the wild-type IL-4BP (Figure 3.28 B). Although IL-4 was used in a very low concentration rate (2.5, 5, 7.5 nM), fast association phase occurred followed by a very slow dissociation. Both the association and dissociation constants showed values very similar to the wild-type interaction (Table 3.8). The equilibrium dissociation constant could not be evaluated due to the high binding affinity of the variant. The calculated K_d based on the kinetic constants is negligibly different from K_d of IL-4BP, which corresponds to loss of binding free energy of 0.1 kcal/mol.

Table 3.8: Kinetic and thermodynamic constants characterizing the binding of IL-4 to the tyrosine variants of IL-4BP

Receptor variant	n	k_{on} (SE) [$\times 10^6 M^{-1} s^{-1}$]	k_{off} (SE) [$\times 10^{-3} s^{-1}$]	K_d [M]		Rel. K_d (Mut./WT)	$\Delta\Delta G$ kcal/mol
				K_d (kin.)	K_d (equilib.)		
Y13F	12	11 (1.4)	26 (2.7)	2.4×10^{-9}	3.2×10^{-9}	40	2.2
Y127F	6	16 (1.0)	1.5 (0.4)	9.3×10^{-11}		1.2	0.1
Y183F	9	6.0 (1.0)	190 (12)	3.1×10^{-8}	2.4×10^{-8}	310	3.4

n: number of measurements; SE: Standard error; K_d (kin.): K_d calculated from kinetic data.

K_d (equilib.): K_d calculated from steady state binding data. The mean standard error for this value was 4.2%.

Rel. K_d : relative value of K_d .

Variant Y13F showed more significant effect (Figure 3.28 A) but still not comparable to the alterations observed with Y13A. The association constant was almost not affected due to the amino acid substitution. The faster dissociation phase caused a decrease in binding affinity over 40-fold. The energetic contribution of this variant counted for merely 2.2 kcal/mol in contrast to the large contribution of Y13A, implying that the IL-4BP binding properties were significantly

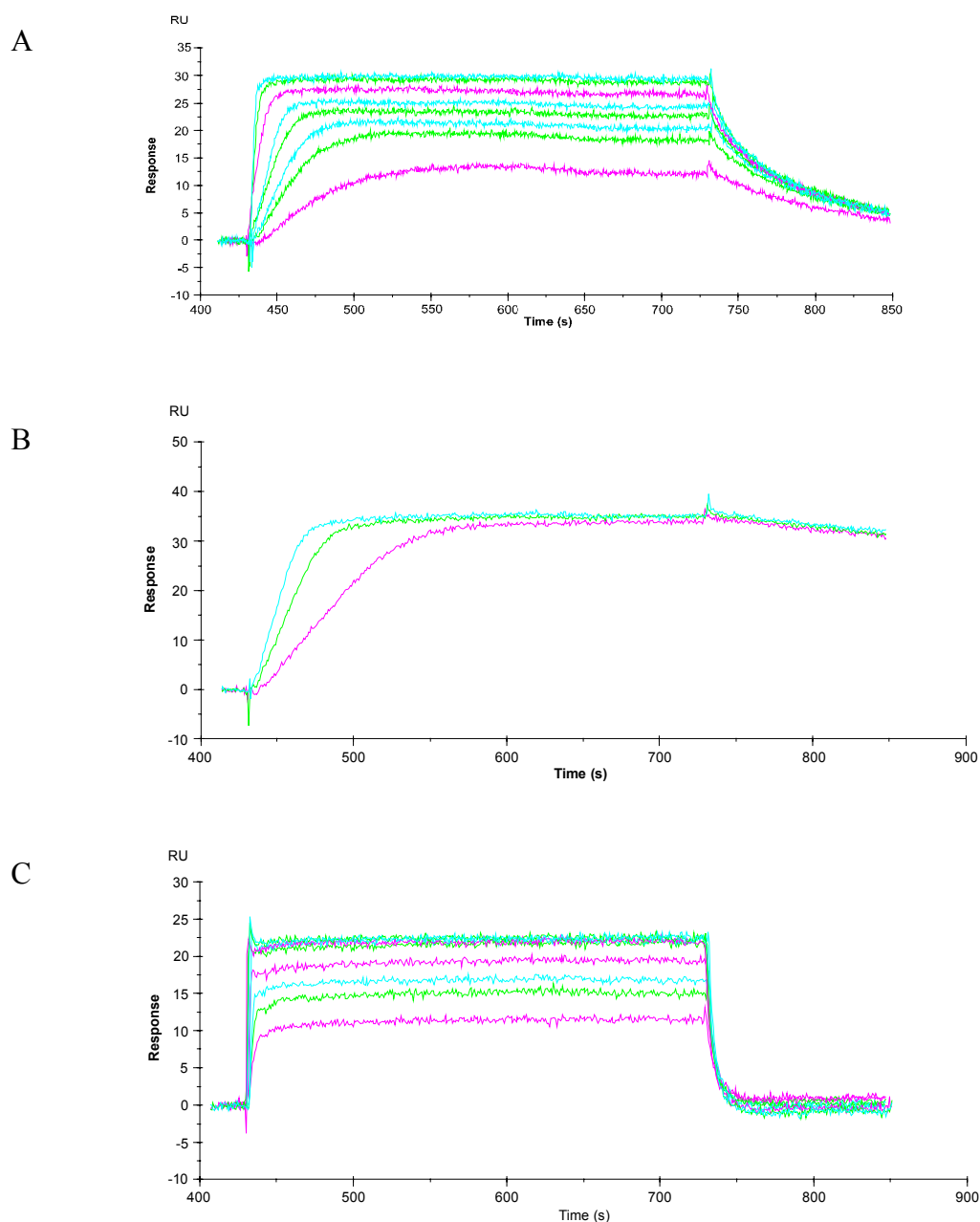


Figure 3.28: Overlay of the sensograms representing the interaction of IL-4 and the tyrosine variants of IL-4BP: (A) Y13F, (B) Y127F, (C) Y183F.

less affected by a phenylalanine substitution at this position than by an alanine replacement.

The largest effect due to the phenylalanine substitution displayed variant Y183F. While the association constant was only slightly changed, the dissociation constant was over 190-fold faster compared to the wild-type receptor (Table 3.8). The binding affinity was reduced over 300-fold, corresponding to apparent binding energy contribution of 3.4 kcal/mol. In relation to the corresponding alanine variant, Y183F still retained an about 2-fold higher binding affinity. However, both variants revealed comparable energetic contribution (Table 3.7).

In summary, the substitution of the mentioned tyrosine side chains with the structurally similar phenylalanine dropped down significantly the energetic contribution of the analyzed variants to the overall loss of binding free energy. It seems that the hydroxyl group of the tyrosine at this position does not take part in hydrogen bonds to IL-4 that are critical for the binding. It is more likely that this tyrosine is involved in hydrophobic interactions through its aromatic ring. The replacement of Y13 and Y183 by phenylalanine caused considerable effects which suggests that their hydroxyl groups contribute to binding contacts. However, comparing the energetic contribution of both variants Y13A and Y13F implies that Y13 has rather structural than functional importance for the interaction between IL-4 and IL-4BP. It is also possible that Y183 is involved in more hydrogen bonds than Y13 and therefore the loss of its hydroxyl group results in a greater functional effect. In addition, the results obtained from the phenylalanine variants to some extent give an explanation for the enormously large sum of binding free energy determined within the alanine mutational analysis.

3.3.4 Analysis of IL-4BP Double Mutants

Since proteins are highly cooperative structures, it has to be considered that the contribution of a particular residue might involve effects of multiple order. In many cases, interactions of several amino acids are coupled to one another and may not be reduced simply to a sum of pairwise interactions. In order to study experimentally the interaction of a certain amino acid residue in a protein with other residues in that protein, it has become common practice to analyse the free energy changes of multiple mutants (Wells, 1990; Jin et al., 1994; Hilser et al., 1998; Clackson et al, 1998; Di Cera, 1998).

The analysis of double mutants considers the changes of binding free energy characterizing two proteins mutated individually at the sites X and Y, respectively and the double mutant form, which is mutated at both sites X and Y. To assess whether the effects between the examined residues are cooperative or additive, the losses of binding free energies characterizing the two

individual mutations are theoretically summarized ($\Delta\Delta G_{\text{add}}$) and compared to the value, which is estimated for the double mutant. If the effects of the mutations are independent (non-cooperative), the change in free energy for the double mutant form is equal to the sum of those for the two site-specific mutations. If the two examined sites are coupled, then the change in free energy for the double mutant differs from the sum of the two single mutants (Carter et al., 1984; Di Cera, 1998). It is possible for $\Delta\Delta G_{\text{add}}$ to be either lower or greater than the experimentally estimated value for the double mutant depending upon whether the interactions between the examined side chains reduce or enhance the functional properties measured (Wells, 1990).

In order to study whether the contact residues within IL-4BP are involved in cooperative interactions or function in an independent manner, a series of double mutants was produced and examined by BIAcore technology. Amino acid side chains from the three IL-4BP clusters identified by the crystal structure of the complex were included in the analysis (Table 3.2). The double mutant forms were constructed for all residues whose binding affinity decreased during the alanine screening over 50 fold (Table 3.7), since they were considered to have significant contribution to the binding. In half of the variants the mutation, D72N was uniformly present, while the second mutated site was subsequently exchanged to L39A, F41A, D67A, V69A, Y127A, or Y183F. The second group of double mutants constantly was modified to Y13F and additionally the mutations L39A, F41A, D67A, V69A, Y127A, or Y183F were introduced. Furthermore, a variant containing both mutations D72N and Y13F was created. Considering the technical limitations of the used device, all the double mutated variants were constructed under the condition that the theoretical sum of the change in free energies ($\Delta\Delta G_{\text{add}}$) for the two introduced mutations does not exceed 8 kcal/mol.

As expected, all examined double mutants demonstrated very low binding affinity to IL-4 (Figure 3.29). Initially, about 100 RU of receptor were immobilized on the biosensor chip and the IL-4 concentration was increased to 750 nM. Under those conditions, binding was recorded only for variants Y13F/L39A, Y13F/F41A, and Y13F/D67A. To analyze variants Y13F/V69A, Y13F/Y127A, and Y13F/Y183F, it was necessary to increase the amount of immobilized receptor to 200 RU and the IL-4 concentration to 3000 nM. The experiments for the remaining variants were performed with 400 RU of receptor immobilized on the chip, and IL-4 concentrations up to 3000 nM. Both kinetic constants for the interaction of IL-4 and the double mutant variants could not be evaluated due to the high concentration of ligand that was applied causing very fast association, on one side, and the extremely rapid dissociation phase, on the other. Values for the equilibrium dissociation constant K_d were derived from the plots representing the receptor saturation levels at different ligand concentrations (Figure 3.30). Generally, the double mutants showed high K_d (between 1.4×10^{-7} and 7.7×10^{-5} M), but as

expected the mutant forms containing Y13F were less affected than the variants carrying D72N (Table 3.9). Although the receptor variants Y13F/D72N and D72N/D67A were immobilized with high density on the chip and extremely high IL-4 concentration was used, saturating binding was

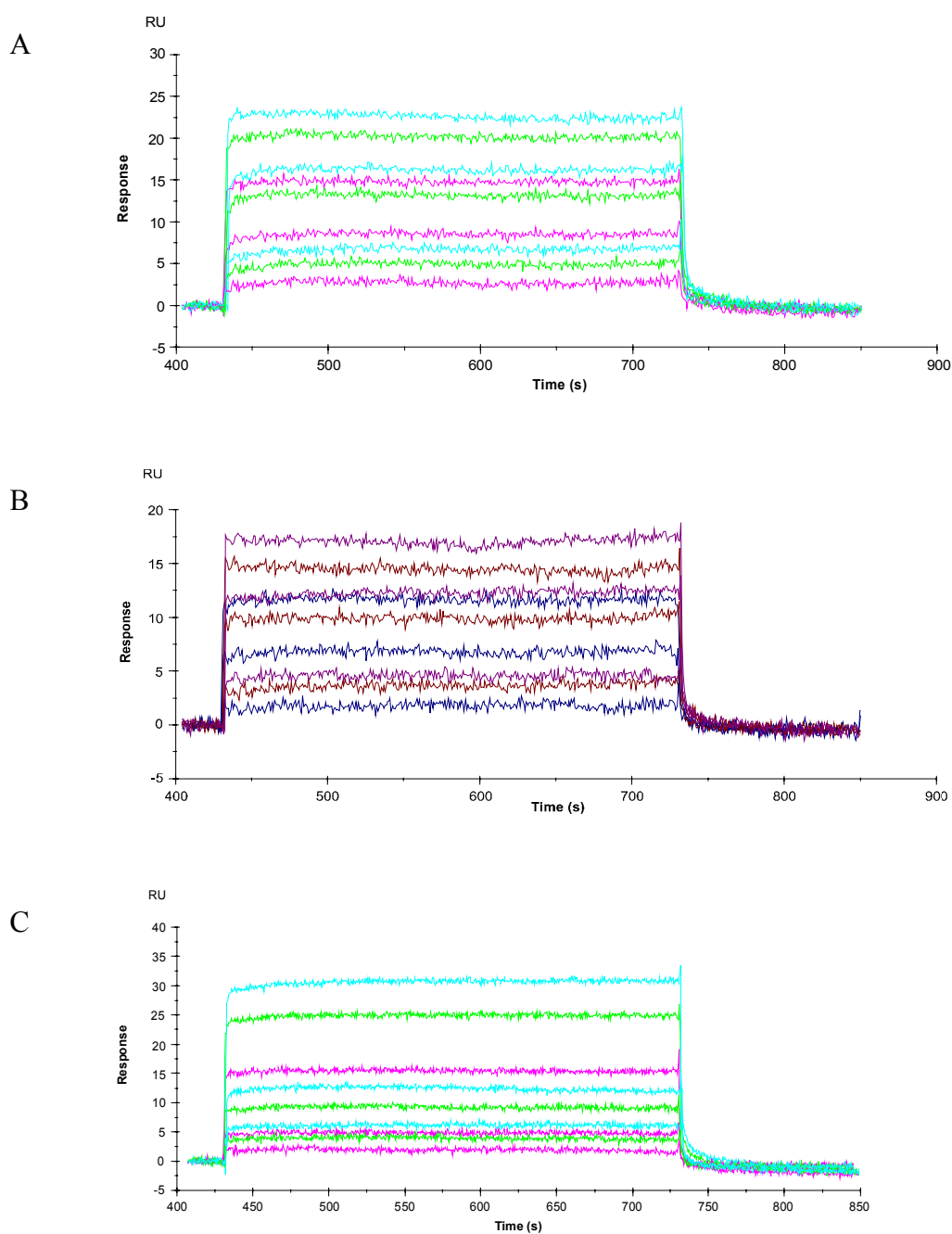


Figure 3.29: Overlay of sensograms which recorded the interaction between IL-4 and double mutants of IL-4BP: (A) Y13F/L39A, (B) Y13F/F41A, (C) D72N/V69A.

not obtained and the equilibrium binding constants could not be determined. It seems that their K_d values exceed the detection limits of the used technical device (typically for steady state analysis $10^{-4} - 10^{-9}$ M), considering the fact that K_d of 7.7×10^{-5} M was still successfully determined. Experiments with higher receptor density were not performed within the present study, since for reliable measurements it is recommended to keep the immobilized receptor at levels of 100-500 RU (BIAapplications Handbook, 1995). Furthermore, for the system of IL-4/IL-4BP it was already reported that density above 50 pg/mm^2 (1 RU corresponds to 1 pg/mm^2) resulted in high bulk-phase signals and drift phenomena (Shen, et al., 1996).

Table 3.9: Equilibrium dissociation constant and loss of binding free energies for the IL-4BP double mutant variants

Receptor variant	n	K_d (equilib.) [M]	$\Delta\Delta G$ [kcal/mol]	$\Delta\Delta G_{\text{add}}$ [kcal/mol]
Y13F/L39A	9	2.6×10^{-7}	4.8	5.4
Y13F/F41A	9	2.4×10^{-7}	4.8	5.0
Y13F/D67A	9	3.9×10^{-7}	5.1	5.0
Y13F/V69A	9	2.2×10^{-7}	4.7	4.8
Y13F/D72N	9	ND	ND	8.2
Y13F/Y127A	9	1.4×10^{-7}	4.4	4.8
Y13F/Y183F	9	4.9×10^{-7}	5.2	5.6
D72N/L39A	9	9.0×10^{-7}	5.5	8.0
D72N/F41A	9	2.3×10^{-6}	6.1	7.6
D72N/D67A	9	ND	ND	7.6
D72N/V69A	9	2.8×10^{-6}	6.2	7.4
D72N/Y127A	9	1.6×10^{-5}	7.2	7.4
D72N/Y183F	9	7.7×10^{-5}	8.2	8.2

n: number of measurements.

K_d (equilib.): K_d calculated from steady state binding data. The mean standard error for this value was 30 %.

$\Delta\Delta G_{\text{add}}$: the sum of $\Delta\Delta G$ for the two individual mutations.

ND: the values could not be accurately determined because they exceeded the limitations of the instrument.

The analysis of double mutants applied to IL-4BP revealed that most of the variants were characterized by values of $\Delta\Delta G$ very similar to the theoretically predicted $\Delta\Delta G_{\text{add}}$, implying that the examined amino acid residues are independent and the observed mutational effects are

additive. However, the variants D72N/F41A and D72N/V69A were found to have higher binding affinity than expected. From all double mutants of IL-4BP, which were successfully analyzed variant D72N/L39A showed the largest difference between the theoretically predicted binding free energy and the experimental value. The residues L39, F41, V69, and D72, examined through the mentioned variants, were shown to be part from one and the same structural cluster (Hage et al., 1999). Therefore, it is likely that they are involved in cooperative contacts, especially considering the fact that the present data suggests a favorable kind of interactions.

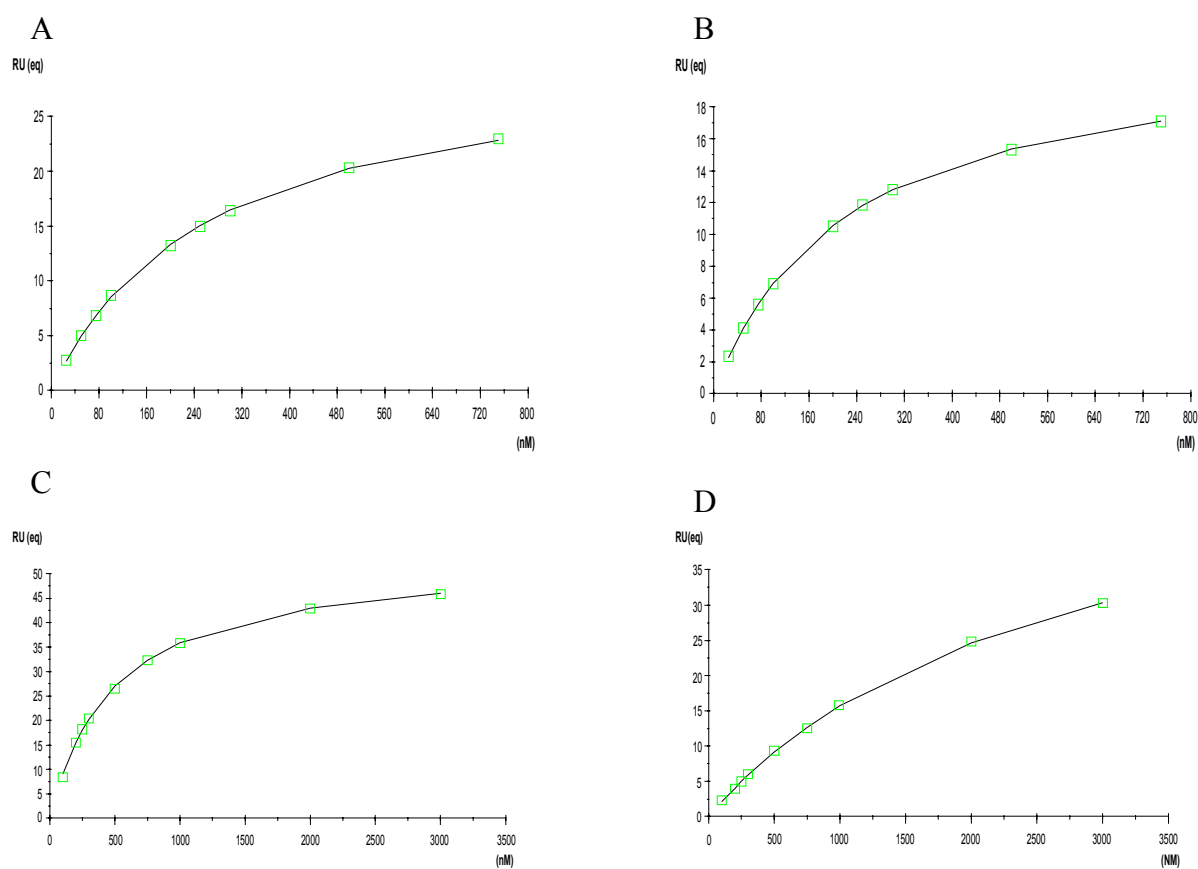


Figure 3.30: Equilibrium phase of some double mutants. (A) Y13F/L39A, (B) Y13F/F41A, (C) Y13F/D67A, (D) Y13F/Y183F D72N/V69A.

3.4 Biosensor Analysis of the Kinetics of Binding of IL-4 Variants to the IL-4BP

To further investigate the binding mechanisms of IL-4 to IL-4BP, two additional alanine IL-4 variants were constructed and the kinetics of their interaction with the receptor was examined. The investigation on the IL-4 binding epitope was extended and the both IL-4 variants R53A and Y56A were studied in the framework of the current project, since the crystal structure of the complex demonstrated that those amino acids were part of the second contact cluster assembled around IL-4 R88 (Hage et al., 1999).

The kinetics of the interaction between the both IL-4 variants and IL-4BP was analyzed using biosensor technology (Figure 3.31). The wild-type IL-4BP was immobilized on the streptavidin-coated chip with density of 90 RU and perfusion with each IL-4 variant in the concentration range of 2.5 to 60 nM was performed. The introduced mutations in the IL-4 molecule nearly did not affect the association phase and the evaluated corresponding rate constants remained very similar to the wild-type interaction (Table 3.10). A larger effect on the dissociation rate constant was observed particularly for the variant R53A, which increased over 20-fold compared to the wild-type. The off-rate of the IL-4 variant Y56A was 6-fold faster. The K_d levels of R53A, determined independently from the steady-state binding and from the ratio k_{off}/k_{on} , were in good agreement. Due to the high binding affinity, which variant Y56A retained it was not possible to evaluate its dissociation equilibrium constant and the presented value was calculated based on the kinetic constants. Overall, as an effect from the alanine substitution both variants showed decreased binding affinity to IL-4BP which was especially noticeable in the case of R53A (over 30-fold) and merely modest (8-fold) for Y56A.

Table 3.10: Constants and loss in binding free energy representing the interaction of the IL-4 variants to the IL-4BP.

IL-4 variant	n	k_{on} (SE) [x $10^6 M^{-1} s^{-1}$]	k_{off} (SE) [x $10^{-3} s^{-1}$]	K_d [M]		Relative K_d (Mut./WT)	$\Delta\Delta G$ [kcal/mol]
				K_d (kin.)	K_d (eq.)		
R53A	9	8.6 (0.7)	21 (1.6)	2.5×10^{-9}	2.7×10^{-9}	36	2.1
Y56A	9	9.9 (0.8)	6.3 (0.9)	6.4×10^{-10}		8	1.2

n: number of measurements.

SE: Standard error.

K_d (kin.): K_d calculated from kinetic data.

K_d (eq.): Data for K_d from equilibrium binding. The mean standard error for this value was 5 %.

$\Delta\Delta G$: loss in free binding energy.

The corresponding values of $\Delta\Delta G$ suggest that the examined residues from the IL-4 contact epitope should be considered as functionally significant, since the energetic contribution of R53A was counted for 2.1 kcal/mol, and this of Y56A for 1.2 kcal/mol. Generally, an introduction of a mutation within IL-4 was followed by more moderate alterations of functional properties compared to IL-4BP (Wang et al., 1997). Therefore, even though the demonstrated effects were less pronounced, they imply that the mentioned amino acids are of importance for the interaction with the receptor, and are part of the binding epitope. Furthermore, the data obtained from the association and dissociation phases is in agreement with the proposal that the amino acids from the second contact cluster stabilize the complex with the receptor (Hage et al., 1999) and in this respect they are consistent with results from earlier mutational studies of other residues from the same cluster (Wang et al., 1997).

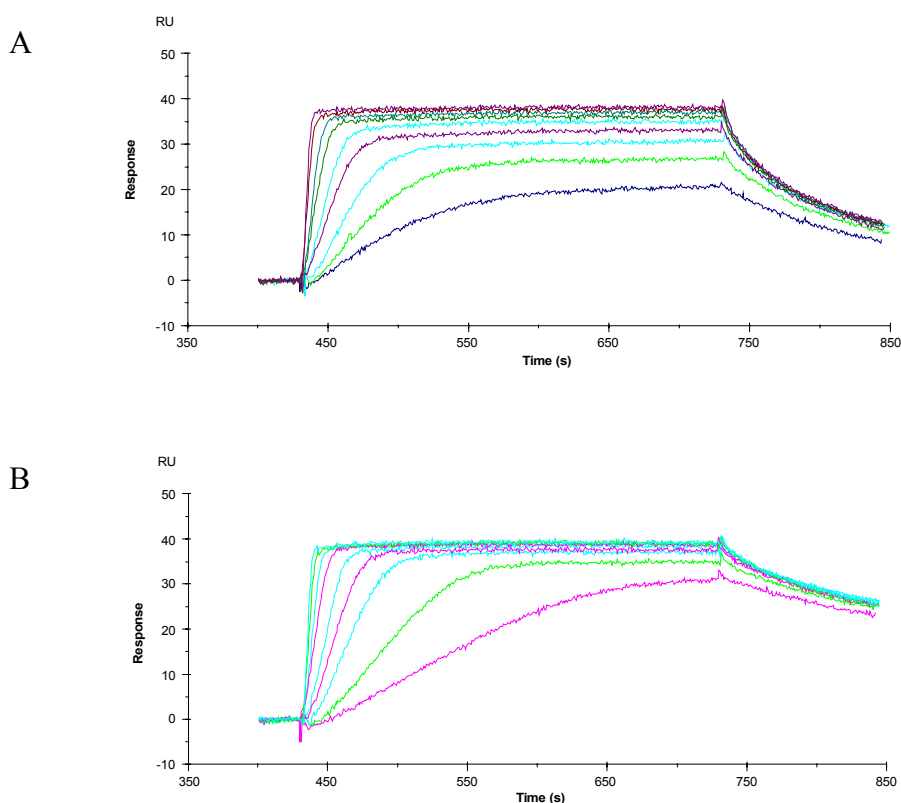


Figure 3.31: Sensograms representing the interaction of IL-4 variants R53A (A) and Y56A (B) with IL-4BP.

4. Discussion

Human IL-4, as most cytokines, has pleiotropic functions and exhibits a wide range of biological effects on various tissues and cells. Responses are induced after IL-4 binds to its receptor. A central goal of receptor research is to understand, at molecular level, how receptors allow cells to sense and to respond to their external environment. A possible approach to this issue is to elucidate the binding determinants within both the ligand and the receptor, and to identify the molecular recognition mechanisms of the interaction between them. Improving the knowledge of the features characterizing the binding mechanisms is not only of theoretical interest, but as well is important for the drug development. Extensive information about the binding epitope of the α chain of the IL-4 receptor is of special benefit for drug design. With regard to the fact that this receptor component is implicated in the binding of two cytokines, which are involved in allergic responses (IL-4 and IL-13), a blocking agent directed against its binding epitope would be of advantage for both IL-4- and IL-13- mediated allergic diseases.

Usually, two powerful methods, structural analysis and mutational analysis, are exploited to characterize sufficiently the interactions occurring within a receptor-ligand system. Only in combination they can explain how energetics and regulatory contacts are encoded into structure, and to provide comprehensive understanding of structure-functional correlations. Structural analysis reveals the contacts that contribute to protein-protein recognition in atomic details (Jones & Thornton, 1996). However, it alone cannot show how these contacts contribute to overall affinity and specificity. Ideally, the high-resolution structure of a complex is used to guide an extensive functional survey of residues present at the interface using site-directed mutagenesis, to allow their individual contributions to be assessed. Furthermore, construction and analyses of double mutants provides additional information about cooperative interactions, which link the behavior of different amino acid residues within the protein molecule.

4.1 Structural Features and Binding Site of Human IL-4BP

Since at the beginning of the presented study there was no structural data about the ligand-binding epitope of IL-4BP, the initial selection of amino acids subjected to alanine substitution relied on two theoretical models of the complex between IL-4 and its receptor, which were available at that time (Bamborough et al., 1994; Gustchina et al., 1995). Both models were built, using as a starting point the extracellular portion of human growth hormone receptor (hGHbp),

since the structural and functional epitopes of the receptor and the ligand have been well characterized (De Vos et al., 1992; Cunningham & Wells, 1993). Based on sequence conservation and the predicted common structural organization for cytokine receptors, the amino acid sequences of a few different extracellular domains of cytokine receptors, including IL-4BP were aligned and examined for similarities to hGHbp.

Although in the hGH/hGHbp complex the major contribution is provided by hydrophobic side chains, the IL-4BP interface proposed by the two models contains several polar and charged residues. Agreeably, as most prominent contact determinants from the receptor side were defined D72 and K91, which were suggested to form ion pairs with IL-4 R88 and E9, respectively. This assumption was supported also by the results from the mutagenesis study of human IL-4, which showed that charged and polar determinants predominate in its high-affinity binding epitope (Wang et al., 1997). According to the alignment of amino acid sequences of hGHbp with IL-4BP A71 and Y129 of IL-4BP superimpose the two most important binding determinants of hGHbp, W104 and W169, respectively. Therefore, those amino acids and their close surrounding from the same loop regions were of principle interest for the mutagenesis study of IL-4BP. Besides this, the models implicated particularly residues D66, D67, V69, S70, N126, Y127, and L128 of IL-4BP in direct contacts with amino acids from the ligand. Additionally, in the mutational analysis were included residues M14 and S15, as well as P92, S93, and E94, since they correlate in the frame of the sequence alignment to amino acids of hGHbp, which have shown certain functional importance for the binding with hGH.

At a later step, when the crystal structure of the complex between human IL-4 and IL-4BP was determined, the set of examined amino acids from IL-4BP interface was extended. Generally, the structure revealed an organization similar to the already observed for other hematopoietic receptors (Hage et al., 1999). IL-4BP consists of two covalently linked domains (D1 and D2). The domains are related to the overall topology of fibronectin type III (FN III) modules and fold into a sandwich comprising seven antiparallel β sheets. Moreover, it contains the strictly conserved four cysteine residues in the N-terminal domain and the strongly conserved “WSXWS” motif near the C-terminus of the second domain, which are distinctive characteristics of the cytokine receptor homology (CRH) region, as defined by Bazan, 1990.

The structural epitope of IL-4BP was shown to be assembled by residues of five loops and has a midline of hydrophobic side chains with patches of tyrosine and serine residues situated on one side and a patch of aspartic acid side chains on the other side (Figure 4.1). An analysis of the possible hydrogen bonds and van der Waals contacts between IL-4 and its receptor revealed that their binding epitopes consist of three structurally independent subunits. Two of them (designated as cluster I and cluster II) were compared to an “avocado fruit”, since they exhibit a conspicuous

amphipathic structure with an outer mantle of hydrophobic side chain moieties and an inner core of polar groups. The third assemblage of trans-interacting side chains was demonstrated to have completely different design. The main characteristic of this cluster is the domination of electrostatic interactions.

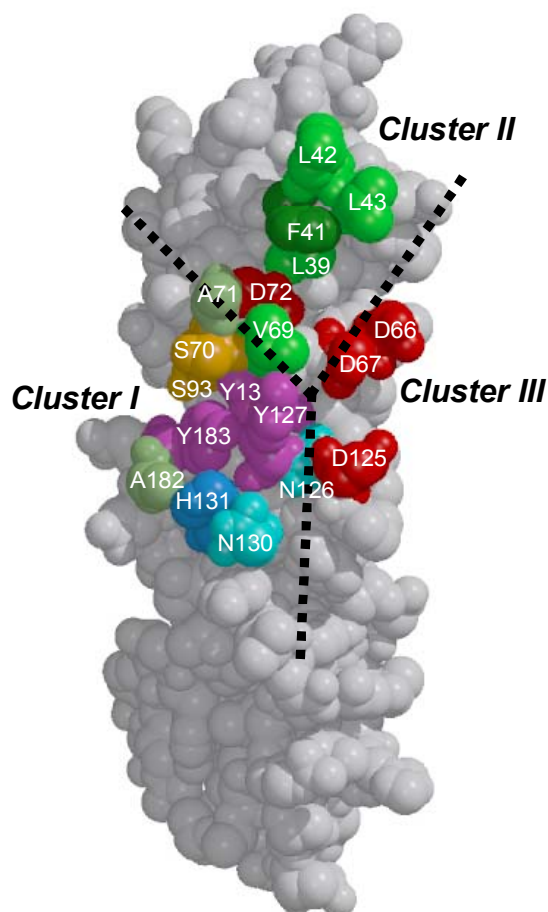


Figure 4.1: Structural epitope of IL-4BP. Contact residues are colored according to their physicochemical properties (red, negatively charged; dark blue, positively charged; light blue, histidine; cyan; glutamine/ asparagine; magenta, tyrosine; orange, serine/threonine, green, hydrophobic) (Hage et al., 1999).

Considering the structure of the above-mentioned clusters, the contacts formed within them between receptor and ligand side chains and the data about the loss of solvent-accessible surface area upon the binding (Table 4.1), a few additional amino acids of IL-4BP were submitted to site-directed mutational analysis. Some of the side chains, which apparently demonstrated considerable change of the accessible surface, were already successfully predicted based on the

theoretical models and included in the study. Since the accessible surface of receptor F41, L42, L43 and Y183 showed a large decrease upon association, they were converted to alanine. Although L39 does not appear to change its solvent accessibility upon the complex formation to the same extent, it is a part of the hydrophobic shell within the second cluster and therefore it was included in the alanine scanning mutagenesis. The solvent-accessible surface area of Y13 does not change upon IL-4 binding. Nevertheless, according to the crystal structure this amino acid is implicated in a hydrogen bond with IL-4 E9 and was of particular interest for the mutational analysis.

Table 4.1: Change in the accessible surface of amino acids within IL-4BP upon formation of the 1:1 complex between IL-4 and IL-4BP (Hage, 1999).

IL-4BP amino acid	Δ Accessible surface [\AA^2]
L39	12
V40	2
F41	106
L42	32
L43	58
D66	23
D67	95
V69	50
S70	71
A71	54
D72	21
K91	1
S93	8
P123	3
D125	98
N126	7
Y127	119
N130	12
H131	27
A182	24
Y183	47

Altogether, in the frame of the entire project, 25 different side chains of IL-4BP distributed over all six loops of the receptor molecule were individually mutated to alanine (Figure 4.2). To refine

the functional epitope, substitutions by more conservative residues were performed, where it was necessary. The binding affinity of the mutated variants to IL-4 was examined by the use of a biosensor-based technology.

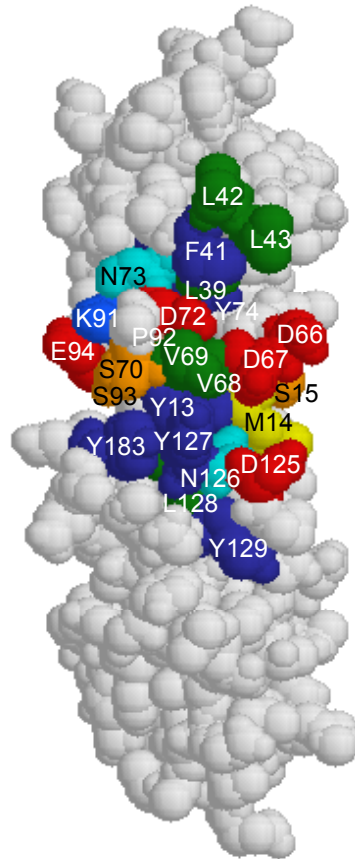


Figure 4.2: Side chains within IL-4BP subjected to site-directed mutagenesis. The colour scheme is according to traditional amino acid properties. Roughly, polar amino acids are presented in bright colours and non-polar in darker. (aspartic acid and glutamic acid, bright red; lysine, mid blue; methionine, yellow; serine, orange; phenylalanine and tyrosine, blue; asparagine, cyan; valine, leucine, green; proline, flesh).

4.2 Defining Functional Important Residues from The Interface of Human IL-4BP for the Interaction with IL-4

The present study has identified all amino acid side chains within the extracellular domain of the IL-4 receptor α chain that are engaged in the high-affinity binding of the ligand. A scanning

mutagenesis strategy was used to dissect the contribution of the particular IL-4BP residues to the binding energy. Such approaches typically assume that no structural disturbances are caused by the mutations, so that the energetic consequences are entirely attributable to the deletion of the contacts.

Undeniably, the site-directed mutational analysis defined the side chain of D72 as one of the major functional determinants for the interaction with the ligand. A mutation at this site to alanine caused 2600-fold decrease of binding affinity, corresponding to energetic contribution of 4.7 kcal/mol. Such an effect definitely indicates affected functional properties and cannot be attributed to structural perturbation due to the introduced mutation. The assumption is based on the analysis of the additional variant D72N. The exchange of the aspartic acid by the structurally similar asparagine is followed by the loss of a negative charge, but generally is not expected to have disruptive effect on the structure. Despite the conservative character of the substitution made, variant D72N demonstrated decrease of binding affinity that basically was the same as the observed for the alanine variant. Thus, the original side-chain D72 and especially its negative charge is directly implicated in a contact to the ligand. The conclusion about the functional importance of D72 for the interaction with IL-4 is consistent with the findings of independent experiments using a cell-based selection strategy (Friedrich et al., 1999; Wietek, 1999). Two different receptor constructs carrying the receptor mutants D72A and D72R, respectively, were expressed in the murine pro-B cell line (Ba/F3) and examined for interaction with IL-4. Proliferation assays verified that cells expressing the charge reverse mutation D72R completely failed to proliferate in the presence of IL-4, while cell populations carrying D72A showed a weak response after treatment with IL-4. In addition, radioligand binding experiments revealed a complete loss of specific IL-4 binding by cells expressing D72R receptors, confirming that D72R receptors are incapable of productive interaction with IL-4. Furthermore, the results from the mutational analysis are in perfect agreement with the crystal structure of the IL-4/IL-4BP complex (Figure 4.3 B), which revealed that a salt pair links the side chain of D72 to IL-4 R88 (Hage et al., 1999).

The results from the alanine scanning mutagenesis pointed three tyrosine residues, Y13, Y127, and Y183, as prominent binding determinants from the receptor side. The mutant variant Y13A showed reduction of binding affinity over 10000-fold compared to the wild-type interaction. Its contribution to the loss of binding free energy counts 5.5 kcal/mol, which is the largest effect observed in the course of the alanine scan for IL-4BP. Further experiments were performed to assess if this effect is functional or structural. Replacement of Y13 by a phenylalanine residue resulted in merely 40-fold decreased binding affinity in comparison with the wild-type. Since the phenylalanine is a structural analog of the originally present amino acid, but without properties

for forming hydrogen bonds, it seems that the reason for the large effect demonstrated by Y13A is rather structural than functional. The alanine variant could still be recognized by the anti-IL-4BP monoclonal antibody and therefore overall structural disruption could be excluded. It is more likely that the substitution caused only local perturbations within the contact cluster, but was not sufficient to destroy the structure as a whole. If Y13 is a structurally important residue for the entire cluster such a substitution will affect not only the contact properties of Y13, but of all amino acids within the cluster and will give an explanation for the large loss of binding free energy demonstrated by Y13A. Further, it has to be considered that in some cases, especially if much smaller amino acid replaces a large one, solvent can occupy the place of the missing side chain. Regarding the crystal structure (Hage et al., 1999), it seems that the effect shown by Y13F represents totally the functional importance of Y13. The hydroxyl group of this residue is implicated in a hydrogen bond with IL-4 E9 (Figure 4.3 A), and on that base it is reasonable to expect a modest functional effect by variant Y13F.

Even more dramatic differences between affinity of the alanine and phenylalanine mutant form were observed in the case of Y127. Variant Y127A was characterized by 80-fold lower binding affinity to IL-4 than IL-4BP, while Y127F did not demonstrate considerable effect (1.2-fold) on the binding and in fact behaved as a wild-type receptor. However, the effect of the alanine substitution is by far not as large as in the case of Y13A and does not support the idea that Y127A is a structurally affected mutant. The structural data suggest that Y127 takes part in a series of hydrophobic interactions with the aliphatic side chain of IL-4 E9 (Hage, 1999). Therefore, it is likely that the reduced binding affinity of variant Y127A represents the contribution of those contacts and they are perhaps not disrupted when variant Y127F plays a part in the interaction with IL-4. According to the structure of the complex with IL-4, the hydroxyl group of receptor Y127 is involved in a hydrogen bond to IL-4 T13 (Figure 4.3 A) and additionally is bridged by a single ordered water molecule to IL-4 N89 (Hage et al., 1999). Nevertheless, the analysis of the mutant form Y127F, which is not able to form such contacts, indicates that they do not have significant contribution to the binding and should not be considered as functionally important for the complex stability.

Replacement of receptor Y183 by alanine and phenylalanine revealed that both variants Y183A and Y183F bound IL-4 with low affinity. The alanine substitution caused a larger effect and the binding affinity of Y183A to IL-4 was reduced 800-fold compared to the wild-type interaction. Due to the introduced mutation, variant Y183F demonstrated an over 300-fold decrease in binding affinity corresponding to 3.4 kcal/mol loss of binding free energy. Definitely, the large energetic effect of mutation Y183F is an indication about the important functional role, which the hydroxyl group of Y183 takes in the interaction with the ligand. The crystal structure of IL-4/IL-

4BP complex showed that this group is involved in a hydrogen bond to IL-4 E9 (Figure 4.3 A), one of the major binding determinants within the ligand (Hage et al., 1999). Another hydrogen bond was suggested to link Y183 to IL-4 K12. Apparently, those are contacts of great significance, which have a crucial role for the stability of the complex with IL-4, since their destruction was followed by a large functional effect. Furthermore, the side chain of receptor Y183 was implicated in van der Waals contacts to IL-4 I5 (Hage, 1999), which might explain to some extent the fact that a substitution by alanine has a greater effect on ligand binding. Small structural perturbations in variant Y183A cannot be excluded to be partially the reason for the reduced binding affinity to IL-4. However, if the mutation Y183A caused some disruptions in the receptor structure they certainly were minor and cannot be compared to the case observed with variant Y13A. Therefore, it seems that within contact cluster I of IL-4BP the residue Y183 provides the largest functional contribution to the ligand binding. Moreover, the site-directed mutational analysis of IL-4BP established the side chain of Y183 as one of the main binding determinants from the receptor side for the high-affinity interaction with IL-4.

Aspartic acids at positions 66, 67, and 125 were converted to alanine and examined for effects on the interaction, as they were determined to be engaged within the third structural cluster of IL-4BP (Hage et al., 1999). The largest reduction in affinity (120-fold) occurred in variant D67A, which energetic contribution was estimated to be 2.8 kcal/mol. Mutations D66A and D125A decreased the affinity to a minor degree: 7- and 10-fold, respectively. The lower effects observed with these variants are in agreement with the suggestion that the third contact cluster is not important for the complex stability (Hage et al., 1999). The amino acids from the cluster were supposed to accelerate complex formation through electrostatic steering. Due to an alanine mutation certainly was affected the association phase of variant D67A, which appeared to be 4-fold slower compared to the wild-type interaction. Apparently, the other two alanine mutants demonstrated negligible changes in association. However, the overall contribution of D125 to the affinity and also to the association of the complex might be partially underestimated, since some contacts to the ligand in which this amino acid is involved are built by its main chain.

The analysis of the hydrophobic sequence of amino acids localized on loop L2 revealed that only L39 and F41 are of certain functional importance for the highly-affinity binding between IL-4 and its receptor. Variant L39A bound IL-4 with over 200-fold lower binding affinity than IL-4BP did, while the binding affinity of F41A decreased over 100-fold. The association phase of both mutant forms was about 2-fold slower than the wild-type exhibited, but their dissociation was significantly affected due to the introduced mutation. Substitution of L42 and L43 by alanine did not result in considerable effects on the binding kinetics. As long as the properties of the alanine variants from this sequence were affected, the effects did not suggest a direct contribution to the

binding, but a supporting function of the original amino acids. Such an assumption is in accordance with the crystal structure, which showed that these amino acids are the main part of a hydrophobic shell surrounding D72 (Figure 4.3 B), and are involved in a number of van der Waals contacts with residues from IL-4 (Hage, 1999). The side chain of V69 localized on another loop (L3) in the receptor molecule completes the hydrophobic cluster around D72. Variant V69A behaved in a similar way to variants L39A and F41A; since it showed a 2-fold slower association and a modest effect on binding affinity (80-fold reduction). Besides the disruption of weak contacts, the substitution of large residues by alanine might be followed by penetration of water molecules in the hydrophobic cluster. Although no one of those residues demonstrated characteristics of a major binding determinant, disorder in the proper hydrophobic environment, which they provide alters to some degree the functional properties of IL-4BP as it affects the complex stability and to a minor extent concerns the association phase.

No one of the residues K91, P92, S93, and E94, which are situated on loop L4 of IL-4BP, indicated significant contribution to the binding when they were exchanged by alanine. The corresponding variants reduced the binding affinity between 2- and 17-fold. In the absence of structural data receptor K91 was of special interest for the study, since a theoretical model of IL-4/IL-4BP complex suggested this residue to be one of the main contact determinants, taking part in electrostatic interactions to IL-4 E9 (Bamborough et al., 1994). For that reason an additional variant K91D was produced and examined, although the analogous alanine variant showed negligible energetic contribution (0.8 kcal/mol). Despite the fact that the charge reversal mutation was expected to cause a grate effect on binding, the affinity in this case was reduced merely 30-fold. Thus, the charge of receptor K91 is not involved in functionally important contacts to the ligand and the residue is not considered as a binding determinant. The site-directed mutagenesis of K91 should be seen as an example for the limited potential and accuracy of the molecular modelling as an approach for defining structural and functional epitopes. Later, in agreement with the above-mentioned findings, the structure of the complex confirmed that the entire loop L4 is not implicated in contacts to the ligand (Hage et al., 1999).

The alanine scanning mutagenesis of IL-4BP did not reveal that some of the remaining amino acids included in the study provide important contribution to binding. Interestingly, variant S70A showed virtually the same binding affinity to IL-4 as the wild-type receptor. This amino acid is involved by its main chain in a hydrogen bond to IL-4 E9 (Figure 4.3 A) and additionally by its side chain forms a second with IL-4 T6 (Hage, 1999). Disruption of the hydrogen bond, in which the side chain of S70 plays a part, clearly showed that this contact is of no functional importance for the stability of the complex. This is supported by the fact that mutations of IL-4 T6, caused just negligible changes on binding affinity (Wang et al., 1997). It is likely that only the contact

made by the main chain of S70 is significant for the interaction with the ligand, but due to limitations of the used method that could not be assessed.

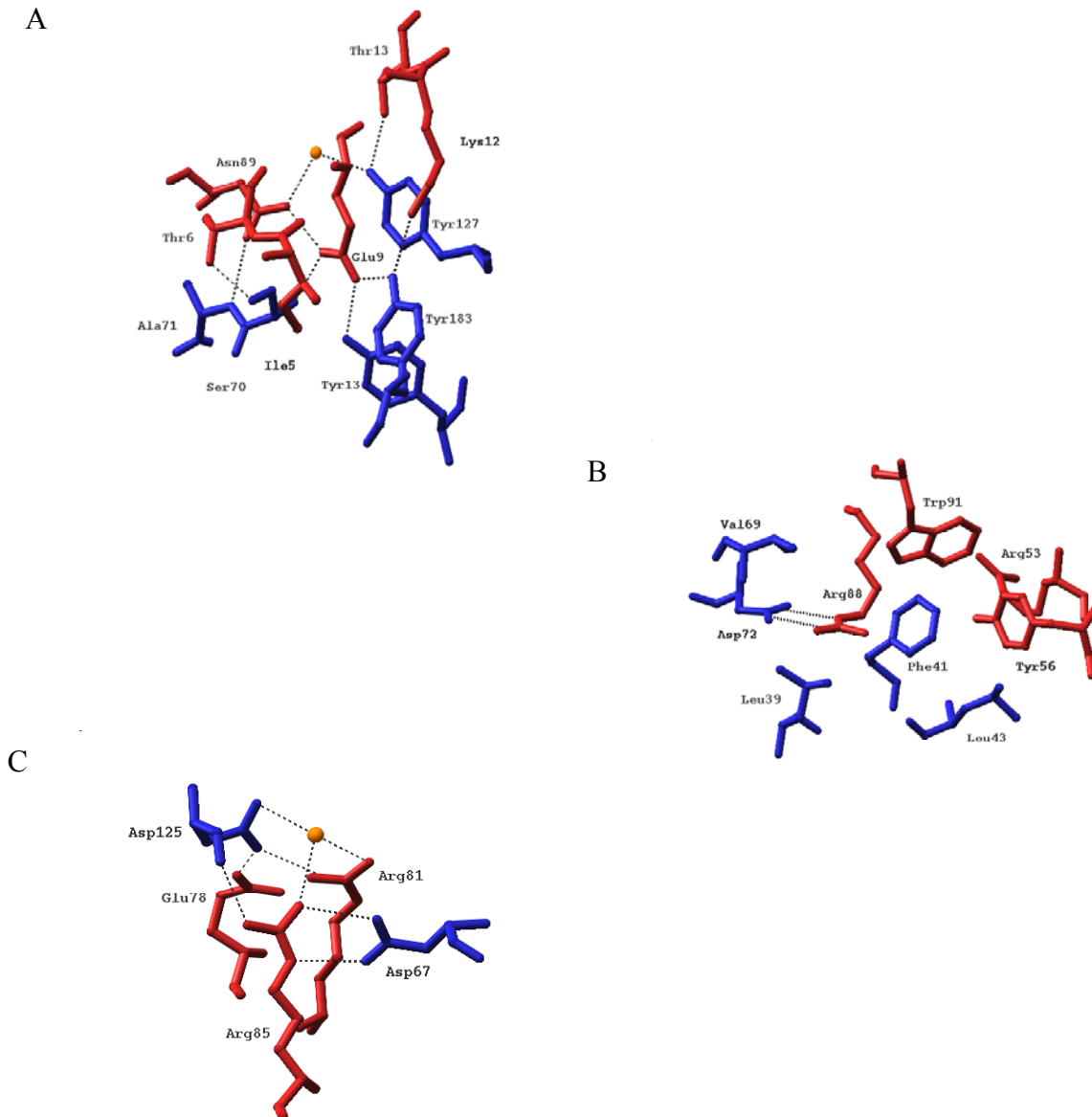


Figure 4.3: Details of the IL-4/IL-4BP contact: A, contact cluster I; B, contact cluster II; C, contact cluster III (Hage et al., 1999).

In conclusion, the site-directed mutagenesis of IL-4PB residues defined clearly its functional epitope for the interaction with IL-4 (Figure 4.4). As major binding determinants were established the side chains of Y183 and D72 from binding clusters I and II, respectively. The contacts made by the side chain of D72 are strongly enhanced by the hydrophobic shell that

encircles it, as it was shown for residues L39, F41, and V69. Meanwhile Y183 is functionally supported by the other two tyrosine side chains, Y13 and Y127, localized within the same cluster. The amino acids included in the third cluster generally indicated lesser contribution to binding. However, D67 certainly is involved in contacts to IL-4 and perhaps is supported in this function by D125.

The existence of further binding determinants is unlikely, but cannot be definitely excluded. Due to restrictions of the applied approach, contributions from alanine could not be analyzed. For instance, the functional importance of A71, which is involved in contacts with ligand residues within the first cluster of IL-4BP and shows relatively large change of accessible surface area upon association, could not be assessed. Furthermore, the site-directed mutational analysis is not able to detect contributions provided by the backbone parts of the amino acids.

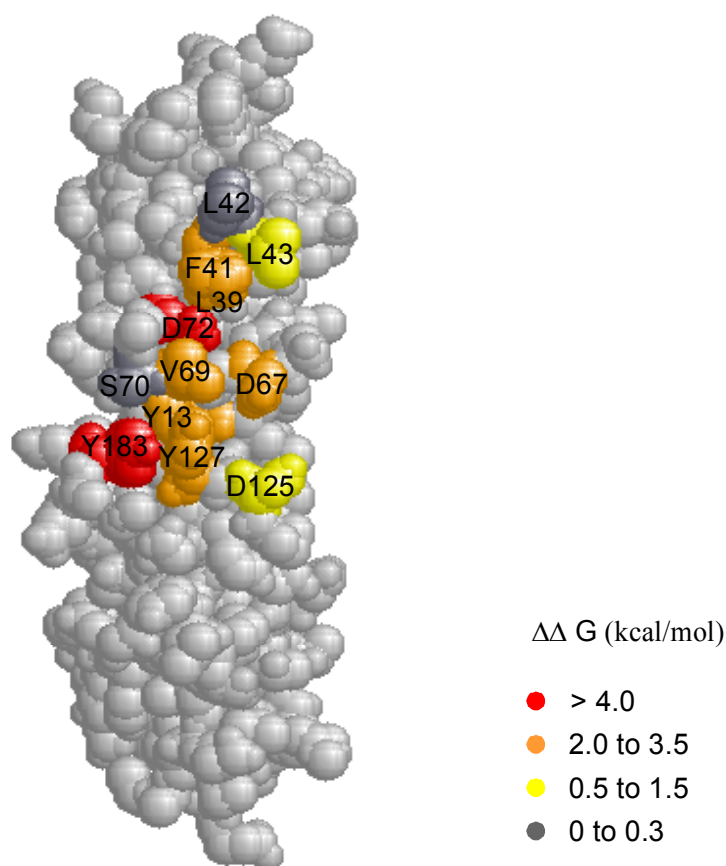


Figure 4.4: Functional epitope of IL-4BP. Residues have been color-coded according to the loss of binding free energy due to alanine substitutions. Mutant variant Y13F has been used to estimate the energetic contribution of Y13, as the alanine form represents a structural mutant.

Based on the results from the alanine scan, the sum of the apparent binding free energy contributions (> 36 kcal/mol) considerably exceeds the estimated binding free energy for the complex (13.8 kcal/mol, corresponding to $K_d=77$ pM). The contributions made only by the residues included in the functional epitope of IL-4BP already give a sum of over 26 kcal/mol. Certainly, some contributions were overestimated due to structural perturbations caused by the introduced alanine residue. Nevertheless, this is only partially the reason for the high sum. The most pronounced instance of structural perturbations is presumably variant Y13A, but even in this case it seems that only approximately 3 kcal/mol from the loss of binding free energy can be attributed to structural effects, while the remaining 2.2 kcal/mol represent disrupted functional properties. Likewise, some alanine variants demonstrated large energetic contributions probably because the side chains of the original amino acids are involved in more than one single contact to the ligand. For example, the crystal structure revealed that the side chain of receptor Y183 takes part in hydrogen bonds to both IL-4 E9 and K12. Furthermore, high loss of binding free energy implies that some of the examined mutations are not independent in their effects. That can be explained by the fact that particular side chains are involved not only in interactions to the ligand but also in intramolecular contacts. If interactions among residues within the receptor molecule are present, as a result the effect of the mutation will be propagated to other residues. In such cases the alanine scanning mutagenesis cannot assess properly the real contribution of the single side chains because the observed effect depends on the state of other residues (Di Cera, 1998). Cooperativity is supposed to take place between residues within the binding epitope of IL-4 (Wang et al., 1997). The small number of amino acids identified in the functional epitope of IL-4BP and the large energetic contribution which they indicate, suggest that cooperative interactions might exist also in IL-4BP.

In summary, the approach based on an alanine scanning mutagenesis is in principle powerful and informative. However, in the course of practical applications some limitations should be considered. Substitution by alanine, although is not supposed to introduce additional new contacts, might cause structural changes and subsequently large energetic consequences. Such effects might be wrongly assessed as functional. Therefore, the residues, which revealed great apparent contribution in the present study, were further mutated to produce structurally similar variants to the wild-type receptor. Furthermore, results might be misinterpreted in cases when interactions of several amino acids are coupled to one another and are not reduced simply to a sum of pairwise interactions. To identify if the effects from the site directed mutagenesis of IL-4BP are independent or not, the present study was completed by analyses of receptor double mutant forms.

4.3 Additivity and Cooperativity in the Functional Epitope of IL-4BP

Additive and cooperative mutational effects between the residues from the functional IL-4BP epitope were examined by applying double mutants. The side chains of amino acids L39, F41, D67, V69, Y127, and Y183 were analyzed for potential intramolecular interactions with Y13 and D72, respectively. In addition, a variant containing mutations at both sites, D72 and Y13, was created.

Comparison of the theoretically predicted $\Delta\Delta G_{\text{add}}$ and the estimated change of binding free energy (Table 3.9) for variants Y13F/Y127A and Y13F/Y183F indicates that the effects between the residues from contact cluster I are additive. This suggests not only that the sites act functionally independent, but also that no one of the introduced mutations caused structural perturbations. Indirectly this fact confirmed the assumption that mutation Y127A in the corresponding single variant was not disruptive to the structure and the observed effect represented basically the functional contribution of this residue to binding. Further, the analysis of double mutants indicated that the hydroxyl group from the side chain of Y13 is not involved in contacts to other residues from the cluster, but just in the interaction with IL-4. Therefore the mutational effect demonstrated by variant Y13F (2.2 kcal/mol) should be seen as the entire contribution of Y13 to ligand binding. The site-directed mutational analysis revealed that Y13 is important probably for the structure of the whole cluster. Since in these double mutated forms of the receptor Y13 was exchanged by the similar phenylalanine residue, which clearly did not affect the structure, it seems that the aromatic ring of Y13 is a crucial structural element supporting the conformation and the integrity of the cluster.

Independent contributions to binding were shown from the side of Y13 and the hydrophobic shell surrounding D72, since the binding free energies of variants Y13F/L39A, Y13F/F41A, and Y13F/V69A negligibly differ from the corresponding $\Delta\Delta G_{\text{add}}$ values. Likewise, additivity was established between the effects of Y13F and the binding determinant from cluster III D67. The binding free energies characterizing the double mutants, which carry the mutations D72N/Y127A and D72N/Y183F were very close to the values predicted by adding the energies of the single mutants. This is a clear indication that the main functional determinant D72 behaves in a completely independent manner from the two tyrosine residues from cluster I.

The analyses of variants D72N/L39A, D72N/F41A, and D72N/V69A suggested that the examined sites in those double mutants are not independent in their effects. As those residues are parts from one and the same binding cluster it is likely that they cooperate and the effects from the individual substitutions are not additive. Further, the values of $\Delta\Delta G_{\text{add}}$ are greater than the estimated $\Delta\Delta G$ for the three variants suggesting favorable interactions between the side chains

(Wells, 1990). The conclusion that the contacts to the ligand in which D72 is involved are enhanced by the hydrophobic shell including L39, F41, and V69 is in agreement with the results from the alanine scan of IL-4BP. Accordingly, the structural analysis defined the contact clusters as assemblies of trans-interacting residues and did not exclude the possibility that within a cluster certain amino acids cooperate (Hage et al., 1999).

The equilibrium dissociation constants and subsequently the binding free energies for two double mutants, Y13F/D72N and D72N/D67A, could not be determined due to their extremely low binding affinity to the ligand. If the effects of the individual substitutions in variants Y13F and D72N were independent, then the change in binding energy caused due to the simultaneous mutation of these sites in variant Y13F/D72N, would be $\Delta\Delta G_{\text{add}} = 7.0$ kcal/mol. Correspondingly, the equilibrium dissociation constant of the double mutated variant would be $K_d = 1.0 \times 10^{-5}$ M, in a case of additivity. Assuming that the mutational effects in sites D72 and D67 are independent, a loss of binding free energy $\Delta\Delta G_{\text{add}} = 7.6$ kcal/mol and $K_d = 2.9 \times 10^{-5}$ M are expected for the interaction between variant D72N/D67A and IL-4. Certainly, those values indicate such a low affinity to the ligand which is at the detection limits of the used BIAcore system. Nevertheless, considering the fact that binding was recorded even for a variant with $K_d = 7.7 \times 10^{-5}$ M (variant D72N/Y183F), detection of interaction also in the case of Y13F/D72N and D72N/D67A should be still possible. Thus, variants Y13F/D72N and D72N/D67A are characterized by considerably lower binding affinity to IL-4 than the theoretically estimated values presuming additive mutational effects. However, this does not necessarily indicate cooperativity between the examined sites. The structural analysis of IL-4BP strongly suggests that the three contact clusters are discrete and independent in their interactions (Hage et al., 1999). Furthermore, if the low binding affinity is seen as a sign for cooperative interactions, the change of binding free energy for those mutants will be greater than the values of the theoretic sum $\Delta\Delta G_{\text{add}}$. This is not very likely, since such values would suggest that the mutant side chains reduce functional properties and the individual substitutions underestimated the contributions of the original residues. Considering the high cumulative loss of binding free energies, which was assessed in the frame of the alanine scan, effects were probably overestimated but not underestimated. Hence, the idea that cooperative interactions between the mutated sites in variants Y13F/D72N and D72N/D67A caused the extremely low binding affinity is not in agreement neither with the results from the alanine site-directed mutagenesis, nor with the structural data. It is more likely that due to the substitutions in the case of D72N/D67A the electrostatic steering between receptor and ligand was affected to a great degree. It was shown that the extraordinarily fast association rate constant, which is the main reason for the high-affinity binding of IL-4 to IL-4BP, is caused by complementary electrostatic potentials of both

interfaces (Shen et al., 1996; Wang et al., 1997). Accordingly, variant D67A demonstrated the slowest association rate constant in the site-directed mutational analysis. The association phase of D72N could not be examined. In addition, alanine substitutions of the hydrophobic side chains surrounding D72 in cluster II revealed small but systematic reduction of the on-rate for L39, F41, and V69, suggesting that perhaps the entire cluster is recognized early in association. The third charged residue within the functional epitope of IL-4BP (D125) did not indicate significant effect on the association. It is likely that the charges of D72 and D67 are critical for the initiation of electrostatic steering between receptor and ligand and therefore their simultaneous loss in variant D72N/D67A results in such low electrostatic potential in the receptor that is under the point, which allows the complex formation. This suggestion is in agreement with the mechanism of association proposed for the complex of hGH and its receptor (Cunningham & Wells, 1993). Accordingly, the association is a multi-step process that starts with the formation of an initial weak complex, which undergoes further desolvation and cooperative rearrangement.

Not all amino acids from IL-4BP examined by site-directed mutagenesis were included in the analysis of double mutants and therefore perhaps not all cases of cooperativity were identified. However, cooperative effects clearly were demonstrated to take part at least between amino acids within contact cluster II. This fact gives to some degree an explanation for the high cumulative loss of binding free energy, which was calculated according to the contribution of alanine variants.

4.4 Comparison of the Structural and the Functional IL-4BP Epitopes

Generally, the functional epitope of IL-4BP defined by mutational analyses is in a good agreement with the structural data. Similarly to the structural epitope, the functional important residues of IL-4BP are assembled in three differentiated clusters. The crystal structure of the IL-4/IL-4BP complex proposed that the clusters are independent, but did not exclude the possibility that cooperative interactions take place in the same contact cluster (Hage et al., 1999). Respectively, the present analysis did not show a clear indication for interactions between the defined clusters. Furthermore, cooperativity was demonstrated to occur between side chains within one and the same cluster.

The structure revealed that 835 Å² of the receptor surface area are buried upon complex formation (Hage et al., 1999). This indicates that the high-affinity interaction between IL-4 and IL-4BP is generated from a relatively small contact area and that its size is not directly connected to binding affinity. Accordingly, amino acids localized out of the structural epitope did not appear

to have significant effects on binding affinity when they were mutated. Although segregation in the contribution of the examined residues present in the structural epitope of IL-4BP was observed, nearly all of them showed considerable effect on binding. Thus, the modest size of the IL-4BP structural epitope determines a corresponding functional epitope, which has a similar size.

The structure of contact clusters I and II was compared to an “avocado fruit” and was suggested to be highly relevant to binding because polar interactions are enhanced in a hydrophobic environment (Hage et al., 1999). Agreeably, the mutational analysis indicated as main binding determinants residues from the central core of IL-4BP clusters I and II. Particularly large contribution to binding demonstrated the side chains of Y183 and D72, respectively. Most of the residues from their close surrounding certainly are implicated in the interaction with IL-4, although the mutations at those sites caused a loss in binding affinity to a lesser extent. Contact clusters I and II were proposed to have the same contribution to binding (Hage et al., 1999). However, based on the findings from the mutagenesis study of IL-4BP it seems that, comparing functional contributions, cluster II has slight prevalence over cluster I. Estimated from the loss of free binding energy in the mutant proteins, the entire cluster II (13.3 kcal/mol) accounts approximately for 95 % of binding energy, while the energetic contribution of cluster I corresponds to around 60 % (8.8 kcal/mol)¹. In agreement with the suggestions based on structural data, the mutational analysis indicated that the residues from the third contact cluster have minor functional role in complex stability and the entire cluster contributes with 30 % (4.2 kcal/mol) to binding energy. Additionally, the importance of this cluster, and particularly of the side chain of D67, for the association phase was confirmed. Alanine substitutions of a few residues present in the defined structural epitope did not produce considerable effect on binding affinity. Those are amino acids localized in the periphery of the binding epitope, and it is likely that the contacts made by their side chains are not of importance for the high-affinity interaction with IL-4. It is possible that some of them are directly involved in binding by their main chains, but due to limitations of the used approach such a suggestion could not be verified. Furthermore, it cannot be excluded that the periphery of the interface has another important role. For instance, it might contribute substantially to the specificity of binding by repulsion of non-target molecules through unfavorable electrostatic or steric interactions, or both.

Comparison between the change of buried surface area upon binding and the change in the free energy of binding when the particular side chain was mutated revealed a very poor correlation

¹ The contribution of cluster I was estimated considering the loss of binding affinity of variants Y13F, Y127A, and Y183A. Variant Y13F was favoured, since it represents better the functional properties of Y13 than the analogous alanine variant. Data about variants L39A, F41A, V69A, and D72A, was used for cluster II. Other variants were not included, as they demonstrated negligible contribution to binding.

(Figure 4.5). The largest decrease of accessible surface upon association was shown to occur for Y127 and F41 (Hage et al., 1999). Substitution of both residues by alanine was followed by modest effect on binding affinity and therefore they were suggested to have basically a supporting role for the interaction with IL-4. Likewise, amino acids L43 and S70 indicated high decrease of accessible surface, but did not affect any binding properties of the receptor when they were mutated. Meanwhile, the two main functional determinants D72 and Y183 are characterized by far lower change in buried surface area. Thus, although the decrease of accessible surface upon binding is useful when the entire epitope is defined, this parameter alone is not sufficient to assess the role of the individual side chains. Presumably, for the nonfunctional residues the energetic cost of desolvation and side chain rearrangement compensates the energy gained through the intermolecular interaction and therefore they do not stabilize the complex.

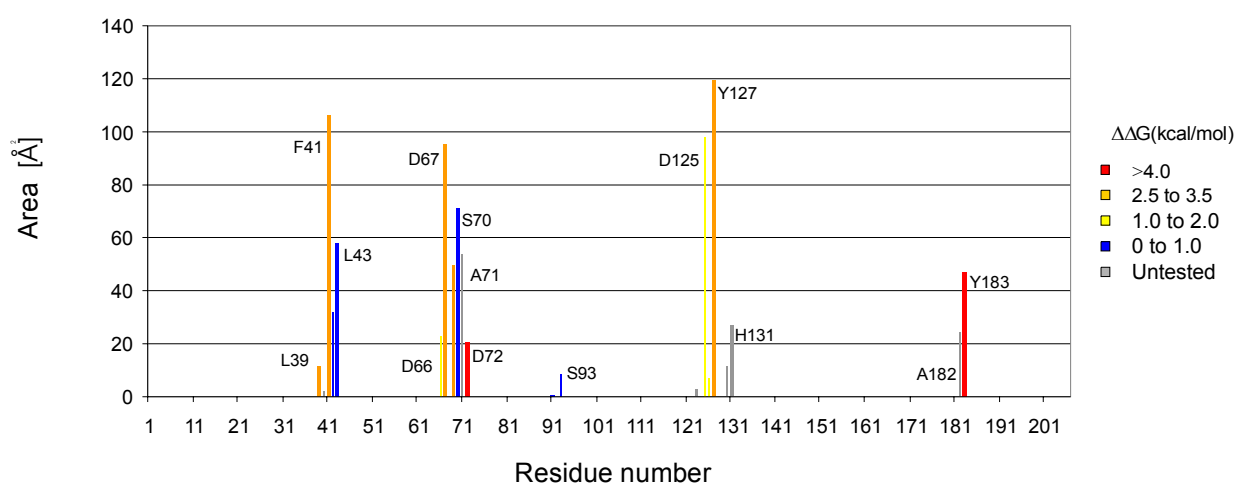


Figure 4.5: Decrease in solvent accessibility on complex formation for IL-4BP (data was taken from Hage, 1999) and loss of binding free energy when the individual side chains were converted to alanine.

In the IL-4BP, molecule is observed a clear hierarchy regarding the functional significance of the particular clusters. The mosaic design of the structural epitope of IL-4BP predetermines the independent functional behaviors of the clusters in the process of binding. Possibly, this fact opens perspectives for drug design based on the mimicry of the assemblies. Compounds with low molecular weight might act as antagonists of IL-4, if significant affinity is assured. The most promising in this sense seems to be cluster II. Mimicry of cluster I might additionally increase the effect.

4.5 Complementarity between the Functional Epitopes of Human IL-4 and IL-4BP

Site-directed mutagenesis has previously been used as a strategy to determine the functional epitope on the ligand side of the interface (Wang et al., 1997). A set of alanine, glutamine, and charge reversed mutant forms of IL-4 were studied for effects on the interaction with IL-4BP by means of the BIAcore technology. The similar approaches used in the previous and current study give a reliable basis to compare the functional epitopes of ligand and receptor. In the framework of the present project two additional IL-4 variants R53A and Y56A were produced and analyzed. The original side chains were shown by the structure to be a part of contact cluster II and were implicated in contacts to residues from IL-4BP.

The results of the systematic mutational analysis of IL-4 contact residues (Wang et al., 1997) confirmed that the functional important residues are localized on the helix AC face of the ligand (Figure 4.6). Furthermore, they are in agreement with the functional significance of the tree clusters of trans-interacting residues identified in the structure of the complex and support the existence of a mosaic binding (Wang et al., 1997, Hage et al., 1999). In like manner to the IL-4BP structure, the contact clusters I and II of IL-4 were shown to resemble an “avocado fruit”. Mutations of the central amino acids within those two clusters, namely E9 and R88, had the largest effects on binding affinity observed among the IL-4 mutant forms. Their energetic contribution to the complex stability was estimated to be over 3.5 kcal/mol for each. Both residues are implicated in direct contacts to the corresponding main binding determinants from the IL-4BP interface. Accordingly, the carboxylate of E9 accepts three bonds from receptor Y13, Y183, and S70, while R88 is linked by a salt pair to the receptor D72. The energetic effect resulting from the substitution of receptor D72 by alanine is greater than from an analogous replacement of IL-4 R88. Since those residues were not demonstrated to take part in other contacts, it is likely that the higher effect in the receptor alanine variant represents the cooperative interactions within IL-4BP cluster II where D72 is localized. Mutations of residues from the periphery of IL-4 clusters I and II indicated modest contributions of the original side chains to the binding. Agreeably, the conversion to alanine of IL-4 residues R53 and Y56, which are parts from the shell of cluster II, was followed by 36- and 8-fold reduction in binding affinity. Similarly, the mutagenesis analysis of IL-4BP amino acids, which surround the main determinants, indicated that their side chains have only indirect but not main functions for the interaction.

The results from substitutions performed in the corresponding clusters III of IL-4 and IL-4BP revealed that the residues from the both sides of the interface are important for the association

phase rather than to contribute significantly to the stability of the complex. Thus, comparison between the energetic effects of mutations introduced in the analogous functional epitopes of IL-4 and IL-4BP demonstrates a striking complementarity: energetically critical and unimportant regions on one molecule match those on the other (Figures 4.4 and 4.6). As a result, the two proteins are able to interact with high affinity and specificity and to form a stable complex through relatively small functional epitopes.

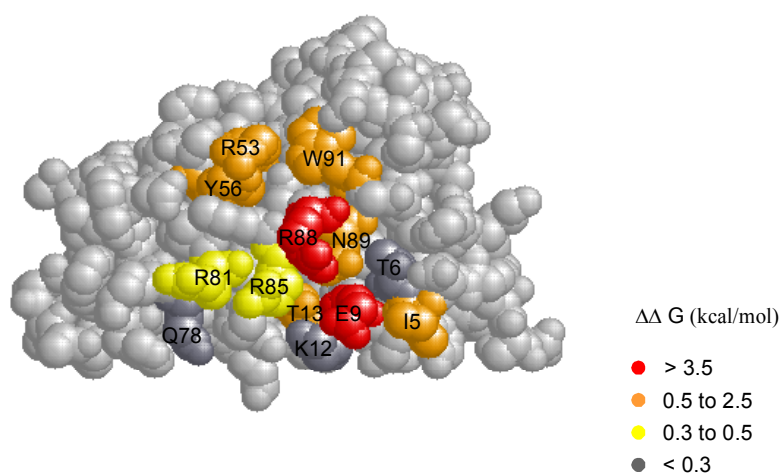


Figure 4.6: The functional epitope of IL-4. Residues are color-coded according to the loss of binding free energy upon site directed mutagenesis. Data from Wang et al., 1997 is taken.

Additivity analysis shows that summation of the disruptive effects of the alanine mutations of amino acids present in the IL-4BP functional epitope produces a value in excess of 26 kcal/mol. By comparison, for the mutations performed within the IL-4 functional epitope this value counts for over 15.5 kcal/mol. The cumulative loss of binding free energy for IL-4 might be slightly higher than the value mentioned above, since data for IL-4 variant E9A is not available and therefore the contribution of variant E9Q was used in this calculation (Wang et al., 1997). The summations of the energetic effects seen for IL-4 and IL-4BP mutant forms, respectively exceed the total change in binding free energy for the interaction of the wild-type ligand and receptor (13.8 kcal/mol). Based on this fact, it was assumed that the individual mutations in both proteins are not completely independent. However, the cumulative loss of binding free energy estimated

for IL-4BP certainly exceeds a lot this for IL-4. This difference cannot be explained with the implication of more main-chain interactions from one side of the interface than from the other, because both proteins, IL-4 and IL-4BP, were shown to build contacts mainly through side chains (Hage, 1999). The substantially greater cumulative loss of binding free energy for the receptor molecule is consistent with the findings that some of the residues within the functional epitope of IL-4BP are involved in cooperative interactions. It seems that the main functional side chains in IL-4 act in a more independent way and if cooperative effects within the epitope exist, they are of minor importance. In part, this probably reflects the rigidity of secondary structural scaffolds on which the complementary epitopes are presented: the major binding determinants from IL-4 are localized on helices whereas those of IL-4BP are displayed from loops.

4.6 Comparison of the IL-4BP Functional Epitope to Other Cytokine Receptors

Structurally the human IL-4BP is similar to the extracellular domains of other type I cytokine receptors that interact with short or long chain helical cytokines (Hage et al., 1999). Based on the structural homology and the established pattern of interaction between hGH and hGHbp (Clackson & Wells, 1995), hydrophobic contacts were suggested to dominate in the complexes of four-helix bundle cytokines (Kossiakoff & De Voss, 1999). However, the present results put together with the mutational analysis of IL-4 and the structure of IL-4/IL-4BP complex indicate that this is not universally the case, since within the epitopes of both the ligand and the receptor, a mixture of charged, polar, and hydrophobic side chains has been identified.

In contrast to IL-4BP, the functional epitope of hGHbp is represented by a compact patch in the center of the contact region in which the hydrophobic residues form a core flanked by charged groups. Two tryptophans of the core (W104 and W169), constituting a “hot spot” for the interaction with hGH, were shown to account for the majority of the binding free energy. A structure-based sequence alignment reveals that IL-4BP Y127 is the direct homologue of W169 in hGHbp (Figure 4.7). Furthermore, M150 in EPB (Middleton et al., 1999) and V230 in gp130 (Horsten et al, 1997; Bravo et al, 1998), which superimpose to the same position, are important binding determinants for the interactions with their corresponding ligands. Similar to hGHbp W169, V230 from gp130 and M150 from EPB are parts of the hydrophobic surface forming the functional epitopes of those receptors. Although reduction in binding affinity was seen when Y127 in IL-4BP was substituted by alanine, the effect indicates rather supporting than major functions of this residue in binding.

The other major binding determinant of hGHbp, W104, according to the sequence alignment corresponds directly to S70 of IL-4BP (Figure 4.7). Mutational analysis clearly demonstrated that the side chain of S70 has no functional importance for the interaction with IL-4. However, the same receptor loop (L3) contains the major binding determinant D72 from the second binding cluster of IL-4BP that is involved in tight interaction with IL-4 R88. It approximately resembles not only W104 of hGHbp, but also F93 of EPB, which is a critical determinant of erythropoietin binding (Barbone et al, 1997). Likewise, the position of IL-4BP D72 correlates to Y172 of GCSF-R that has been suggested to take part in functionally very important hydrogen bonds to residues from the ligand (Layton et al, 1997; Aritomi et al, 1999). Thus, it seems that the presence of residues critical for binding in loop L3 might be a common feature of class I cytokine receptors.

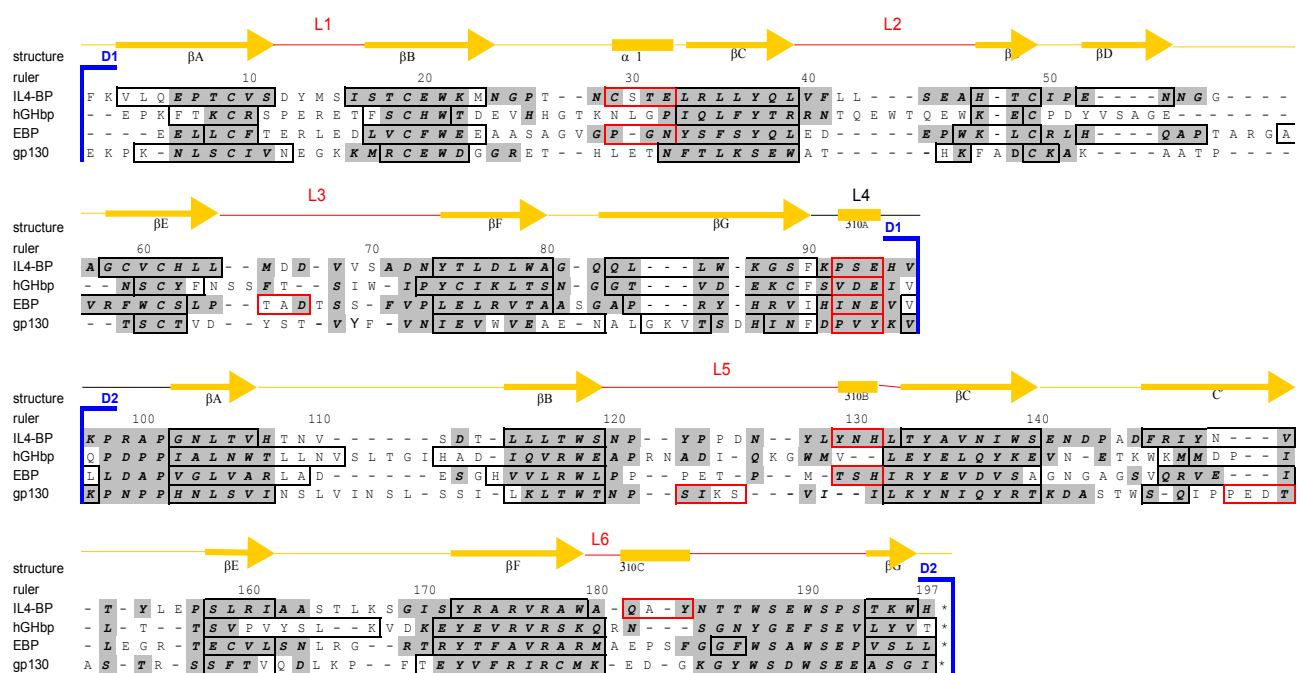


Figure 4.7: Structure-based sequence alignment of different extracellular domains of cytokine receptors (IL-4BP, hGHbp, EBP, and gp130). Amino acid sequences are given in one letter code; deletions are marked “-“, sequence numbering and secondary structure designations are given for IL-4BP. β strands and $\alpha/3_{10}$ helices are depicted by black and red boxes, respectively. A gray background indicates structural superposition (Hage et al., 1999).

In accordance with the sequence alignment, no important side chains of hGHpb and EPB correspond to IL-4BP Y183. Nevertheless, the structurally guided mutagenesis of IL-4BP residues revealed that Y183 is the main binding component of cluster I engaged in interaction

with the ligand. Comparison with GCSF-R shows that within the same receptor loop where IL-4BP Y183 is localized (L6), is positioned residue R287, which obtained the greatest effect on binding after alanine substitution (Layton et al., 1997). Another residue Y13, which is also present in the first contact cluster of IL-4BP has as a structural homologue R43 from hGHbp. Structurally Y13 is a part from the hydrophobic shell surrounding the main binding determinant Y183 of IL-4BP and in like manner L43 is a peripheral element from the functional epitope of hGHbp. Agreeably, both side chains are characterized by modest effects on binding, when replaced in a structurally non-disruptive way.

The aspartic acid at position 67 from the third contact cluster of IL-4BP appears to be homologous to D89 in EBP that has been implicated in contacts to EPO at site 2 (Syed et al., 1998). Although data from mutagenesis of EPB D89 currently is not available, generally it is known that the interactions between EPB and EPO at site 2 are less extensive than at site 1. Similarly, the present analysis indicates that the residues within cluster III of IL-4BP provide lesser contribution to the stability of the complex with IL-4. The other aspartic acid present in the same cluster of IL-4BP D125 resembles D164 in hGHbp. Substitution by alanine of both side chains was followed by relatively small effects on binding affinity (Clackson et al., 1998).

The functions in binding of the hydrophobic sequence localized within loop L2 and comprising L39, F41, L42, and L43 is unique for the IL-4/IL-4BP receptor complex. This sequence represents the main part of the hydrophobic shell in cluster II, which is completed by V69 from loop L3. According to the structural alignment, IL-4BP V69 superimposes I103 from hGHbp and L171 from GCSF-R. The effects on binding affinity observed after the hydrophobic residues at this position were mutated to alanine suggest that in all receptors they have indirect functional contribution to the binding (Clackson & Wells, 1995; Layton et al., 1997).

In summary, the functional epitope of IL-4BP significantly differs from other structurally well-characterized cytokine receptors, such as hGHbp and EBP, for which the majority of binding energy is attributed to a few hydrophobic residues. In contrast, both the present study and the mutational analysis of IL-4 indicate that the critical contacts in the IL-4/IL-4BP complex are provided by polar and charged residues. Correspondingly, the crystal structure of IL-4/IL-4BP complex revealed that the relative position of IL-4BP is remarkably altered compared to hGHbp (Hage et al., 1999). Thus, both the spatial orientation of IL-4 and IL-4BP in the complex and the functional properties of the contact establish novel features different from the binding in the homodimeric hGH receptor complex. The molecular arrangement of GCSF and its receptor was shown to be similar to that of IL-4/IL-4BP complex (Aritomi et al., 1999). Furthermore, the distribution of hydrophobic and polar contacts found in the two complexes is comparable. The importance of charged residues and polar contacts was demonstrated also for the interaction

between p35 and p40, the two subunits of IL-12, which is a heterodimeric cytokine similar to the class I cytokine-receptor complexes in its overall architecture (Yoon et al., 2000). Based on these data, two distinct models of interactions seem to exist for the binding between cytokines and their receptors. In the first case, the interfaces are dominated by hydrophobic residues, as it has been established for the receptor systems of hGH and EPO. In the second, charged and polar contacts are dominating, while the hydrophobic have only indirect contribution to the binding, as it was shown for the complexes of IL-4, GCSF and the two subunits of IL-12. Moreover, the binding epitope of IL-4BP is further distinguished from those receptors by its unique mosaic-like topography consisting of three discrete contact clusters.

5. Summary

The cytokine IL-4 is a basic regulator of immune responses that plays a pivotal role in the pathophysiology of allergic diseases. Its effects depend upon binding to and signaling through a receptor complex composed of the IL-4R α chain and the common gamma chain (γ_c). A first and crucial event in receptor activation is the interaction between IL-4R α chain and IL-4, which is characterized by high affinity ($K_d \approx 100$ pM) and specificity. Signal transduction pathways are mediated after the subsequent recruitment of γ_c . Therefore the IL-4 receptor complex is seen as a promising therapeutic target for treatment of allergic disorders.

The aim of the present study was to define the functional epitope of IL-4BP that is engaged in the high-affinity interaction with IL-4. Side chains of IL-4BP amino acids, implicated in contacts to the ligand, were analyzed systematically by the means of site-directed mutagenesis. In a first step, all residues of interest were replaced by alanine. To verify whether the observed effects in the alanine variants were functional or structural, in a few cases, the original amino acids were further substituted by structurally similar residues. Moreover, double mutants were constructed with the purpose to examine cooperative and additive interactions between residues within the functional epitope of IL-4BP. All IL-4BP mutant variants were expressed in an eukaryotic expression system (Sf9 insect cells). Variants, which retained relatively high binding affinity to the ligand, were successfully purified by IL-4 affinity chromatography. An alternative purification procedure using a monoclonal antibody against IL-4BP was established for low-affinity variants. The effects on binding kinetics, due to the introduced mutations, were measured employing biosensor technology.

The mutagenesis analysis revealed that IL-4BP takes part in the high-affinity interaction with IL-4 through a relatively small functional epitope. As major binding determinants were identified the side chains of two amino acids localized within contact clusters I and II, respectively. The residues of six additional amino acids contribute to the binding to a minor extent. In contrast to other cytokine receptors, in which the major contributions to binding are from hydrophobic side chains, the IL-4BP functional epitope is assembled from charged, polar, and hydrophobic residues. Furthermore, the critical contacts for binding to IL-4 are provided by charged and polar residues, while the hydrophobic side chains have only supporting functions in the interaction. The energetic segregation observed within the IL-4BP binding interface is highly relevant and complementary to the already described IL-4 functional epitope.

The mosaic design of the binding epitope proposed by the crystal structure of the IL-4/IL-4BP complex was confirmed in this study. The three contact clusters were demonstrated to act in an

independent manner. However, cooperative interactions between residues present in one and the same cluster were observed. Moreover, the clusters could be distinguished according to their apparent contribution and functional importance for the binding. Estimated from the loss of free binding energy in the affected mutant variants, contact cluster II has the greatest contribution to binding followed by cluster I and cluster III, respectively. Both clusters I and II appear to have important functions in stabilizing the complex between IL-4 and its receptor, since mutations introduced in those assemblies resulted in considerably affected binding properties. In contrast, substitutions of residues from cluster III caused merely small effects on binding affinity, indicating that the cluster plays a role mainly in electrostatic steering in order to accelerate complex formation.

The mutational analysis presented in this thesis, together with the already established IL-4 functional epitope and the structure of the intermediate complex between IL-4 and IL-4BP, improves the understanding of the molecular mechanisms of receptor binding and activation for members of the cytokine receptor family. Detailed knowledge about the molecular recognition between cytokines and their receptors is not only of theoretical interest, but is also important as a base for drug design.

6. Literature

- Aman, M.J., Tayebi, N., Obiri, N., Puri, R.K., Modi, W.S. & Leonard, W.J. (1996) cDNA cloning and characterisation of the human interleukin 13 receptor α chain. *J. Biol. Chem.* **271**, 29265-29270
- Anderson, G.G. & Morrison, J.F. (1998) Molecular biology and genetics of allergy and asthma. *Arch. Dis. Chil.* **78**, 488
- Aritomi, M., Kunishima, N., Okamoto, T., Kuroki, R., Ota, Y. & Morikawa, K. (1999) Atomic structure of the GCSF-receptor complex showing a new cytokine-receptor recognition scheme. *Nature* **401**, 713-717
- Baixeras, E., Roman-Roman, S., Jitsukawa, S., Genevee, C., Mechiche, S., Viegas-Pequignot, E., Hercend, T. & Triebel, F. (1990) Cloning and expression of a lymphocyte activation gene (Lag-1) *Mol. Immunol.* **27**, 1091-1102
- Bamborough, P., Hedgecock, C.J.R. & Richards, W.G. (1994) The interleukin-2 and interleukin-4 receptors studied by molecular modeling. *Structure* **15**, 839-851
- Barbone, F.P., Middleton, S.A., Johnson, D.L., McMahon, F.J., Tullai, J., Gruninger, R.H., Schilling, A.E., Jolliffe, L.K. & Mulcahy, L.S. (1997) Mutagenesis studies of the human erythropoietin receptor. *J. Biol. Chem.* **272**, 4985-4992
- Bazan, J.F. (1990) Structural design and molecular evolution of a cytokine receptor superfamily. *Proc. Natl., Acad. Sci. USA* **87**, 6934-6938
- Beckmann, M.P., Cosman, D., Fanslow, W., Maliszewski, C.R. & Lyman, S.D. (1992) Interleukins: Molecular biology and immunology. *Chem. Immunol.* **51**, 107-134
- Bennett, B.L., Cruz, R., Lacson, R.G., Manning, A.M. (1997) Interleukin-4 suppression of TNF α -stimulated E-selectin gene transcription is mediated by STAT6 antagonism of NF κ B. *J. Biol. Chem.* **272**, 10212-10219
- BIAcore Handbook (1995) Biacore 2000 Handbook, *Pharmacia*
- Birnboim, H.C. & Doly, J. (1979) A rapid extraction procedure for screening recombinant plasmid DNA. *Nucl Acid Res* **7**, 1513-1523.
- Bravo, J., Staunton, D., Heath, J.K. & Jones, E.Y. (1998) Crystal structure of a cytokine-binding region of gp 130. *The EMBO J.* **17**, 1665-1674
- Brusselle, G., Kips, J., Joos, G., Bluethmann, H. & Pauwels, R. (1995) Allergen-induced airway inflammation and bronchial responsiveness in wild-type and interleukin-4-deficient mice. *Am. J. Respir. Cell Mol. Biol.* **12**, 254-259
- Brusselle, G.G., Kips, J.C., Tavernier, J.H., van der Heyden, J.G., Cuvelier, C.A., Pauwels, R.A. & Bluethmann, H. (1994) Attenuation of allergic airway inflammation in IL-4 deficient mice. *Clin. Exp. Allergy* **24**, 73-80
- Callard, R. & Gearing A. (1994) The cytokine facts book, p53
- Carter, P., Winter, G., Wilkinson, J., & Fersht, R. (1984) *Cell* **38**, 835-840
- Chen, H.J. & Paul, W.E. (1997) Cultured NK1.1(+)CD4(+) T cells produce large amounts of IL-4 and IFN γ upon activation by anti-CD3 or CD1. *J. Immunol.* **159**, 2240-2249
- Chomarat, P. & Banchereau, J. (1997) An update on interleukin-4 and its receptor. *Eur. Cytokine Netw.* **8**, 333-344
- Clackson, T. & Wells, J.A. (1995) A hot spot of binding energy in a hormone-receptor interface. *Science* **267**, 383-386

- Clackson, T., Ultsch, M.H., Wells, J.A. & de Vos, A.M. (1998) Structural and functional analysis of the 1:1 growth hormone: receptor complex reveals the molecular basis for receptor affinity. *J. Mol. Biol.* **277**, 1111-1128
- Coffman, R.L., Ohara, J., Bond, M.W., Carty J., Zlotnik, A. & Paul, W.E. (1986) B cell stimulatory factor 1 enhances the IgE response of lipopolysacchride-activated B cells. *J. Immunol.* **136**, 4538-4541
- Cohn, L., Homer, R.J., MacLeod, H., Mohrs, M., Brombacher, F. & Bottomly, K. (1999) Th2-induced airway mucus production is dependent on IL-R α , but not on eosinophils. *J.Immunol.* **162**, 6178-6183
- Cookson, W.O. & Moffatt, M.F. (1998) Alchemy for asthma. *Nature Medicine* **4**, 500-501
- Corry, D.B., Folkesson, H.G., Warnock, M.L., Erle, D.J., Matthay, M.A., Wiener-Kronish, J.P. & Locksley, R.M. (1996) Interleukin 4, but not interleukin 5 or eosinophils, is required in a murine model of acute airway hyperreactivity. *J. Exp. Med.* **183**, 109-117
- Cunningham, B.C. & Wells, J.A. (1993) Comparison of a structural and a functional epitope. *J. Mol. Biol.* **234**, 554-563
- Cunningham, B.C. & Wells, J.A. (1995) *Science* **244**, 1081-1085
- D'Eustachio, P., Brown, M., Watson, C. & Paul, W.E. (1988) The IL-4 gene maps to chromosome 11, near the gene encoding IL-3. *J. Immunol.* **141**, 3067
- David, M., Petricoin, E., Benjamin, C., Pine, R., Weber, M.J. & Larner, A.C. (1995) requirement for MAP kinase activity in interferon α and interferon β -stimulated gene expression through STAT protein. *Science* **269**, 1721-1723
- De Vos, A.M., Ultsch, M. & Kossiaffoff, A.A. (1992) Human growth hormone and extracellular domain of its receptor: crystal structure of the complex. *Science* **255**, 306-312
- Defrance, T., Aubry, J.P. Rousset, F., Vandervliet, B., Bonnefoy, J.Y., Arai, N., Takebe, Y., Yokota, T., Lee, F., Arai, k., (1987) Human recombinant interleukin-4 induces Fc ϵ receptors (CD23) on normal human b lymphocytes. *J. Exp. Med.* **165**, 1459-67
- Dh, R., Hiles, I., Panayotou, G., Roche, S., Fry, M.J., Gout, I., Totty, N.F., Truong, O., Vicendo, P., Yonezawa, K., et al., (1994): PI-3 kinase is a dual specificity enzyme: autoregulation by an intrinsic protein-serine kinase activity. *EMBO J.* **13**, 522-533.
- Di Cera, E. (1998) Site – specific analysis of mutational effects in proteins. *Advances in Protein Chemistry* **51**, 59-119
- Dubucquoi, S., Desreumaux, P., Janin, A., Klein, O., Goldman, M., Tavernier, J., Capron, M. & Capron, A. (1994) Interleukin-5 secretion by eosinophils – association with granules and immunoglobulin-dependant secretion. *J. Exp. Med.* **179**, 703-708
- Duschl, A. & Sebald, W. (1996) Transmembrane and intracellular signalling by interleukin-4: receptor dimerization and beyond. *Eur. Cytokine Netw.* **7**, 37-49
- Fernandez-Botran, R. & Vitetta, E.S. (1990) A soluble, high-affinity, interleukin-4 binding protein is present in the biological fluids of mice. *Proc. Natl., Acad. Sci. USA* **87**, 4202-4206
- Fernandez-Botran, R. & Vitetta, E.S. (1991) Evidence that natural murine soluble interleukin 4 receptors may act as transport proteins. *J. Exp. Med.* **174**, 673-681
- Franke, T.F., Kaplan, D.R. & Cantley, L.C. (1997) PI3K: downstream action blocks apoptosis. *Cell* **88**, 435-437.
- Friedrich, K. & Wietek, S. (2001) Experimental regulation of STAT gene expression reveals an involvement of STAT5 in IL-4-driven cell proliferation. *Biol. Chem.* **382**, 343-351
- Friedrich, K., Wietek, S., Lischke, A., Wellbrock, C., Kreitman, R.J., Pastan, I. & Sebald, W. (1999) A two-step selection approach for identification of ligand-binding determinants in cytokine receptors. *Anal. Biochem.* **268**, 179-186

- Frisch, C., Schreiber, G., Johnson, C.M. & Fersht, A.R. (1997) Thermodynamics of the interaction of barnase and barstar: changes in free energy *versus* changes in enthalpy on mutation. *J Mol Biol* **267**, 696-706
- Gascan, H., Gauchat, J.F., Roncarolo, M.G., Yssel, H. & de Vries, J.E. (1991) Human B cell clones can be induced to proliferate and to switch to IgE and IgG4 synthesis by interleukin 4 and signal provided by activated CD4+ T cell clones. *J. Exp. Med.* **173**, 747-750
- Gavett, S.H. et al. (1994) *Am. J. Respir. Cell Mol. Biol.* **10**, 587
- Gavett, S.H. et al. (1995) *J. Exp. Med.* **182**, 1527
- Gershoni, J.M. & Palade, G.E. (1983) *Anal. Biochem.* **131**, 1-15
- Grabstein, K., Eisenman, J., Mochizuki, D., Shanebeck, K., Conlon, P., Hopp, T., March, C. & Gillis, S. (1986) Purification of homogeneity of B cell stimulating factor. *J. Exp. Med.* **163**, 1405
- Gruenig, G., Watnock, M., Wakil, A.E., Venkayya, R., Brombacher, F., Rennick, D.M., Sheppard, D., Mohrs, M., Donaldson, D.D., Locksley, R.M. & Corry, D.B. (1998) Requirement for IL-13 independently of IL-4 in experimental asthma. *Science* **282**, 2261-2263
- Grunewald, S.M., Brocker, E.B., Sebald, W. & Duschl, A. (1998) Cytokine antagonists and allergy. *Eur. Cytokine Netw.* **9**, 92-94
- Grunewald, S.M., Werthmann, A., Schnarr, B., Klein, C.E., Brocker, E.B., Mohrs, M., Brombacher, F., Sebald, W. & Duschl, A. (1998) An antagonistic IL-4 preventstype I allergy in mouse. Inhibition of the IL-4/IL-13 receptor system completely abrogates humoral immune response to allergen and development of allergic symptoms in vivo. *J. Immunol.* **160**, 404
- Gustchina, A., Zdanov, A., Schalk-Hihi, C. & Wlodawer, A. (1995) A model of the complex between interleukin-4 and its receptor. *Proteins* **21**, 140-148
- Hage, T. (1999) PhD Thesis, Julius-Maximilians University of Wuerzburg
- Hage, T., Sebald, W. & Reinemer, P. (1999) Crystal structure of the interleukin-4/receptor α chain complex reveals a mosaic binding interface. *Cell* **97**, 271-281
- Hamelmann, E., Wahn, U. & Gelfand, E.W. (1999) Role of Th2 cytokines in the development of allergen-induced airway inflammation and hyperresponsiveness. *Int. Arch. Allergy Immunol* **118**, 90-94
- Henderson, W.R., Chi, E.Y. & Maliszewski, C.R. (2000) Soluble IL-4R inhibits airway inflammation following allergen challenge in a mouse model of asthma. *J. Immunol.* **164**, 1086-1095
- Hermann, R.G., Whitefield, P.R. & Bottomly, W. (1980) *Gene* **8**, 179-191
- Hilser V.J., Dowdy D., Oas, T.G. & Freire E. (1998) The structural distribution of cooperative interactions in proteins: analysis of the native state ensemble. *Proc. Natl. Acad. Sci. USA* **95**, 9903-9908
- Hoffman, R.C., Castner, B.J., Gerhart, M., Gibson, M.G., Rasmussen, B.D., March, C.J., Weatherbee, J., Tsang, M., Gustchina, A., Schalk-Hihi, C., Reshetnikova, L. & Wlodawer, A. (1995) Direct evidence of a heteromeric complex of human interleukin-4 with its receptor. *Prot. Sci.* **4**, 382-386
- Horovitz, A. & Fersht, A.R. (1990) Strategy for analysing the co-operativity of intramolecular interactions in peptides and proteins. *J Mol. Biol.* **214**, 613-617
- Horsten, U., Muller-Newen, G., Gerhartz, C., Wollmer, A., Wijdenes, J., Heinrich, P.C. & Grotzinger J. (1997) Molecular modeling-guided mutagenesis of the extracellular part of gp 130 leads to the identification of contact site in the interleukin-6-IL-6 receptor-gp 130 complex. *J. Biol. Chem.* **272**, 23748-23757
- Howard, M., Farrar, J., Hilfiker, M., Johnson, B., Takatsu, K., Hamaoka, T., Paul, W.E. (1982) Identification of T-cell derived B-cell growth factor distinct from interleukin 2. *J. Exp. Med.* **155**, 914

- Hsieh, C.S., Heimberger, A.B., Gold J.S., O'Garra, a. & Murphy, K.M. (1992) Differential regulation of T helper phenotype development by interleukins 4 and 10 in an alpha beta T-cell receptor transgenic system. *Proc. Natl. Acad. Sci. USA* **89**, 6065-6069
- Hu-li, J., Shevach, E.M., Mizuguchi, J., Ohara, J., Mosmann, T. & Paul, W.E. (1987) B cell stimulatory factor 1 (interleukin 4) is a potent stimulant for normal resting T-lymphocytes. *J. Exp. Med.* **165**, 157-172
- Idzerda, R.L., March, C.J., Mosely, B., Lyman, S.D., VandenBos, T., Gimpel, S.D., Din, W.S., Grabstein, K.H., Widmer, M.B., Park, L.S., Cosman, D. & Beckmann, M.P. (1990) Human interleukin-4 receptor confers biological responsiveness and defines a novel receptor super-family. *J. Exp. Med.* **171**, 86
- Izuhara K., Umeshita-Suyama, R., Akaiwa, M., Shirakawa, T., Deichmann, K.A., Arima, K. & Hopkin, J.M. (2000) Recent advances in understanding how IL-13 signals are involved in the pathogenesis of bronchial asthma. *Arch. Immunol. Ther. Exp.* **48**, 502-512
- Jarvis, D.L. & Garcia A. (1994) Long-term stability of baculoviruses stored under various conditions. *BioTechniques* **16**, 508-513
- Jensen, P.L. (2000) The IL-13 receptor complex. *Stem Cells* **18**, 61-62
- Jin, L. & Wells, J. A. (1992) Dissecting the energetics of an antibody-antigen interface by alanine shaving and molecular grafting. *Protein Sci.* **3**, 2351-2357
- Jones, S. & Thornton, M. (1996) Principles of protein-protein interactions. *Proc. Natl. Acad. Sci. USA* **93**, 13-20
- Karlsson, R. & Fealt, A (1997) Experimental design for kinetic analysis of protein-protein interactions with surface plasmon resonance biosensors. *J. Immunol. Meth.* **200**, 121-133
- Koph, M., Le Gros, G., Bachmann, M., Lamers, M.C., Bluethmann, H. & Koehler, G. (1993) Disruption of murine IL-4 gene blocks Th2 cytokine responses. *Nature*, **362**, 245-248
- Kossiakoff, A. & de Vos, A.M. (1998) Structural basis for cytokine hormone-receptor recognition and receptor activation. *Adv Prot Chem* **52**, 67-108
- Kruse, ., Shen, B.J., Arnold, S, Tony, H.P., Mueller, T. & Sebald, W. (1993) Two distinct functional sites of human interleukin 4 are identified by variants impaired in either receptor binding or receptor activation. *EMBO J.* **12**, 5121
- Kruse, N., Lehrnbecher, T. & Sebald, W. (1991) Site-directed mutagenesis reveals the importance of disulfide bridges aromatic residues for structure and proliferative activity of human interleukin-4. *FEBS Lett.* **286**, 58-60
- Kruse, N., Tony, H.-P. & Sebald, W. (1992) Conversion of human interleukin-4 into a high affinity antagonist by a single amino acid replacement. *The EMBO J* **11**, 3237-3244
- Kuby, J. (1994) Immunology. *Second Edition*, 1-19
- Kühn, R., Rajewsky, K. & Müller, W. (1991) Generation and analysis of interleukin 4 deficient mice. *Science* **254**, 707-710
- Lau, F. T. & Fersht, A. R. (1987) *Nature* **326**, 811-812
- Layton, J., Iaria, J., Smith, D. & Treutlein, H. (1997) Identification of a ligand-binding site on the Granulocyte Colony-stimulating Factor Receptor by molecular modeling and mutagenesis. *J. Biol. Chem.* **272**, 29735-29741
- Le Beau, M.M., Lemons, E.R.S., Espinosa, R., Larson, R.A., Arai, N. & Rowley, J.D. (1988) IL-4 and IL-5 map to human chromosome 5 in a region encoding growth factors and receptors and are deleted in myeloid leukemias with a del(5q) *Blood* **73**, 647
- Le, H.V., Ramanathan, L., Labdon, J.E., Mays-Ichinco, C.A., Sytp, R., Arai, N., Hoy, P., Takebe, Y., Nagabhushan, T.L. & Trotta, P.P. (1988) Isolation and characterisation of multiple variants of recombinant human interleukin 4 expressed in mammalian cells. *J. Biol. Chem.* **263**, 10817

- Leahy, D.J., Hendrickson, W.A., Aukhil, I. & Erickson, H.P. (1992) Structure of a fibronectin type III domain from tenascin phased by MAD analysis of the selenomethionyl protein. *Science* **258**, 987-991.
- Lee, F., Yokota, T., Otsuka, T., Meyerson, P., Villaret, D., Coffman, R., Mosmann, T., Rennick, D., Roehm, N., Smith, C., Zlotnick, A. & Arai, K. (1986) Isolation and characterisation of mouse interleukin cDNA clone that expresses B-cells stimulatory factor 1 and T-cell and mast-cell-stimulating activities. *Proc. Natl. Acad. Sci. USA* **83**, 2061
- Leonard W.J. & O'Shea, J.J. (1998) JAKS and STATS: biological implications, *Annu. Rev. Immunol.* **16**, 293-322
- Letzelter, F., Wang, Y. & Sebald, W. (1998) The interleukin-4 site-2 epitope determining binding of the common receptor γ chain *Eur. J. Biochem.* **257**, 11-20
- Lonjou, C., Barnes, K., Chen, H., Cookson, W.O., Deichmann, K.A., Hall, I.P., Holloway, J.W., Laitinen, T., Palmer, L.J., Wjst, M. & Moton, N.E. (2000) A first trial of retrospective collaboration for positional cloning in complex inheritance: assay of the cytokine region on chromosome 5 by COAG. *Proc. Natl. Acad. Sci. USA* **97**, 10942-10947
- Look, D.C., Pelletier, M.R., Tidwell, R.M., Roswit, W.T. & Holtzman, M.J. (1995) STAT-1 depends on transcriptional synergy with Sp1. *J. Biol. Chem.* **270**, 30264-30267
- Lukacs, N.W., Strieter, R.M., Chensue, S.W. & Kunkel, S.L. (1994) *Am. J. Respir. Cell Mol. Biol.* **10**, 526
- Manian, P. (1997) Genetics of asthma: a review. *Chest* **112**, 1397
- Marone G. (1998) Asthma: recent advances. *Immunology Today* **19**, 5-9
- Marsh, D.G. et al. (1996) *Science* **264**, 1152
- Matthews, R.E.F. (1982) Classification and nomenclature of viruses. Fourth report of international committee on taxonomy of viruses. Karger, Basel
- McCarthy, J.E., Schairer, H.U. & Sebald, W. (1985) Translation initiation frequency of atp genes from Escherichia coli: identification of an intercistronic sequence that enhances translation. *Embo J* **4**, 519-526
- McKenzie A.N. (2000) Regulation of T helper type immunity by IL-4 and IL-13. *Pharmacol. Ther.* **88**, 143-151
- Middleton, S.A., Barbone, F.P., Johnson, D.L., Thurmond, R.L., McMahon, F.J., Jin, R., Livnah, O., Tullai, J., Farrell, F.X., Goldsmith, M.A., Wilson, I.A. & Jolliffe L.K. (1999) Shared and unique determinants of the erythropoietin (EPO) receptor are important for binding EPO and EPO mimetic protein. *J. Biol. Chem.* **274**, 14163-14169
- Miossec, P. (1994) Acting on the cytokine balance to control autoimmunity and chronic inflammation. *Eur. Cytoline Netw.* **4**, 245f.
- Miyajima, A., Kitamura, T., Harada, N., Yokota, T., & Arai, K. (1992) Cytokine receptors and signal transduction. *Annu. Rev. Immunol.* **10**, 295-331
- Miyazaki, T., Kawahara, A., Fujii, H., Nakagawa, Y., Minami, Y., Liu, Z., Oishi, I., Silvennoinen, O., Witthahn, B.A., Ihle, J.N. (1994) Functional activation of Jak1 and Jak3 by selective association with IL-2R subunits. *Science* **266**, 1045-47
- Murata, T., Taguchi, J. & Puri, R.K. (1998) Interleukin -13 receptor α' but not α chain: a functional component of interleukin-4 receptors. *Blood* **91**, 3884-3891
- Nanavaty, U., Goldstein, A.D. & Levine S.J. (2001) Polymorphisms in candidate asthma genes. *Am. J. Med. Sci.* **321**, 11-16
- Nelms, K., Keegan, A.D., Zamorano, J., Ryan, J.J. & Paul, W.E. (1999) The IL-4 receptor: signaling mechanisms and biologic function. *Annu. Rev. Immunol.* **17**, 701-738

- Nice, E.C. & Catimel, B. (1999) Instrumental biosensors: new perspectives for the analysis of biomolecular interactions. *BioEssays* **21**, 339-352
- Nicola, N. & Hilton, D. (1998) General classes and function of four-helix bundle cytokines. *Adv Prot Chem* **52**, 1-65
- Nicola, N.A. ed. (1994) "Guidebook to cytokines and their receptors". *Oxford University Press, Oxford*, 1-7
- Noben-Trauth, N., Schultz, L.D., Brombacher, F., Urban, J.F.; Gu, H. & Paul, W.E. (1997) An interleukin 4 independent pathway for CD4+ T-cell IL-4 production is revealed in IL-4 receptor deficient mice. *Proc. Natl. Acad. Sci. USA* **94**, 10838-10843
- Noelle, R., Kramme, R.P., Ohara, J., Uhr, J.W., Vitetta, E.S. (1984) Increased expression of Ia antigens on resting B cells: an additional role for B-cell growth factor. *Proc. Natl. Acad. Sci. USA* **81**, 6149-6153
- Obiri, N.I., Debinski, W., Leonard, W.J. & Puri, R.K. (1995) Receptor for interleukin 13- interaction with interleukin 4 by a mechanism that does not involve the common γ chain shared by receptors for interleukin 2, 4, 7, 9, and 15. *J. Biol. Chem.* **270**, 8797-8804
- Ohara, J. & Paul, W.E. (1988) Up-regulation of interleukin-4/B-cell stimulatory factor 1 receptor expression. *Proc. Natl. Acad. Sci. USA* **85**, 8221-8225
- Ohara, J., Lahet, S., Inman, J. & Paul, W.E. (1985) Partial purification of murine B-cell stimulatory factor -1. *J. Immunol.* **135**, 2518
- Otzen, D.E. & Fersht, A.R. (1999) Analysis of protein-protein interactions by mutagenesis: direct versus indirect effects. *Prot. Engin.* **12**, 41-45
- Patel, B.K.R., Pierce, J.H. & LaRochelle, W.J. (1998) Regulation of Interleukin-4-mediated signalling by naturally occurring dominant negative and attenuated forms of human STAT-6. *Proc. Natl. Acad. Sci. USA* **95**, 172-177
- Paul, W.E. & Seder, R.A. (1994) Lymphocyte responses and cytokines. *Cell* **76**, 241-251
- Pene, J., Rousset, F., Briere, F., Chretien, I., Bonnefoy, J.Y., Spits, H., Yokota, T., Arao, N., Arai, K.I., Bancherea, J. & de Vries, J.E. (1988) IgE production by normal human lymphocytes is induced by interleukin-4 and suppressed by IFN γ and α and prostaglandin E2. *Proc. Natl. Acad. Sci. USA* **85**, 6880-6884
- Powers, R., Garrett, D.S., March, C.J., Frieden, E.A., Gronenborn, A.M. & Clore, G.M. (1992) Three-dimensional solution structure of human interleukin-4 by multidimensional heteronuclear magnetic resonance spectroscopy. *Science* **256**, 1673-1677
- Prasad, M.R., Bahekar, R.H. & Rao, (2000) Recent perspectives in the design of antiasthmatic agents. *Pharmazie* **55**, 457-482
- Ramshaw, H., Woodcock, J., Bagley, C., McClure, B., Hercus, T. & Lopez, A. (2001) New approaches in the treatment of asthma. *Immunol. Cell Biol.* **79**, 154-159
- Rebollo, A., Gomez, J. & Martinez-A., C. (1996) lessons from immunological, biochemical and molecular pathways of the activation mediated by IL-2 and IL-4. *Adv. Immunol.* **63**, 127-196
- Renz, H., Bradley, K., Enssle, K., Loader, J.E., Larsen, G.L. & Gelfand, E.W. (1996) prevention of development of immediate hyperresponsiveness following in vivo treatment with soluble IL-4 receptor. *Int. Arch. Allergy Immunol.* **109**, 167-176
- Reusch, P., Arnold, S., Heusser, C., Wagner, K., Weston, B. & Sebald, W. (1994) Neutralizing monoclonal antibodies define two different functional sites in human interleukin-4. *Eur J Biochem* **222**, 491-499
- Romagnani, S. (1991) Human TH1 and TH2 subsets: doubt no more. *Immunol. Today* **12**, 256-257
- Russell, S.M., Keegan, A.D., Harada, N., Nakamura, Y., Noguchi, M., Leland, P., Friedmann, M.C., Miyajima, A., Puri, R.K., Paul, W.E. & Leonard, W.J. (1993) Interleukin-2 receptor γ chain: a functional component of the interleukin-4 receptor. *Science* **262**, 1880-1883

- Sambrook, J., Fritsch, E.F. & Maniatis, T. (1989) Molecular cloning: a laboratory manual. Cold Spring Harbour Laboratory Press, USA.
- Schaefer, T.S., Sanders, L.K. & Nathans, D. (1995) Co-operative transcriptional activity of Jun and STAT-3 β , a short form of STAT-3. *Proc. Natl. Acad. Sci. USA* **92**, 9097-9101
- Schreiber, G. & Fersht, A.R. (1995) Energetics of protein-protein interactions: analysis of barnase-barstar interface by single mutations and double mutant cycles. *J Mol. Biol.* **248**, 478-486
- Seder, R.A. & Paul, W.E. (1994) Acquisition of lymphokine-producing phenotype by CD4+ T-cells. *Annu. Rev. Immunol.* **12**, 635-673
- Seder, R.A., Gazzinelli, R., Sher, A. & Paul, W.E. (1993) IL-12 acts directly on CD4+ T cells to enhance priming for IFN γ production and diminishes IL-4 inhibition of such priming. *Proc. Natl. Acad. Sci. USA* **90**, 10188-10192
- Seder, R.A., Paul, W.E., Davis, M.M. & Fazekas de St. Groth, B. (1992) The presence of interleukin 4 during in vitro priming determines the lymphokine-producing potential of CD4+ T cells from T cell receptor transgenic mice. *J. Exp. Med.* **176**, 1091-1098
- Shen, B. (1996) Molecular recognition during binding of human IL-4 to its receptor. PhD Thesis, Julius-Maximilians University of Wuerzburg
- Shen, B-J. (1996) Thesis work, University of Wuerzburg
- Smerz-Bertling, C. & Duschl, A. (1995) Both interleukin-4 and interleukin-13 induce tyrosine phosphorylation of the 140 kD subunit of the interleukin-4 receptor. *J. Biol. Chem.* **270**, 966-970
- Smith, L.J., Redfield, C., Boyd, J., Lawrence, G., Edwards, R.G., Smith, R.A.G. & Dobson, C.M. (1992) Human interleukin 4- the solution structure of a four-helical bundle protein. *J. Mol. Biol.* **224**, 899-904
- Snapper, C.M., Hornbeck, P.V., Atasoy, U., Pereira, G.M. & Paul, W.E. (1988) Interleukin 4 induces membrane Thy-1 expression on normal murine B cells. *Proc. Natl. Acad. Sci. USA* **85**, 6107-6111
- Sprang, S.R. & Bazan, J.F. (1993) Cytokine structural taxonomy and mechanisms of receptor engagement. *Curr. Opin. Struct. Biol.* **3**, 815-827
- Sugamura, K., Asao, H., Kondo, M., Tanaka, N., Ishii, N., Nakamura, M. & Takeshita, T. (1995) The common γ -chain for multiple cytokine receptors. *Adv. Immunol.* **59**, 225-277
- Sugamura, K., Asao, H., Kondo, M., Tanaka, N., Ishii, N., Ohbo, K., Nakamura, M. & Takeshita, T. (1996) The interleukin-2 receptor γ chain: its role in the multiple cytokine receptor complexes and T cell development in XSCID. *Annu. Rev. Immunol.* **14**, 179-205
- Sun, X.J., Wang, L.M., Zhang, Y., Yenush, L., Myers, M.G.J., Glasheen, E., Lane, W.S., Pierce, J.H. & White, M.F. (1995) Role of IRS-2 in insulin and cytokine signalling. *Nature* **377**, 173-177
- Takeshita, T., Asao, H., Ohtani, K., Ishii, N., Kumaki, S., Tanaka, N., Munakata, H., Nakamura, M. & Sugamura, K. (1992) Cloning of the γ chain of the human IL-2 receptor. *Science* **257**, 551-556
- Tanaka, H., Nagai, H. & Maeda, Y. (1998) Effect of anti-IL-4 and anti-IL-5 antibodies on allergic airway hyperresponsiveness in mice. *Life. Sci.* **62**, 169-174
- Tartof, K.D. & Hobbs, C.A. (1987) Improved media for growing plasmid and cosmid clones. *Bethesda Res. Lab. Focus* **9**:12
- Tepper, R.I. & Mule, J.J. (1994) Experimental and clinical studies of cytokine gene-modified tumor cells. *Hum. Gene. Ther.* **5**, 153-164
- Tepper, R.I., Levinson, D.A., Stanger, B.Z., Campos-Torres, Abbas, A.K. & Leder, P. (1990) IL-4 induces allergic-like inflammatory disease and alters T cell development in transgenic mice. *Cell* **62**, 457-467

- Thornhill, M.H., Wellicoms, S.M., Mahiouz, D.L., Lanchbury, J.S., Kyan-Aung, U. & Haskard, D.O. (1991) TNF combines with interleukin 4 or IFN γ to selectively enhance endothelial cell adhesiveness for T cells. The contribution of vascular cell adhesion molecule-1-dependent and independent binding mechanisms. *J. Immunol.* **146**, 592-598
- Toker, A. & Cantley, L.C. (1997) Signalling through the lipid products of phosphoinositide-3-OH kinase. *Nature* **387**, 673-676.
- Tomkinson, A., Duez, C., Cieslewicz, G., Pratt, J.C., Joetham, A., Shanafelt, C., Gundel, R. & Gelfand, E.W. (2001) A murine IL-4R antagonist that inhibits IL-4- and IL-13-induced responses prevents antigen-induced airway eosinophilia and airway hyperresponsiveness. *J. Immunol.* **166**, 5792-5800
- Tony H.P., Shen, B.J., Reusch, P. & Sebald, W. (1994) Design of human interleukin-4 antagonists inhibiting interleukin-4-dependent and interleukin-13-dependent responses in T cells and B cells with high efficiency. *Eur. J. Biochem.* **225**, 659
- Tsicopoulos, A., Janin, A., Akoum, H., Lamblin, C., Vorng, H., Hamid, Q., Tonnel, A.B. & Wallaert, B. (2000) Cytokine profile in MSGs from patients with bronchial asthma. *Allergy Clin. Immunol.* **106**, 687-696
- Turner, B., Rapp, U., App, H., Greene, M., Dobashi, K. & Reed, J. (1991) Interleukin-2 induces tyrosine phosphorylation and activation of p72-74 Raf-1 kinase in a T-cell line. *Proc. Natl. Acad. Sci. USA* **88**, 1227f.
- Vaughn, J.L., Goodwin, R.H. & Tompkins, G.J. (1977) *In vitro* **13**, 213-217
- Velazquez, L., Fellous, M., Stark, G.R. & Pellegrini, S. (1992) A protein tyrosine kinase in the interferon α/β signalling pathway. *Cell* **70**, 313-322
- Walker, C. et al. (1992) *Am. Rev. Respir. Dis.* **146**, 109
- Walter, M.R., Cook, W.J., Zhao, B.G., Cameron, R.P., Ealick, S.E., Walter, R.L., Reichert, P., Nagabhushan, T.L., Trotta, P.P. & Bugg, C.E. (1992) Crystal structure of recombinant human interleukin-4. *J. Biol. Chem.* **267**, 20371-20376
- Wang, H.Y., Paul, W.E. & Keegan, A.D. (1996) IL-4 function can be transferred to the IL-2 receptor by tyrosine containing sequences found in the IL-4 receptor alpha chain. *Immunity* **4**, 113-121.
- Wang, Y., Shen, B-J. & Sebald, W. (1997) A mixed – charge pair in human interleukin 4 dominates high-affinity interaction with the receptor α chain. *Proc. Natl. Acad. Sci. USA* **94**, 1657-1662
- Welham, M.J., Learmonth, L., Bone, H., Schrader, J.W. (1995) Interleukin-13 signal transduction in lymphohemopoietic cells. Similarities and differences in signal transduction with interleukin-4 and insulin. *J. Biol. Chem.* **270**, 12286-12296
- Wells, J.A. (1990) Additivity of mutational effects in proteins. *Biochemistry*, **29**, 8509-8517
- Wietek, S. (1999) Gezielte Beeinflussung der Signaltransduktion des humanen Interleukin-4 Rezeptors durch Expression von mutierten Komponenten der Signalweiterleitungs-Kaskade. PhD Thesis, Julius-Maximilians University of Wuerzburg
- Wills-Karp, M., Luyimbazi, J., Xu, X., Schofield, B., Neben, T.Y., Karp, C.L. & Donaldson, D.D. (1998) Interleukin-13: central mediator of allergic asthma. *Science* **282**, 2258-2261
- Wlodawer, A., Pavlovsky, A. & Gustchina, A. (1992) Crystal structure of human recombinant interleukin-4 at 2.25 Å resolution. *FEBS lett.* **309**, 59-64
- Yanisch-Perron, C., Vieira, J. & Messing, J. (1985) Improved M13 phage cloning vectors and host strains: nucleotide sequences of M13amp18 and pUC19 vectors. *Gene* **33**, 103-119
- Yokota, T., Otsuka, T., Mosmann, T., Banchereau, J., Defrance, T., Blanchard, D., de Vries, J.E., Lee, F. & Arai, K. (1986) Isolation and characterisation of a human interleukin cDNA clone homologous to mouse B-cell stimulatory factor 1 that expresses B-cell and T-cell-stimulatory activities. *Proc. Natl. Acad. Sci. USA* **83**, 5894

- Yoon, C., Johnston, S., Tang, J., Stahl, M., Tobin, J.F. & Somers, W.S. (2000) Charged residues dominate a unique interlocking topography in the heterodimeric cytokine interleukin-12. *EMBO J.* **19**, 3350-3541
- Yoshimoto, T. & Paul, W.E. (1994) CD4pos, NK1.1pos T-cells promptly produce Interleukin-4 in response to in vivo challenge with anti-CD3. *J. Exp. Med.* **179**, 1285-1295
- Zamorano, J. & Keegan, A.D. (1998) Regulation of apoptosis by tyrosine containing domains of IL-4R α :Y497 and Y713, but not the Stat-6-docking tyrosine, signal protection from apoptosis. *J. Immunol.* **161**, 859-867

7. Appendices

Appendix 1 Kinetic and equilibrium theory for the evolution of data obtained from BIAcore experiments

For the association of an analyte A with an immobilized ligand B



a kinetic of first order is assumed:

$$d[\mathbf{AB}] / dt = k_a \times [\mathbf{A}] \times [\mathbf{B}] - k_d \times [\mathbf{AB}] \quad (2)$$

k_a : association rate constant

k_d : dissociation rate constant

For the starting concentration of free B, $[\mathbf{B}_0]$ is valid:

$$[\mathbf{B}_0] = [\mathbf{B}] + [\mathbf{AB}] \quad (3)$$

Equation (2) can therefore be rearranged to give:

$$d[\mathbf{AB}] / dt = k_a \times [\mathbf{A}] ([\mathbf{B}_0] - [\mathbf{AB}]) - k_d \times [\mathbf{AB}] \quad (4)$$

If one equates $[\mathbf{B}_0]$ with the maximal signal of the BIAcore experiment \mathbf{R}_{max} , $[\mathbf{AB}]$ with the actually measured signal \mathbf{R} and $[\mathbf{A}]$ with the used concentration of analyte C, equation (4) can be written as:

$$d\mathbf{R} / dt = \frac{k_a \times \mathbf{C} \times \mathbf{R}_{max}}{y} - \frac{(k_a \times \mathbf{C} + k_d)}{k_s} \times \mathbf{R} \quad (5)$$

Equation (5) is the equation of a straight line with k_s as gradient.

$$k_s = k_a \times C + k_d \quad (6)$$

The graphical representation of k_s against C results also in a straight line with k_s as gradient and the k_d as ordinate segment.

By measurement at different analyte concentrations C through this graphical representation k_a as well as k_d can be determined. In practice, the determination of k_d by graphical representation is not very accurate, because in general is valid:

$$k_a \times C \gg k_d$$

The determination of k_d therefore is achieved according to another method.

For the dissociation a time law of first order is assumed:

$$R_t = R_0 \times e^{-k_d(t-t_0)}$$

This can be transformed into

$$\ln(R_0/R_t) = k_d \times (t - t_0)$$

A graphical representation of $\ln(R_0/R_t)$ against $(t - t_0)$ results in a straight line with k_d as gradient.

Appendix 2 **Vector pRPR9IL-4FD**
(with IL-4BP cDNA 1278-1970 bp)

5' TTCTCATGTTTGACAGCTTATCATCGATTTTATGAATATACAAATAATTGGAGCCAACCT 3'
1 60

5' GCAGGTGATGATTATCAGCCAGCAGAGAATTAAGGAAAACAGACAGGTTTATTGAGCGCT 3'
120

5' TATCTTCCCTTTATTTTTGCTGCGGTAAGTCGCATAAAAACCATTCTTCATAATTCAAT 3'
180

5' CCATTTACTATGTTATGTTCTGAGGGGAGTGAAAATTCCCCTAATTCGATGAAGATTCTT 3'
240

5' GCTCAATTGTTATCAGCTATGCGCCGACCAGAACACCTTGCCGATCAGCCAAACGTCTCT 3'
300

5' TCAGGCCACTGACTAGCGATAACTTTCCCCACAACGGAACAACCTTCATTGCATGGGATC 3'
360

5' ATTGGGTACTGTGGGTTTAGTGGTTGTAAAAACACCTGACCGCTATCCCTGATCAGTTTC 3'
420

5' TTGAAGGTAAACTCATCACCCCAAGTCTGGCTATGCAGAAATCACCTGGCTCAACAGCC 3'
480

5' TGCTCAGGGTCAACGAGAATTAACATTCCGTCAGGAAAGCTTGGCTTGGAGCCTGTTGGT 3'
540

5' GCGGTCATGGAATTACCTTCAACCTCAAGCCAGAATGCAGAATCACTGGCTTTTTTGGTT 3'
600

5' GTGCTTACCCATCTCTCCGCATCACCTTTGGTAAAGGTTCTAAGCTTAGGTGAGAACATC 3'
660

5' CCTGCCTGAACATGAGAAAAACAGGGTACTCATACTCACTTCTAAGTGACGGCTGCATA 3'
720

5' CTAACCGCTTCATACATCTCGTAGATTTCTCTGGCGATTGAAGGGCTAAATTCTTCAACG 3'
780

5' CTAACTTTGAGAATTTTTGTAAGCAATGCGGCGTTATAAGCATTTAATGCATTGATGCCA 3'
840

5' TTAAATAAAGCACCAACGCCTGACTGCCCCATCCCCTCTTGCTCTGCGACAGATTCCCTGG 3'
900

5' GATAAGCCAAGTTCATTTTTCTTTTTTTCATAAATTGCTTTAAGGCGACGTGCGTCCTCA 3'
960

5' AGCTGCTCTTGTGTTAATGGTTTCTTTTTTGTGCTCATACGTTAAATCTATCACCGCAAG 3'
1020

5' GGATAAATATCTAACACCGTGCGTGTTGACTATTTTACCTCTGGCGGTGATAATGGTTGC 3'
1080

5' ATGTACTAAGGAGGTGTATGGAACAACGCATAACCCTGAAAGATTATGCAATGCGCTTT 3'
1140

5' GGGCAAACCAAGACAGCTAAAGATCAAGAATGTTGATCTTCAGTGTTCGCCTGTCTGTT 3'
1200

5' TTGCACCGGAATTTTTGAGTCTGCCTCGAGCTGGTATAAGTTTTATTGCTTATAGCAAT 3'
1260

5' AAGGTTGAGGTGATTTTATGAAAAGAATATCGCATTTCTTCTTGCATCTATGTTTCGTTT 3'
1320

5' TTTCTATTGCTACAAATGCCTATGCATTTAAGGTCTTGCAGGAGCCCACCTGCGTCTCCG 3'
1380

5' ACTACATGAGCATCTCTACTTGCGAGTGGAAGATGAATGGTCCCACCAATTGCAGCACCG 3'
1440

5' AGCTCCGCCTGTTGTACCAGCTGGTTTTTCTGCTCTCCGAAGCCCACACGTGTATCCCTG 3'
1500

5' AGAACAACGGAGGCGGGGTGCGTGTGCCACCTGCTCATGGATGACGTGGTCAGTGCGG 3'
1560

5' ATAACTATACACTGGACCTGTGGGCTGGGCAGCAGCTGCTGTGGAAGGGCTCCTTCAAGC 3'
1620

5' CCAGCGAGCATGTGAAACCCAGGGCCCCAGGAAACCTGACAGTTCACACCAATGTCTCCG 3'
1680

5' ACACTCTGCTGCTGACCTGGAGCAACCCGTATCCCCCTGACAATTACCTGTATAATCATC 3'
 1740
 5' TCACCTATGCAGTCAACATTTGGAGTGAAAACGACCCGGCAGATTTTCTAGAAATCTATAACG 3'
 1800
 5' TGACCTACCTAGAACCCCTCCCTCCGCATCGCAGCCAGCACCCCTGAAGTCTGGGATTTCTT 3'
 1860
 5' ACAGGGCACGGGTGAGGGCCTGGGCTCAGGCCTATAACACCACCTGGAGTGAGTGGAGCC 3'
 1920
 5' CCAGCACCAAGTGGCACAACCTCCTACAGGGAGCCCTTCGAGCAGCACTAGGATCCCGCAA 3'
 BamHI 1980
 5' AAGCGGCCTTTGACTCCCTGCAAGCCTCAGCGACCGAATATATCGGTTATGCGTGGGCGA 3'
 2040
 5' TGGTTGTTGTCATTGTCGGCGCAACTATCGGTATCAAGCTGTTTAAGAAATTCACCTCGA 3'
 2100
 5' AAGCAAGCTGATAAACCGATACAATTAAGGCTCCTTTTGGAGCCTTTTTTTTTGGAGAT 3'
 2160
 5' TTTCAACGTGAAAAAATTATTATTCGCAATTCCTTTAGTTGTTTCCTTTCTATTCTCACTC 3'
 2220
 5' CGCTGAAACTGTTGAAAGTTGTTTAGCAAAAACCTCATAACAGAAAATTCATTTACTAACGT 3'
 2280
 5' CTGGAAAGACGACAAAACCTTTAGATCCGGCCAAGCTTCGTCGACCCTGCCTCGCGCGTTT 3'
 2340
 5' CGGTGATGACGGTGAAAACCTCTGACACATGCAGCTCCCGGAGACGGTCACAGCTTGTCT 3'
 2400
 5' GTAAGCGGATGCCGGGAGCAGACAAGCCCGTCAGGGCGCGTCAGCGGGTGTGGCGGGTG 3'
 2460
 5' TCGGGGCGCAGCCATGACCCAGTCACGTAGCGATAGCGGAGTGTATACTGGCTTAACAT 3'
 2520
 5' GCGGCATCAGAGCAGATTGTAAGTGCAGAGTGCACCATATGCGGTGTGAAATACCGCACAGA 3'
 2580
 5' TCGGTAAGGAGAAAATACCGCATCAGGCGCTCTTCCGCTTCCTCGCTCACTGACTCGCTG 3'
 2640
 5' CGCTCGGTTCGTTCCGGCTGCGGCGAGCGGTATCAGCTCACTCAAAGGCGGTAATACGGTTA 3'
 2700
 5' TCCACAGAATCAGGGGATAACGCAGGAAAGAACATGTGAGCAAAAAGGCCAGCAAAAAGGCC 3'
 2760
 5' AGGAACCGTAAAAAGGCCGCGTTGCTGGCGTTTTTCCATAGGCTCCGCCCCCTGACGAG 3'
 2820
 5' CATCACAAAAATCGACGCTCAAGTCAGAGGTGGCGAAACCCGACAGGACTATAAAGATAC 3'
 2880
 5' CAGGCGTTTTCCCCCTGGAAGCTCCCTCGTGCGCTCTCCTGTTCCGACCCTGCCGCTTACC 3'
 2940
 5' GGATACCTGTCCGCCTTTCTCCCTTCGGGAAGCGTGGCGCTTTCTCATAGCTCACGCTGT 3'
 3000
 5' AGGTATCTCAGTTCGGTGTAGGTCGTTTCGCTCCAAGCTGGGCTGTGTGCACGAACCCCC 3'
 3060
 5' GTTCAGCCCGACCGCTGCGCCTTATCCGGTAACTATCGTCTTGAGTCCAACCCGGTAAGA 3'
 3120
 5' CACGACTTATCGCCACTGGCAGCAGCCACTGGTAACAGGATTAGCAGAGCGAGGTATGTA 3'
 3180
 5' GCGGGTGCTACAGAGTTCTTGAAGTGGTGGCCTAACTACGGCTACACTAGAAGGACAGTA 3'
 3240
 5' TTTGGTATCTGCGCTCTGCTGAAGCCAGTTACCTTCGGAAAAAGAGTTGGTAGCTCTTGA 3'
 3300
 5' TCCGGCAAACAAACCACCGCTGGTAGCGGTGGTTTTTTTTGTTTGAAGCAGCAGATTACG 3'
 3360
 5' CGCAGAAAAAAGGATCTCAAGAAGATCCTTTGATCTTTTCTACGGGGTCTGACGCTCAG 3'
 3420
 5' TGGAACGAAAACCTCACGTTAAGGGATTTTGGTCATGAGATTATCAAAAAGGATCTTCACC 3'
 3480
 5' TAGATCCTTTTAAATTAATAATGAAGTTTTAAATCAATCTAAAGTATATATGAGTAAACT 3'
 3540

7. Appendices

5' TGGTCTGACAGTTACCAATGCTTAATCAGTGAGGCACCTATCTCAGCGATCTGTCTATTT 3'
3600

5' CGTTCATCCATAGTTGCCTGACTCCCCGTCGTGTAGATAACTACGATACGGGAGGGCTTA 3'
3660

5' CCATCTGGCCCCAGTGCTGCAATGATACCGCGAGACCCACGCTCACCGGCTCCAGATTTA 3'
3720

5' TCAGCAATAAACCAGCCAGCCGGAAGGGCCGAGCGCAGAAGTGGTCTGCAACTTTATCC 3'
3780

5' GCCTCCATCCAGTCTATTAATTGTTGCCGGGAAGCTAGAGTAAGTAGTTCGCCAGTTAAT 3'
3840

5' AGTTTGCGCAACGTTGTTGCCATTGCTGCAGGCATCGTGGTGTACGCTCGTCGTTTGGT 3'
3900

5' ATGGCTTCATTCAGCTCCGGTTCCTCAACGATCAAGGCGAGTTACATGATCCCCATGTTG 3'
3960

5' TGCAAAAAAGCGGTTAGCTCCTTCGGTCTCCGATCGTTGTCAGAAGTAAGTTGGCCGCA 3'
4020

5' GTGTTATCACTCATGGTTATGGCAGCACTGCATAATTCTCTTACTGTCATGCCATCCGTA 3'
4080

5' TTAAAAGTGCTCATCATTGAAAACGTTCTTCGGGGCGAAAACCTCTCAAGGATCTTACCG 3'
4140

5' CTGTTGAGATCCAGTTCGATGTAACCCACTCGTGCACCCAACCTGATCTTCAGCATCTTTT 3'
4200

5' ACTTTCACCAGCGTTTCTGGGTGAGCAAAAACAGGAAGGCAAAATGCCGCAAAAAAGGGA 3'
4260

5' AGATGCTTTTCTGTGACTGGTGAGTACTCAACCAAGTCATTCTGAGAATAGTGTATGCGG 3'
4320

5' CGACCGAGTTGCTCTTGCCCGGCGTCAACACGGGATAATACCGCGCCACATAGCAGAACT 3'
4380

5' ATAAGGGCGACACGGAAATGTTGAATACTCATACTCTTCCTTTTTCAATATTATTGAAGC 3'
4440

5' ATTTATCAGGGTTATTGTCTCATGAGCGGATACATATTTGAATGTATTTAGAAAAATAAA 3'
4500

5' CAAATAGGGTTCCGCGCACATTTCCCCGAAAAGTGCCACCTGACGTCTAAGAAACCATT 3'
4560

5' ATTATCATGACATTAACCTATAAAAATAGGCGTATCACGAGGCCCTTTCGTCTTCAAGAA 3'
4620

Appendix 3 A Part of the Expression Vector pAcGP67B (with IL-4BP cDNA 4267-4887 bp)

```

5' GATAACCATCTCGCAAATAAATAAGTATTTTACTGTTTTTCGTAACAGTTTTGTAATAAAA 3'
   4020                                                                                   4080
5' AAACCTATAAATATTCCGGATTATTCATACCGTCCCACCATCGGGCGCGGATCTATGCTA 3'
                                                                                     4140
5' CTAGTAAATCAGTCACACCAAGGCTTCAATAAGGAACACACAAGCAAGATGGTAAGCGCT 3'
                                                                                     4200
5' ATTGTTTTTATATGTGCTTTTGGCGGCGGCGGCATTCTGCCTTTGCGGCGGATCTTGGA 3'
                                                                                     4260
5' TCCATGAAGGTCTTGCAGGAGCCCACCTGCGTCTCCGACTACATGAGCATCTCTACTTGC 3'
                                                                                     4320
5' GAGTGGAAGATGAATGGTCCCACCAATTGCAGCACCGAGCTCCGCCTGTTGTACCAGCTG 3'
                                                                                     4380
5' GTTTTTCTGCTCTCCGAAGCCCACACGTGTATCCCTGAGAACAACGGAGGCGGGGGTGC 3'
                                                                                     4440
5' GTGTGCCACCTGCTCATGGATGACGTGGTCAGTGCGGATAACTATACACTGGACCTGTGG 3'
                                                                                     4500
5' GCTGGGCAGCAGCTGCTGTGGAAGGGCTCCTTCAAGCCCAGCGAGCATGTGAAACCCAGG 3'
                                                                                     4560
5' GCCCCAGGAAACCTGACAGTTCACACCAATGTCTCCGACACTCTGCTGCTGACCTGGAGC 3'
                                                                                     4620
5' AACCCGTATCCCCCTGACAATTACCTGTATAATCATCTCACCTATGCAGTCAACATTTGG 3'
                                                                                     4680
5' AGTGAAAACGACCCGGCAGATTTTCAAGTCTATAACGTGACCTACCTAGAACCCTCCCTC 3'
                                                                                     4740
5' CGCATCGCAGCCAGCACCCCTGAAGTCTGGGATTTCTACAGGGCACGGGTGAGGGCCTGG 3'
                                                                                     4800
5' GCTCAGGCCTATAACACCACCTGGAGTGAGTGGAGCCCCAGCACCAAGTGGCACAACCTCC 3'
                                                                                     4860
5' TACAGGGAGCCCTTCGAGCAGCACTAGGATCCCGGGCCATGGGAATTCGGAGCGGCCGC 3'
                                                                                     4920
5' TGCAGATCTGATCCTTTCTGGGACCCGGCAAGAACCAAAAACCTCACTCTCTTCAAGGAA 3'
                                                                                     4980
5' ATCCGTAATGTTAAACCCGACACGATGAAGCTTGTCGTTGGATGGAAAGGAAAAGAGTTC 3'
                                                                                     5060
5' TACAGGGAAACTTGGACCCGCTTCATGGAAGACAGCTTCCCATTGTTAACGACCAAGAA 3'
                                                                                     5120
5' GTGATGGATGTTTTCTTGTGTCAACATGCGTCCCCTAGACCCAACCGTTGTTACAAA 3'
                                                                                     5180
5' GCCCGGCGTCAATACGGGATAATACCGCGCCACATAGCAGAACTTTAAAAGTGCTCATCA 3'
                                                                                     5240

```

Appendix 4 Sequence of the Expression Vector R^{IS}pRC109 (with IL-4 cDNA 1281-1673 bp)

```

5' TTCTCATGTTTGACAGCTTATCATCGATTTTATGAATATACAAATAATTGGAGCCAACCT 3'
   1                                                                 60
5' GCAGGTGATGATTATCAGCCAGCAGAGAATTAAGGAAAACAGACAGGTTTATTGAGCGCT 3'
   60                                                                 120
5' TATCTTCCCTTTATTTTTGCTGCGGTAAGTCGCATAAAAACCATTCTTCATAATTCAAT 3'
   120                                                                 180
5' CCATTTACTATGTTATGTTCTGAGGGGAGTGAAAATTCCCCTAATTCGATGAAGATTCTT 3'
   180                                                                 240
5' GCTCAATTGTTATCAGCTATGCGCCGACCAGAACACCTTGCCGATCAGCCAAACGTCTCT 3'
   240                                                                 300
5' TCAGGCCACTGACTAGCGATAACTTTCCCCACAACGGAACAACCTTCATTGCATGGGATC 3'
   300                                                                 360
5' ATTGGGTACTGTGGGTTTAGTGGTTGTAAAAACACCTGACCGCTATCCCTGATCAGTTTC 3'
   360                                                                 420
5' TTGAAGGTAACTCATCACCCCAAGTCTGGCTATGCAGAAATCACCTGGCTCAACAGCC 3'
   420                                                                 480
5' TGCTCAGGGTCAACGAGAATTAACATTCCGTCAGGAAAGCTTGGCTTGGAGCCTGTTGGT 3'
   480                                                                 540
5' GCGGTCATGGAATTACCTTCAACCTCAAGCCAGAATGCAGAATCACTGGCTTTTTTGGTT 3'
   540                                                                 600
5' GTGCTTACCCATCTCTCCGCATCACCTTTGGTAAAGGTTCTAAGCTTAGGTGAGAACATC 3'
   600                                                                 660
5' CCTGCCTGAACATGAGAAAAACAGGGTACTCATACTCACTTCTAAGTGACGGCTGCATA 3'
   660                                                                 720
5' CTAACCGCTTCATACATCTCGTAGATTTCTCTGGCGATTGAAGGGCTAAATTCTTCAACG 3'
   720                                                                 780
5' CTAACTTTGAGAATTTTTGTAAGCAATGCGGCGTTATAAGCATTTAATGCATTGATGCCA 3'
   780                                                                 840
5' TTAAATAAAGCACCAACGCCTGACTGCCCATCCCCATCTTGCTCTGCGACAGATTCCCTGG 3'
   840                                                                 900
5' GATAAGCCAAGTTCATTTTTCTTTTTTTCATAAATTGCTTTAAGGCGACGTGCGTCCTCA 3'
   900                                                                 960
5' AGCTGCTCTTGTGTTAATGGTTTCTTTTTTGTGCTCATACGTTAAATCTATCACCGCAAG 3'
   960                                                                 1020
5' GGATAAATATCTAACACCGTGCGTGTTGACTATTTTACCTCTGGCGGTGATAATGGTTGC 3'
   1020                                                                 1080
5' ATGTACTAAGGAGGTGTATGGAACAACGCATAACCCTGAAAGATTATGCAATGCGCTTT 3'
   1080                                                                 1140
5' GGGCAAACCAAGACAGCTAAAGATCAAGAATGTTGATCTTCAGTGTTTCGCCTGTCTGTT 3'
   1140                                                                 1200
5' TTGCACCGGAATTTTTGAGTCTGCCTCGAGTAATTTACCAACACTACTACGTTTTAACT 3'
   1200                                                                 1260
5' GAAACAAACTGGAGACTGCCATGCACAAGTGCGATATCACCTTACAGGAGATCATCAAAA 3'
   1260                                                                 1320
5' CTTTGAACAGCCTCACAGAGCAGAAGACTCTGTGCACCGAGTTGACCGTAACAGACATCT 3'
   1320                                                                 1380
5' TTGCTGCCTCCAAGAACAACACTGAGAAGGAAACCTTCTGCAGGGCTGCGACTGTGCTCC 3'
   1380                                                                 1440
5' GGCAGTTCTACAGCCACCATGAGAAGGACACTCGCTGCCTGGGTGCGACTGCACAGCAGT 3'
   1440                                                                 1500
5' TCCACAGGCACAAGCAGCTGATCCGATTCCCTGAAACGGCTCGACAGGAACCTCTGGGGCC 3'
   1500                                                                 1560
5' TGGCGGGCTTGAATTCCTGTCCTGTGAAGGAAGCCAACCAGAGTACGTTGGAAAACCTTCT 3'
   1560                                                                 1620
5' TGGAAAGGCTAAAGACGATCATGAGAGAGAAATATTCAAAGTGTTTCGAGCTGATAAGGAT 3'
   1620                                                                 1680

```

5' CCCGCAAAGCGGCCTTTGACTCCCTGCAAGCCTCAGCGACCGAATATATCGGTTATGCG 3'
 1740
 5' TGGGCGATGGTTGTTGTCATTGTTCGGCGCAACTATCGGTATCAAGCTGTTTAAGAAATTC 3'
 1800
 5' ACCTCGAAAGCAAGCTGATAAACCGATACAATTAAGGCTCCTTTTGGAGCCTTTTTTTT 3'
 1860
 5' TGGAGATTTTCAACGTGAAAAAATTATTATTCGCAATTCCTTTAGTTGTTCTTTCTATT 3'
 1920
 5' CTCACTCCGCTGAAACTGTTGAAAGTTGTTTAGCAAAACCTCATAACAGAAAATTCATTTA 3'
 1980
 5' CTAACGTCTGGAAAGACGACAAAACCTTTAGATCCGGCCAAGCTTCGTTCGACCCTGCCTCG 3'
 2040
 5' CGCGTTTCGGTGATGACGGTGAAAACCTCTGACACATGCAGCTCCCGGAGACGGTCACAG 3'
 2100
 5' CTTGTCGTGAAGCGGATGCCGGGAGCAGACAAGCCCGTCAGGGCGCGTCAGCGGGTGTG 3'
 2160
 5' GCGGGTGTTCGGGGCGCAGCCATGACCCAGTCACGTAGCGATAGCGGAGTGTATACTGGCT 3'
 2220
 5' TAACTATGCGGCATCAGAGCAGATTGTACTGAGAGTGCACCATATGCGGTGTGAAATACC 3'
 2280
 5' GCACAGATGCGTAAGGAGAAAATACCGCATCAGGCGCTCTTCCGCTTCCTCGCTCACTGA 3'
 2340
 5' CTCGCTGCGCTCGGTCGTTCCGGCTGCGGGAGCGGTATCAGCTCACTCAAAGGCGGTAAT 3'
 2400
 5' ACGGTTATCCACAGAATCAGGGGATAACGCAGGAAAGAACATGTGAGCAAAGGCCAGCA 3'
 2460
 5' AAAGGCCAGGAACCGTAAAAAGGCCGCGTTGCTGGCGTTTTTCCATAGGCTCCGCCCCC 3'
 2520
 5' TGACGAGCATCACAAAATCGACGCTCAAGTCAGAGGTGGCGAAACCCGACAGGACTATA 3'
 2580
 5' AAGATACCAGGCGTTTTCCCCCTGGAAGCTCCCTCGTGCGCTCTCCTGTTCCGACCCTGCC 3'
 2640
 5' GCTTACCGGATACCTGTCCGCCTTTCTCCCTTCGGGAAGCGTGGCGCTTTCTCATAGCTC 3'
 2700
 5' ACGCTGTAGGTATCTCAGTTCGGTGTAGGTCGTTTCGCTCCAAGCTGGGCTGTGTGCACGA 3'
 2760
 5' ACCCCCCGTTTCAGCCCGACCGCTGCGCCTTATCCGGTAACTATCGTCTTGAGTCCAACC 3'
 2820
 5' GGTAAGACACGACTTATCGCCACTGGCAGCAGCCACTGGTAACAGGATTAGCAGAGCGAG 3'
 2880
 5' GTATGTAGGCGGTGCTACAGAGTTCTTGAAGTGGTGGCCTAACTACGGCTACACTAGAAG 3'
 2940
 5' GACAGTATTTGGTATCTGCGCTCTGCTGAAGCCAGTTACCTTCGGAAAAAGAGTTGGTAG 3'
 3000
 5' CTCTTGATCCGGCAAACAAACCACCGCTGGTAGCGGTGGTTTTTTTTGTTTGAAGCAGCA 3'
 3060
 5' GATTACGCGCAGAAAAAAGGATCTCAAGAAGATCCTTTGATCTTTTCTACGGGGTCTGA 3'
 3120
 5' CGCTCAGTGGAACGAAAACCTCACGTTAAGGGATTTTGGTTCATGAGATTATCAAAAAGGAT 3'
 3180
 5' CTTACCTAGATCCTTTTAAATTAATAATGAAGTTTTAAATCAATCTAAAGTATATATGA 3'
 3240
 5' GTAAACTTGGTCTGACAGTTACCAATGCTTAATCAGTGAGGCACCTATCTCAGCGATCTG 3'
 3300
 5' TCTATTTTCGTTTCATCCATAGTTGCCTGACTCCCCGTCGTGTAGATAACTACGATACGGGA 3'
 3360
 5' GGGCTTACCATCTGGCCCCAGTGCTGCAATGATACCGCGAGACCCACGCTCACCGGCTCC 3'
 3420
 5' AGATTTATCAGCAATAAACCCAGCCAGCCGGAAGGGCCGAGCGCAGAAGTGGTCTGCAAC 3'
 3480
 5' TTTATCCGCCTCCATCCAGTCTATTAATTGTTGCCGGGAAGCTAGAGTAAGTAGTTCGCC 3'
 3540

5' AGTTAATAGTTTGCGCAACGTTGTTGCCATTGCTGCAGGCATCGTGGTGTCACGCTCGTC 3'
 3600
 5' GTTTGGTATGGCTTCATTCAGCTCCGGTTCCCAACGATCAAGGCGAGTTACATGATCCCC 3'
 3660
 5' CATGTTGTGCAAAAAAGCGGTTAGCTCCTTCGGTCCTCCGATCGTTGTCAGAAGTAAGTT 3'
 3720
 5' GGCCGCAGTGTTATCACTCATGGTTATGGCAGCACTGCATAATTCTCTTACTGTCATGCC 3'
 3780
 5' ATCCGTAAGATGCTTTTCTGTGACTGGTGAGTACTCAACCAAGTCATTCTGAGAATAGTG 3'
 3840
 5' TATGCGGCGACCGAGTTGCTCTTGCCCCGGCGTCAACACGGGATAATACCGCGCCACATAG 3'
 3900
 5' CAGAACTTTAAAAGTGCTCATCATTGGAAAACGTTCTTCGGGGCGAAACTCTCAAGGAT 3'
 3960
 5' CTTACCGCTGTTGAGATCCAGTTCGATGTAACCCACTCGTGCACCCAACCTGATCTTCAGC 3'
 4020
 5' ATCTTTTACTTTTACCAGCGTTTCTGGGTGAGCAAAAACAGGAAGGCAAAATGCCGCAA 3'
 4080
 5' AAAGGAATAAGGGCGACACGGAAATGTTGAATACTCATACTCTTCCTTTTTTCAATATTA 3'
 4140
 5' TTGAAGCATTATCAGGGTTATTGTCTCATGAGCGGATACATATTTGAATGTATTTAGAA 3'
 4200
 5' AAATAAACAAATAGGGGTTCCGCGCACATTTCCCCGAAAAGTGCCACCTGACGTCTAAGA 3'
 4260
 5' AACCATTATTATCATGACATTAACCTATAAAAATAGGCGTATCACGAGGCCCTTTCGTCT 3'
 4320
 5' TCAAGAA 3'

Acknowledgements

The present work was carried out at the Department for Physiological Chemistry II of the Theodor-Boveri-Institute of the University of Würzburg between June 1997 and January 2000. I would like to thank all these who worked together with me, who supported me and who were responsible for the nice working atmosphere:

I am very much thankful to Prof. Dr. W. Sebald for the opportunity to carry out my Ph.D. in his working group, the lots of discussions and invaluable guidance he gave to me. Especially I would like to thank him for introducing me to the BIAcore technology.

I particularly wish to thank Prof. Dr. E. Buchner (Department of Genetics) for being the second referee of this work and for representing this work in front of the Faculty of Biology.

I thank very much Mrs. Mayer for her general support and her kindness and helpfulness with finding lodging.

I am grateful to Dr. Y. Wang and Michael Blässe for introducing me into the project and some of the used techniques.

I would like to say many thanks to Christian Söder for the excellent technical assistance in protein purification.

To Wolfgang Hädelt I would like to thank for the excellent technical assistance in DNA sequencing.

I would like to say thank you to Dr. Thorsten Hage for his helpful discussions and technical support.

Many thanks also to Dr. Joachim Nickel for various useful scientific discussions. For the friendly and nice atmosphere in lab 349 I am thankful to Michael Blässe, Dr. Thorsten Hage, Thomas Hom, Dr. Felix Letzelter, Dr. Joachim Nickel and Angelika Wagner.

I am thankful to my husband Dr. Stefan Wietek for his useful comments and discussions and for his technical help with the formation of the present thesis. I highly appreciate his patience, understanding and moral support in the time of my Ph.D. work.

To my parents and my brother I would like to thank for the moral support and courage, which they gave me and for their efforts to keep in order all my affairs in Bulgaria during my foreign stage.

I would like to address my thanks to all the other people, who have not been mentioned here by names, but who helped me during my thesis work and who made my stage in Würzburg an exciting experience.

Lebenslauf

Persönliche Daten:	Name:	Irina Wietek geb. Simeonova
	Anschrift:	Motorstr. 46 D-80809 München Tel.: 089 / 35 70 96 71 Mobil: 0178 / 687 58 78
	geboren am:	6. Januar 1972 in Sofia (Bulgarien)
	Familienstand:	verheiratet
	Nationalität:	Bulgarisch
Berufstätigkeit:	seit 07/00	Analyst Customer Integration bei der eLabsEurope AG, München
	09/95-06/97	Labor für Molekulare Pathologie, Universitätsklinik für Geburtshilfe und Gynäkologie, Sofia (molekulare Basis und Diagnose vererbbarer Erkrankungen)
Promotion:	seit 06/97	Biozentrum der Universität Würzburg, Prof. W. Sebald (Medizinische Fakultät, Abteilung Physiologische Chemie) "Human Interleukin-4 binding protein epitope involved in high-affinity binding of Interleukin-4: Molecular analysis and characterisation"
Studium:	07/95	Diplom in Biochemie und Mikrobiologie; Gesamtnote: ausgezeichnet
	01-07/95	Diplomarbeit im Labor für Molekulare Pathologie, Universitätsklinik für Geburtshilfe und Gynäkologie, Sofia: „DNS-Analyse von Familien mit spinaler Muskelatrophie“; Gesamtnote: ausgezeichnet
	09/93-12/94	Spezialisierung in Klinischer Chemie, Abteilung Biochemie, Universität Sofia und Abteilung für Klinisches Labor und Klinische Immunologie, Medizinische Universität Sofia
	09/90-07/93	Biochemie und Mikrobiologie an der Universität Sofia, Fakultät für Biologie; Vor-Diplom
Stipendium	09/90-07/95	St. Kliment Ohridsky Universität Sofia
Schulbildung:	09/86-06/90	Nationales Gymnasium für Mathematik und Naturwissenschaften
	09/79-06/86	Grundschule

Erklärung

Ich erkläre hiermit ehrenwörtlich, daß ich die Dissertation „Human Interleukin-4 binding protein epitope involved in high-affinity binding of Interleukin-4: Molecular analysis and characterisation“ selbständig angefertigt und keine anderen als die von mir angegebenen Quellen und Hilfsmittel benutzt habe.

Ich erkläre, daß diese Dissertation weder in der gleichen noch in einer anderen Form in einem anderen Prüfungsverfahren vorgelegen hat.

Außer den mit dem Zulassungsgesuch urkundlich vorgelegten Graden habe ich keine weiteren akademischen Grade erworben oder zu erwerben versucht.

München, den 23. Juli 2001

Irina Wietek